

Optimizing Window Size Through Calibrated Building Energy Simulations: A Case for SAFAD Building of the University of San Carlos

A Thesis Project Proposal

Presented to the

Faculty of

The Department of Electrical

And Electronics Engineering of the

University of San Carlos

Cebu City, Philippines

In Partial Fulfillment

Of the Requirements for the Degree

Master of Science in Electrical Engineering

By

Ivan John A. Naparota, REE

Engr. Isabelo A. Rabuya, MS

Adviser

Engr. Mark Anthony Cabilo, MEng

Co - Adviser

March 2020

Chapter 1

The Problem and Its Settings

1.1 Introduction

Buildings have significant impact to the society and to the environment. They are responsible for 36% of the world's total energy consumption and for 40% of the world's total greenhouse gas emission [1]. In the Philippines, buildings account for 20% of national energy consumption [2]. The increasing population of buildings puts a burden on the country's supply of energy because of the direct relationship between buildings and the country's energy demand. Since the Philippines is still heavily dependent to non-renewable energy sources [2], environmental concerns will really be tied up with the country's pursuit for industrialization.

Energy efficiency in buildings (EEB) is a vital step to lighten the environmental and economic burden due to buildings [3]. The concept of EEB is to use lesser energy for building operations (e.g. heating, cooling, lighting, etc.), without compromising the health or comfort of its occupants as well as the functionality of the building. EEB could be seen in many forms: building energy management (building commissioning, energy monitoring, energy benchmarking and standardization, energy labelling, etc.), behavioral aspect (e.g. giving the occupants direct control of the building systems to alter the energy consumption), and technical aspect (improving the system of the building) [4]. The technical aspect of EEB could be in the form of improving the mechanical systems (e.g. heating, ventilation, and air conditioning systems), improving lighting systems, assessing building performance for retrofitting, micro-generation using renewable energy sources, or enhancing the building's envelope (walls, windows, roofs, etc.)

Windows are found to be the most vital component among building envelope in the loss of energy in the building [5]. The heat flow through the window is basically characterized by its thermal properties – U-value (thermal transmittance), g-value (total solar energy transmittance), and air leakage [6]. The heat gain and heat loss through windows can be associated into these three following parameters: window size, window orientation, and window's thermal properties [7]. Moreover, aside from heat, glazed

windows are major contributors of the penetration of daylight in the building space [8]. Because of these characteristics of windows, they are found to improve the energy performance of buildings when optimized properly.

1.2 Statement of the Problem

Windows are found to be the most crucial feature of a building in permitting the gain and loss of energy [5] making them capable of not only providing daylight [9] but also influencing the building's total energy consumption [10] [11][12]. On the other hand, window size is regarded to be one of the most influential window parameter to the energy consumption [13] and daylight provision [13][9] in buildings.

Optimizing window size should not be treated as a single objective optimization process when you are in a country like the Philippines because of several factors. First, the country's energy demand mostly comes from cooling and lighting. These two types of energy consumption have contradicting characteristics in the viewpoint of an optimum window size. Harnessing natural light is a common approach to minimize lighting energy consumption, and to do that, intuitively, larger windows need to be applied. However, to lessen cooling energy consumption, limiting the entrance of solar energy in a conditioned building space is very important, which in turn requires smaller windows. And second, note that the Philippines is located in the Asian tropics where there is an abundant supply of daylight, altering window size for the sole purpose of minimizing energy consumption may sacrifice the visual comfort of building occupants. Allowing too much penetration of daylight (to minimize lighting energy consumption) may cause over glare to the building occupants, while inhibiting too much daylight (to minimize cooling energy consumption) may go against the preference of most of the building occupants. These contradicting factors in deciding the optimum window size in an extremely hot and humid climate like the Philippines need to be considered, thus, multi-objective optimization process needs to be performed [14] [9].

Few studies about optimizing window size can already be found in the literature, however, studies with Philippines as the location is nowhere to be found.

To have a study that optimizes window size with considerations mentioned above, and which is for specific application for a building located in the Philippines, the present work aims to study the optimum window to wall ratio (WWR) for every orientation that corresponds to the four cardinal direction (North, South, West, and East) in a school building in the Philippines that could lessen its cooling and lighting energy demand with the adequate exploitation of daylight inside the building space. Specifically, this study aims to achieve these following objectives:

- i. Establish calibrated models of the SAFAD building that will serve as baseline models.
- ii. Determine the WWR range that will give the least total energy consumption for every orientation.
- iii. Perform day-lighting assessment of WWR proposed from the previous step using UDI (Useful Daylight Illuminance) metric and conclude to the optimum WWR value that gives the right amount of daylight.

1.3 Significance of the Study

The results of this study would contribute to the advancement of existing body of knowledge since this study is conducted because of the observed gaps, namely: absence of studies that consider total energy consumption and daylight assessment in an extremely hot and humid climate location, and lack of research about enhancing energy performance of buildings through the enhancement of building envelope that is designed for applications specific to the Philippines.

The advancement of window optimization is already evident in other countries, but since results differ with varying scenarios (climate, building characteristics, etc.), it is a must that studies conducted specifically in the Philippines grow in number to back-up future guidelines and implementing rules and regulations in designing and/or retrofitting energy efficient buildings in the Philippines.

Since EEB is yet to be developed in the Philippines, the result of this study could possibly influence the mindset of building designers in the country in the decision making process during the stage of designing buildings – that building features like windows do not only contribute to the aesthetics of a building but also to its energy performance and occupants' visual comfort.

The success of this study is a step for the design of highly energy efficient buildings with the consideration of occupants' visual comfort in the Philippines to support the bigger goal of the country relating to energy efficiency.

1.4 Scope and Limitations

This work aims to study the optimum values of WWR for every orientation that corresponds to the four cardinal directions (North, South, East, and West) that could deliver the least cooling and lighting energy consumption and exploit adequate amount of daylight for occupants based on a school building situated in the Philippines. Therefore, the parameters being investigated are only the window size in terms of window to wall ratio (WWR) and window orientation. There are other window parameters that could affect the energy consumption of a building, namely solar heat gain coefficient (SHGC) and U – value. SHGC measures how well a window blocks heat from the sun, the lower the SHGC the better a window is at blocking heat from the sun. On the other hand, U – value is the measure of the amount of heat energy transferred from a window, the lower the U – value the better the ability of a window in reducing heat transfer. However, the two mentioned parameters were already beyond the scope of the optimization process performed in this study. Also, it is worth noting that during the optimization of window size, it was simulated that there were no shading objects, and the window material was fixed to the existing material of the window of the case study building. Shading objects were removed to maximize the entrance of daylight and so that the window can be optimized without the need for any shading objects (e.g., overhangs, etc.), and the simulated window material were the existing material so that the result will be highly relevant to the case study building. Moreover, the output being considered in arriving to the optimum WWR are

lighting and cooling energy consumption only. The day-lighting assessment is done using the UDI metric only. Lighting and cooling are the only energy considered because the school building does not have heating and humidification systems, moreover, heating is very rare in the Philippines.

The building model used is an existing and occupied school building from the University of San Carlos in Cebu, Philippines. The building details used for the modelling process were gathered through walkthrough audits, equipment specifications, and data available from the University's database. Because it does not represent the entirety of school buildings in the Philippines nor in all countries in the Asian tropics, the results in this study does not guarantee its applicability to all school buildings in the mentioned region; thus the results of this study are only valid to buildings with the same details.

1.5 Definition of Terms

- Building envelope - outer elements of a building – walls, windows, doors, roofs, and floors, including those in contact with earth
- UDI – useful daylight illuminance; a metric developed by Nabil and Mardaljevic [16] to assess the daylight of the entirety of a working space while considering the different sky conditions happening in a year
- WWR – window to wall ratio; the transparent to opaque area ratio in a wall

Chapter 2

Review of Related Literature

2.1 Role of Windows in Buildings

Windows are found to be major contributors in the loss of energy in the building space. In Norway, it was reported that 40% of the heat loss in a typical office building are due to windows, outranking the contribution from other parts of the building envelope specifically walls, air leakages, thermal bridges, floor, and roof [5]. The heat flow through the window is basically characterized by its thermal properties – U-value (thermal transmittance), g-value (total solar energy transmittance), and air leakage [6]. Moreover, the heat gain and heat loss through windows can be associated into these three following parameters: window size, window orientation, and window thermal properties [7]. Furthermore, aside from heat, glazed windows are also major contributors in the penetration of daylight in the building space [8]. Because of these, there have been many research works that optimizes windows to enhance the energy performance of buildings [17].

2.1.1 Window Size Optimization for Energy Consumption

Window size is said to be the most influential window parameter to the energy consumption and daylighting in a building. A sensitivity analysis [8] reveals that among studied parameters, namely window to floor ratio, shading transmittance, shading front and back reflectance, space aspect ratio, insulation thermal resistance, and glazing type, window to floor ratio has the most impact to annual day-lighting, annual heating demand, and annual cooling demand. It was also found out [9] that among WWR, wall reflectance, and window orientation, WWR has the highest influence on lighting energy demand and to four day-lighting assessment metrics. The high influence of window size to the cooling energy demand, heating energy demand, and daylighting made it a subject for many optimization studies to save energy consumption.

The first found record of window size optimization study in the viewpoint of energy consumption is from Francisco Arumi [18]. He studied the effect of WWR on the heating, cooling, and lighting energy demand in Austin, Texas and concluded to an optimum range of window area from 10-40% that can potentially save energy up to 50% relative to a “windowless” configuration. Later on, a study from Johnson et al. [19] has been recorded, again optimizing to get the least total energy consumption but this time window orientation and the window’s glazing properties are included in the studied parameters. Then years later, along with window size, building’s geometric details have been included in recorded optimization studies, specifically the building’s aspect ratio [20] and the room size [21]. The former considers heating and cooling energy demand while the latter considers total energy consumption as the metric for optimization and were studied for residential and office buildings respectively. Then another research work which studied the same parameters as [21] is from Ghisi and Tinker [22] only they differ in the metric used for optimization, in which this time it is more focused on the lighting energy consumption. Specifically, it was about the integration of daylight into the building space to lessen lighting energy demand. Later on, consideration of shading devices [10] in the study of window size has been recorded. Along with wall thermal properties [23], building insulation, thermal mass, different glazing systems, and even colour of wall [24] [25] [26] were studied to maximize further energy savings. Then the inclusion of other building features such as curtain walls can also be found [27] in the literature. More recent related studies can still be found [28] [29] [12] [11] [30] [31]. The parameters being studied are not so different to the earlier studies aside from one [12] where they included in the parameters being studied the window position. In the case of two other studies [11][31], they used different approaches in the optimization process which is through optimization algorithms aside from the most common graphical analysis. The former used *harmony search algorithm* which is an algorithm inspired from the musical process of searching for the perfect harmony and the latter used *genetic algorithm* which is an evolutionary algorithm that is inspired by the natural selection.

Giving the exact value of the optimum window size to summarize the results of the aforementioned studies is however not possible because optimum window size is a case to case basis, as observed in the mentioned studies, optimum window size depends on various factors. It could be climate, building type, glazing properties, or simply the priority of the optimization process. However for simple understanding, in terms of lighting along with heating energy demand, larger window size is more favourable [32] [26] while for the purpose of lesser cooling energy demand, a smaller window size is more favourable [32].

2.1.2 Window Size Optimization: Energy and Day-lighting Assessment

It is found that integration and effective use of daylight in buildings is key in achieving energy savings [22]. But it is important in optimizing windows that aside from minimizing the energy consumption, there should be an assessment of day-lighting in the building space [33]. Thus, multi-objective optimization of window size with simultaneous evaluation of energy performance and daylighting is important. However, compared to studies that focuses solely on energy there are only few studies that conduct simultaneous evaluation of energy performance and daylight assessment.

A study from Ochoa et al. [33] optimizes window size with simultaneous evaluation of total energy and day-lighting. In that study, to assess the day-lighting performance there should be at least 50% of the total occupancy hours that illuminance of 500lux is observed in the office space. For the visual comfort side of daylighting, two criteria were used. Uniformity ratio is between two reference points of not more than 3.5 and Daylight Glare Index (DGI) of not more than 22 both for a minimum of 50% total annual occupancy hours. The window size that will give the least total energy consumption at the same time passes the day-lighting performance and passes one of the two criteria for visual comfort will be deemed as optimum. A similar study [34] was also conducted. This time, solar shading set-point and window size for an energy efficient office building in Frankfurt, Germany was being considered. The day-lighting performance and visual comfort was assessed through Daylight Autonomy (DA) with 500lux being the threshold and Useful Daylight Illuminance (UDI) respectively. DA₅₀₀ is the percentage of the total annual occupancy

hours that had the illuminance of at least 500 lux being met inside the office space [35]. UDI however measures the frequency of daylight in the building space within a specific range (100-500lux, 500-2000lux, >2000lux), 100-500 lux being the range for considered effective with daylight alone or the supplementation of artificial lighting, 500-2000 lux is either desirable or at least tolerable, and >2000 lux is said to cause visual and/or thermal discomfort [16]. The range of window size that will give the least total energy consumption and at the same time passes the defined criteria for day-lighting assessment will be concluded as the optimum range. They also added a robustness test to investigate how variable is the optimum range of window size when subjected to change in building geometry (surface area to volume ratio) and Heating, Ventilation, and Air Conditioning (HVAC) efficiency. This study was replicated with minimal changes by Goia [14]. This time, it considers four different European climate (Oslo, Frankfurt, Athens, and Rome) and added a robustness test through changing the efficiency of artificial lighting. The workflow of this study is basically the same from the previous one. A research conducted by Lartigue et al. studied the effect of window to wall area ratio (WWR) and the window type characterized by its visual and thermal characteristics (visual and solar transmittance, and U-value) to the heating load, cooling load and day-lighting performance [36]. Day-lighting performance is quantified using Annual Deficient Daylight Time (ADDT) and a threshold of 300 lux is set for the ADDT metric. The goal was to minimize the ADDT₃₀₀ since this will mean that there is a minimal duration of illuminance lower than the 300 lux threshold in a year. Another research studied the effect of WWR, wall reflectance, and window orientation to the various day-lighting metrics (Average Daylight Factor, Average Uniformity, Daylight Autonomy, Useful daylight Illuminance, and simplified Daylight Glare Probability) and annual lighting energy demand of an office building in Indonesia [9]. He performed a sensitivity analysis through multiple linear regression to know which among the studied parameters greatly influenced the considered output. Multi objective optimization using Pareto analysis was performed to arrive to the optimum parameters. However, in the viewpoint of energy performance, it is notable that they only considered lighting energy demand. There was an investigation on the effect of building aspect ratio,

building orientation, depth of overhang for south facade, WWR for each facade, window position for each facade, and window visible transmittance to the Annual Glaring Index (AGI) and Annual Energy Requirement (AER) in an existing office in Canada [13]. A very recent study that optimizes WWR in an existing hotel building with solar shading situated in China's climate condition can also be found [37]. There was a simultaneous consideration of visual performance through Daylight Factor and cooling energy demand. First objective of the study was to find the minimum WWR that will meet China's day-lighting requirement. Then computer simulation was applied using the found WWR to calculate the baseline cooling load. The cooling load was again calculated through heat balance equation with various WWR values and solar shading scenarios. A range of WWR values that deliver lesser cooling load with respect to the baseline cooling load was then proposed. Finally, the range of WWR that were proposed previously were tested to verify if they passed the day-lighting requirement. During this stage, the final optimum WWR was then proposed.

2.2 Useful Daylight Illuminance

One of the most used daylighting metrics is a fifty year old metric which is Daylight Factor (DF). DF is the ratio of the indoor illuminance due to daylight in a particular point of a working space to the outdoor horizontal illuminance under an unobstructed overcast sky [16]. It is a very common metric for daylighting assessment because of its simplicity and is still used in the present [37]. However, because it does not capture the scenario during non-overcast skies, this metric is said to be "unrealistic" [16].

Another common daylighting metric is the Daylight Autonomy (DA) metric. There are some studies that uses this metric [14][34] [9] in optimizing window parameters. DA is just like a histogram of the number of occurrence (hourly or sub hourly) of a certain illuminance value (e.g. 500 lux) annually [16]. Unlike the DF metric, it utilizes the annual illuminance data thus the overcast and non – overcast skies are now being captured. However, the limitation of this metric is that the assessment of daylight is made independently point by point. For example, two different points aligned along the centre of

the window in an office room are to be studied, one point is nearer the window and the other is farther. DA will give you for example that point “near” experienced 2000/4380 daylighting hours of 500 lux and point “farther” experienced 2000/4380 daylighting hours of 500 lux which is for example the desired illuminance. From the example scenario, it is good that the two points in the office experienced the desired illuminance (500 lux) almost 50% of the daylighting hours. However, there is a huge possibility that for that one whole year, was an instance that point “near” experienced a higher illuminance while point “farther” experienced the desired illuminance. This will make visual discomfort in point “near” while maintaining the right amount of daylight for point “farther”.

The mentioned limitations of DF and DA are the gaps that Nabil and Mardaljevic [16] addressed resulting in the creation of the metric UDI (Useful Daylight Illuminance). They first did a survey from the existing literature on what is the acceptable illuminance value that is most accepted by occupants. They concluded that “useful daylight illuminance” is within 100-2000 lux.

- 100 – 500 lux being the range for considered effective with daylight alone or the supplementation of artificial lighting
- 500 – 2000 lux is either desirable or at least tolerable
- > 2000 lux is said to cause visual and/or thermal discomfort

Mutual consideration of different points in a working space should be done in this metric to conclude for the entirety of the working space. Should there be at least one of the points being studied that does not fall in the 100 - 2000 lux range, it would mean that the working space in general is not experiencing the “useful daylight illuminance”. Also, it utilizes annual illuminance data to account for different sky conditions. With these, the authors were able to address the limitations of the previous metrics presented.

2.3 Climate in Optimizing Window Size

Climate is a vital factor in concluding to the optimum window size [4]. A study [20] wherein south window size, building aspect ratio, and insulation thickness of the

building were investigated for five different locations in Turkey. It shows that the optimum value of south window size that could reduce cooling and/or heating load is 90 and 25% WWR for those locations that are experiencing cold (Erzurum, Ankara) and hot climate (Diyarbakir, Izmir, Antalya) respectively. Added to that is a study [21] about getting the window size for different orientations and building size that will give the least energy consumption. It is located in seven different cities in Brazil and one city in the United Kingdom. It is difficult to summarize all the results of the optimum window sizes because of the many parameters considered, but for easier comparison, considering only the width to depth ratio of room of 1:2, room index of 5, and orientation of north, the optimum window sizes are: 87% WWR for Leeds in UK, and 49, 62, 64, 51, 51, 40, 32% WWR for Belém, Brasília, Curitiba, Florianópolis, Natal, Rio de Janeiro, and Salvador, respectively. Another study [32] showed five different climate zones in Asia (Manila, Taipei, Shanghai, Seoul, and Sapporo) for an office building typology wherein they arrived to a varying optimum values of WWR for each climate zones studied. Another study [14] investigated the WWR for four different climate zones in Europe. However, because the building being studied is an energy efficient building, values of optimum WWR is usually in between 30-45% WWR. But considering south facing facades, it has the most varying optimum value of WWR which can be as high as 60% for cold climates and as small as 20% WWR for warmer climate.

2.3.1 Daylighting and Climate Condition in Cebu, Philippines

Cebu, Philippines is located in the Asian tropics around 10° latitude and 123° longitude. It has around 12 daylighting hours in between sunrise and sunset on average. The lowest daylighting hours is normally on December of around 11.5 hours and highest on June which is almost 13 hours [38] (see Figure 2.1).

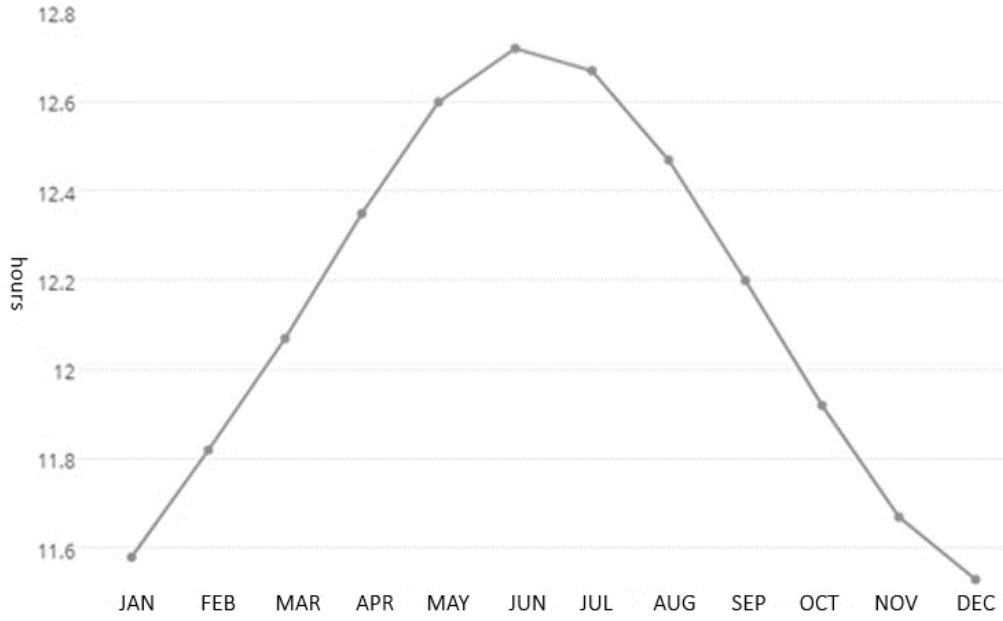


Figure 2.1 Monthly Daylighting Hours Data of Cebu, Philippines [38]

Climate in the Philippines is classified by ASHRAE into three different climate zones (0A, 1A, and 2A) [39] (see Table 2.1). Most of the municipalities and cities belong to climate zone 0A which is classified as extremely hot regions and only one city in the Philippines belongs to the hot region. The letter A after the thermal zone number means that the region is humid, this is why major part of buildings' energy consumption in the Philippines come from cooling and lighting. Thus heating and humidification is rarely used in the country.

Cebu is classified by ASHRAE as extremely hot and humid. The data is from a weather station placed in Mactan, Cebu, Philippines. It has greater than 6000 annual cooling degree days with base of 10°C. Cooling degree day is equal to the °C difference between the mean temperature in a given day and the base temperature 10°C – minimum outside temperature where cooling is not needed inside a building space. Heating is not needed for the entire year according to heating degree days below 18.3°C data available from NASA [38]. Cooling is very much needed during the month of May and very less needed during the month of February (see Figure 2.2).

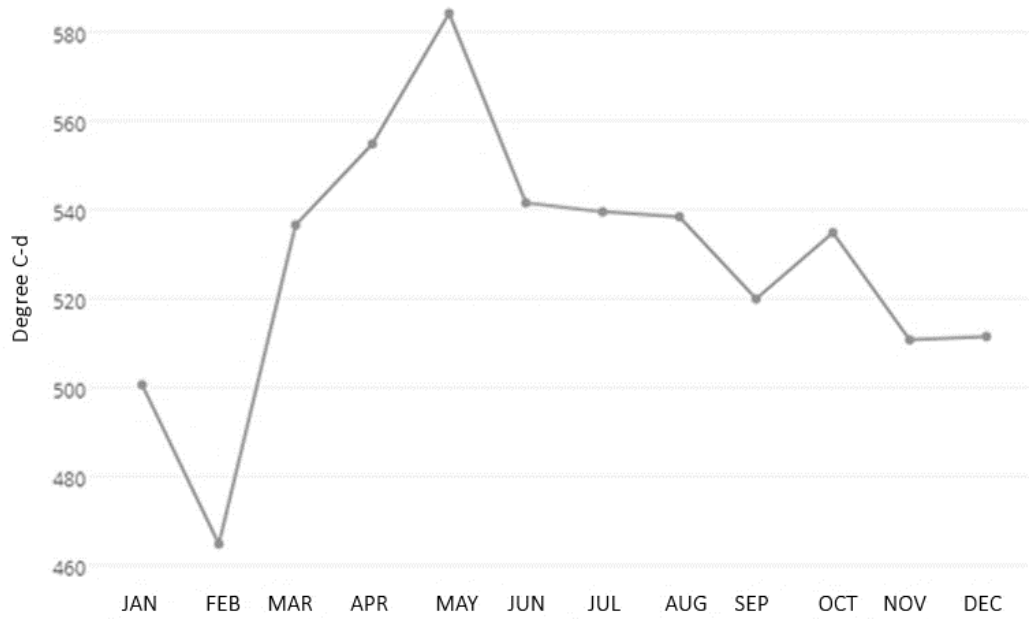


Figure 2.2 Annual Cooling Degree Days of Cebu, Philippines [38]

Table 2.1 Thermal Climate Zone Definitions from ASHRAE [39]

Thermal Climate Zone Definitions			
Thermal Zone	Name	I-P Units	SI Units
0	Extremely hot	$10,800 < \text{CDD}50^{\circ}\text{F}$	$6000 < \text{CDD}10^{\circ}\text{C}$
1	Very hot	$9,000 < \text{CDD}50^{\circ}\text{F} \leq 10,800$	$5,000 < \text{CDD}10^{\circ}\text{C} \leq 6000$
2	Hot	$6,300 < \text{CDD}50^{\circ}\text{F} \leq 9000$	$3500 < \text{CDD}10^{\circ}\text{C} \leq 5000$
3	Warm	$\text{CDD}50^{\circ}\text{F} \leq 6300$ and $\text{HDD}65^{\circ}\text{F} \leq 3600$	$\text{CDD}10^{\circ}\text{C} \leq 3500$ and $\text{HDD}18^{\circ}\text{C} \leq 2000$
4	Mixed	$\text{CDD}50^{\circ}\text{F} \leq 6300$ and $3600 < \text{HDD}65^{\circ}\text{F} \leq 5400$	$\text{CDD}10^{\circ}\text{C} \leq 3500$ and $2000 < \text{HDD}18^{\circ}\text{C} \leq 3000$
5	Cool	$\text{CDD}50^{\circ}\text{F} \leq 6300$ and $5400 < \text{HDD}65^{\circ}\text{F} \leq 7200$	$\text{CDD}10^{\circ}\text{C} \leq 3500$ and $3000 < \text{HDD}18^{\circ}\text{C} \leq 4000$
6	Cold	$7200 < \text{HDD}65^{\circ}\text{F} \leq 9000$	$4000 < \text{HDD}18^{\circ}\text{C} \leq 5000$
7	Very cold	$9000 < \text{HDD}65^{\circ}\text{F} \leq 12,600$	$5000 < \text{HDD}18^{\circ}\text{C} \leq 7000$
8	Subarctic/arctic	$12,600 < \text{HDD}65^{\circ}\text{F}$	$7000 < \text{HDD}18^{\circ}\text{C}$

Table 2.2 Stations and Climate Zones in the Philippines [39]

Country/Location	WMO#	Lat	Long	CZ	Precipitation	
					mm	in.
BAGUIO	983280	16.42	120.60	2A	3686	145
CAGAYAN DE ORO	987480	8.48	124.63	0A	1667	66
CALAPAN	984310	13.42	121.18	0A	1885	74
CATANDUANES RADAR	984470	13.98	124.32	1A	3343	132
CATBALOGAN	985480	11.78	124.88	0A	2555	101
CLARK AB	983270	15.17	120.57	0A	2059	81
CUBI POINT NF	984260	14.80	120.27	0A	3685	145
DAET	984400	14.13	122.98	0A	3563	140
DAGUPAN	983250	16.05	120.33	0A	2429	96
DAVAO AIRPORT	987530	7.12	125.65	0A	1805	71
DUMAGUETE	986420	9.30	123.30	0A	1215	48
GEN. SANTOS	988510	6.12	125.18	0A	1044	41
IBA	983240	15.33	119.97	0A	3802	150
ILOILO	986370	10.70	122.57	0A	2024	80
INFANTA	984340	14.75	121.65	0A	3937	155
LAOAG	982230	18.18	120.53	0A	2226	88
LEGASPI	984440	13.13	123.73	0A	2618	103
LUMBIA AIRPORT	985430	8.43	124.28	0A	1888	74
MACTAN	986460	10.30	123.97	0A	1607	63
MALAYBALAY	987510	8.15	125.08	0A	2580	102
MANILA	984250	14.58	120.98	1A	2134	84
MASBATE	985430	12.37	123.62	0A	1793	71
MUNOZ	983290	15.72	120.90	0A	1942	76
NINOY AQUINO INTERN	984290	14.52	121.00	0A	2134	84
PUERTO PRINCESA	986180	9.75	118.73	0A	1541	61
ROXAS	985380	11.58	122.75	0A	1990	78
SAN JOSE	985310	12.35	121.03	0A	2352	93
SANGLEY POINT	984280	14.50	120.92	0A	1907	75
SCIENCE GARDEN	984300	14.63	121.02	0A	2134	84

SINAIT	982220	17.88	120.45	0A	2478	98
TACLOBAN	985500	11.25	125.00	0A	2241	88
TAGBILARAN	986440	9.60	123.85	0A	1411	56
TAYABAS	984270	14.03	121.58	1A	2439	96
ZAMBOANGA	988360	6.90	122.07	0A	1221	48

2.3.2 Studies with Climate Relevant to the Philippines

Some of the studies mentioned in the previous sections have the same climate with the Philippines.

Ghisi and Tinker [21] studied the window area, orientation, and room size to minimize the total energy consumption in seven cities in Brazil and a city in UK. Some of the considered locations in the study are classified by ASHRAE [39] as 0A and 1A, which are also the climate classification of most cities in the Philippines. Results show that the energy consumption is lower for the room ratios whose façade is smaller and the ideal window area depends on the orientation and facade area. However, daylight assessment is beyond the scope of this study.

Another study which is conducted in Brazil (climate zone 1A) can be found [10]. The parameters being studied are WWR, window control, window material, and interior shading. Results show that 30% WWR is ideal when considering a good trade-off of lighting and air conditioning/ventilation consumption, decreasing or increasing further results in increase in lighting or cooling consumption, respectively. There is 13.4% reduction of energy consumption from baseline with little increase savings of 13.6% when using low-e glasses and 14.4% using interior shading. But again, daylight assessment is beyond the scope of the study.

Another study [9] which has the same climate as the Philippines, was conducted in a neighbour country of the Philippines which is in Bandung, Indonesia. Bandung is classified by ASHRAE as climate zone 0A which represents most of the cities in the Philippines. They studied the effect of WWR, wall reflectance, and window orientation to

various day-lighting metrics (Average Daylight Factor, Average Uniformity, Daylight Autonomy, Useful daylight Illuminance, and simplified daylight glare probability) and total lighting energy consumption. The optimum configuration of building envelope parameters in the context of the study are: WWR 30%, wall reflectance of 0.8, and south orientation. But the scope of this study only extends to lighting energy consumption and day-lighting assessment. It does not consider cooling and/or heating energy consumption.

2.4 Philippines: Energy Efficiency in Buildings Guidelines

A study from Regulatory Indicators for Sustainable Energy (RISE) [40] shows that the Philippines lacks building energy codes to be followed during the design and retrofit of buildings to enhance their energy performance. RISE is a set of indicators that evaluates the quality of policies to support sustainable energy goals in terms of energy access, energy efficiency, and renewable energy. Philippines scored zero in all sub indicators of building energy codes (e.g. codes for new residential and commercial, are renovated buildings required to meet building energy codes, are there mandates for new building stocks to improve their energy performance, etc.).

Philippines has really no strict guidelines in terms of EEB. The country has yet to institutionalize rules and regulations for energy efficiency and conservation, the Energy Efficiency and Conservation Act of 2017 [41].

However, even having no implementing rules and regulations, there are resting codes and guidelines currently in the Philippines in terms of EEB. The Philippine Green Building Code of the Philippines [42] and the Guidelines For Energy Conserving Design of Buildings and Utility Systems of 2008 [43].

2.5 EnergyPlus for Window Size Optimization: Energy and Daylight

EnergyPlus has been widely used for many window size optimization studies, especially in the view point of energy [8] [28] [12] and even up to the more advanced methods of optimization in the present [11] [31]. However, it is found that *EnergyPlus* has limitations in evaluating daylighting. Ramos and Ghisi [44] found that *EnergyPlus* has

limitations in the calculation of daylight factor and external illuminance values when compared to more advanced day-lighting tool like *Radiance* software. He compared measured data of external illuminance in Brazil to the model developed by Perez et al. [45] which is the model used by *EnergyPlus* for external illuminance. *EnergyPlus* shows overestimation in the external illuminance values. Moreover, *EnergyPlus* shows inaccuracy in the calculation of internal illuminance due to reflections as compared to *Radiance*. However, it is worth noting that in the viewpoint of internal illuminance calculation, *EnergyPlus* has maximum difference of only 20% when compared to *Radiance*, which means that *EnergyPlus* can still deliver acceptable result for internal illuminance. Which is also the reason why Goia et al. [34] still used *EnergyPlus* for their daylighting assessment. In their study, window size is being optimized with simultaneous evaluation of energy and daylighting (UDI and DA). It also considers solar shading devices. This study was replicated [14] and considered four different European climate (Oslo, Frankfurt, Athens, and Rome). Both studies use *EnergyPlus* for building energy simulation. Another study [33] was conducted to optimize again the window size with simultaneous evaluation of total energy consumption and day-lighting by performing whole building computer simulation in *EnergyPlus*.

2.5.1 Modelling Windows in EnergyPlus

EnergyPlus [46] follows the thermal and solar/optical modelling procedure of windows from *WINDOW 4* [47] and *WINDOW 5* [48] programs.

2.5.1.1 Thermal Calculation

The temperatures for every face of glazing layers is solved through heat balance equation for every face [49]. There are two faces for every glazing layer and the number of equations is the number of total faces. For example, double glazed window will have four faces (refer to Figures 3 and 4) and will require four equations to solve.

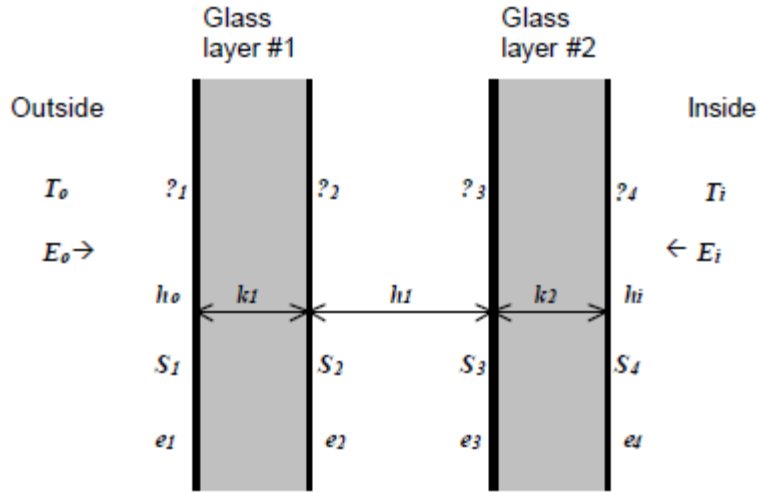


Figure 2.3 Double glazed windows [49]

Here

E_o, E_i = Incident exterior and interior long-wave radiation (W/m^2)

h_o, h_i = Outside and inside air film convective conductance ($\text{W/m}^2\text{-K}$)

S_i = Radiation (short-wave and long-wave) from zone lights absorbed on face i (W/m^2)

T_o, T_i = Outside and inside air temperature (K)

ϵ_i = Long-wave emissivity of face i

h_j = Conductance of gas in gap j ($\text{W/m}^2\text{-K}$)

σ = Stefan-Boltzmann constant

$$E_o \epsilon_1 - \epsilon_1 \sigma \theta_1^4 + k_1 (\theta_2 - \theta_1) + h_o (T_o - \theta_1) + S_1 = 0 \quad (1)$$

$$k_1 (\theta_1 - \theta_2) + h_1 (\theta_3 - \theta_2) + \sigma \frac{\epsilon_2 \epsilon_3}{1 - (1 - \epsilon_2)(1 - \epsilon_3)} (\theta_3^4 - \theta_2^4) + S_2 = 0 \quad (2)$$

$$h_1 (\theta_2 - \theta_3) + k_2 (\theta_4 - \theta_3) + \sigma \frac{\epsilon_2 \epsilon_3}{1 - (1 - \epsilon_2)(1 - \epsilon_3)} (\theta_2^4 - \theta_3^4) + S_3 = 0 \quad (3)$$

$$E_i \epsilon_4 - \epsilon_4 \sigma \theta_4^4 + k_2 (\theta_3 - \theta_4) + h_i (T_i - \theta_4) + S_4 = 0 \quad (4)$$

Figure 2.4 Heat balance equations for Double glazed windows [49]

The detailed thermal calculation is presented in [49].

2.5.1.2 Daylighting

Methods from DOE-2 [50] is used in the calculation of interior daylight illuminance from windows [49]. It is calculated by dividing the window into smaller parts and calculating the daylight that reaches the reference point coming from each part. Luminance of the sky, angle of incidence of light on each part, and glazing visible transmittance at this

angle are considered. Then the calculated daylight coming from each part of window is summed up to arrive to the total direct illuminance at the reference point. Illuminance due to reflection of light from room surfaces to the reference point is also calculated. The daylight factor is then calculated hourly by obtaining the ratio of interior to exterior horizontal illuminances. The exterior horizontal illuminance is obtained using the model from Perez et al. [45].

2.5.2 EnergyPlus Calibration and Validation

Like any other computer models, to use a Building Energy Model (BEM) with certain degree of confidence, it is necessary that the model closely represent the actual performance of the building being modelled. Achieving that, means that the discrepancies between BEM predictions and actual performance of building should be reduced through calibration process. Calibration is the “fine tuning” of the BEM parameters (i.e., geometry, material description, etc.) or input parameters outside the physical system of the building (schedule, weather, etc.) to match the output of the model to the actual output of the building [51].

2.5.2.1 Problems with BEM Calibration

Despite the theoretical advantage of using BEMs in predicting and analyzing building performance, as what Coakley et. al mentioned in their literature review [52], BEMs are underutilized in the Architecture, Engineering, and Construction (AEC) industry, generally because of problems in the model itself and/or how the calibration procedure is performed. They cited studies that show significantly large discrepancy (up to 100% discrepancy) between model prediction and actual metered energy use, this issue does not contribute to the confidence to the model output most especially if the BEM is to be used in the design process where it is expected to predict future building performances on previously unobserved conditions. This is also the reason why it is now more common to see BEMs that are used in post-construction stage (i.e., retrofit analysis, etc.) of the building, rather than its initial intended purpose which is in building’s design stage [53]. But, to use BEMs with certain degree of confidence during post-construction stage of

buildings, calibration is needed to bring the model output closer to the actual performance of building being studied. However, BEM is a model which is derived from fundamental principles (e.g., energy balance, heat transfer, etc.), these principles are used to model the complex system of the building and require large number of parameters that are interconnected with each other. This overwhelming number of interconnected parameters added with the fact that there are only limited measurable outputs will result to tuning lots of uncertain parameters that would be hard for the energy modeler to deal with during the calibration procedure. Also, because of the large number of parameters, tuning a model will become a problem that has no unique solution, meaning, there would be many possible combinations of parameter values that will result to a good goodness-of-fit to measured data. Furthermore, even if calibration is an important thing to do to confidently use BEMs, there is no existing standardized methodology in calibrating BEMs or at least a consensus between researchers of how to perform a calibration procedure. As what Reddy et. al said, “calibration has been an art form that inevitably relies on user knowledge, past experience, statistical expertise, engineering judgment, and an abundance of trial and error” [54][51].

2.5.2.2 Assessing Calibrated Building Energy Models

In the present, statistical indices are the most common and used criteria for assessing the performance of BEMs [53], depending on the results of these statistical indices is the judgment whether a BEM is worthy to be considered calibrated or not.

Currently, a model is deemed calibrated if it passed the standards set by ASHRAE 14 [55] for two statistical indices. These two statistical indices are Mean Bias Error (MBE) and Coefficient of Variation of the Root Mean Squared Error (CV RMSE). MBE measures the overall error in the model. It is the summation of differences (per data point) between the simulated and measured data. However, in this index, positive errors will compensate negative errors, therefore, making this statistical index the sole basis for calibration will give a poor measure of the model’s accuracy. To compensate for MBE’s issue of compensation, CV RMSE is to be used alongside MBE, as CV RMSE is immune to compensation effect as it is just a variant of sum of squares errors (SSE) – the difference

between simulated and actual is squared. The SSE is divided by the number of data points to get the mean squared error (MSE), the square root of the MSE is then calculated to report it as root mean squared error (RMSE). And this RMSE is divided by the mean of actual data to get an index which is the coefficient of variation (CV) of the RMSE that captures how in-sync the model output is to the measured data. The formulas for MBE and CV RMSE are reported below.

1. MBE (Mean Bias Error)

$$MBE = \frac{\sum_{i=1}^n (m_i - s_i)}{\sum_{i=1}^n (m_i)}$$

Where: m_i and s_i are the measured and simulated total energy consumption for every instance; n is the number of data points.

2. Coefficient of variation of the root mean squared

$$CV\ RMSE = \frac{\sqrt{\frac{\sum_{i=1}^n (m_i - s_i)^2}{n}}}{\bar{m}}$$

Where: m_i and s_i are the measured and simulated total energy consumption for every instance; n is the number of data points and \bar{m} is the average of the measured data points.

Though it is currently accepted that ASHRAE's standard is to be followed, it is worth mentioning that there are three international guidelines that set the criteria for MBE and CVRMSE (as presented in Table 2.3), namely: American Society of Heating, Refrigerating, and Air-Conditioning Engineers (ASHRAE) Guidelines 14 [55], International Performance Measurements and Verification Protocol (IPMVP) [56], and M&V Guidelines for Federal Energy Management Program [57]. Criteria for the two statistical indices differ if model is validated hourly or monthly.

However, these guidelines only cover the calibration of model in the viewpoint of energy consumption, it does not cover other aspects of the building, like environmental aspect (i.e., space illuminance, temperature, humidity, etc.) [55].

These guidelines also do not cover uncertainty analysis for the model, uncertainty analysis could help boost confidence on the model's output by quantifying the model's exposure to uncertainties since calibrated models will not have unique solutions and also are subject for tuning hundreds or thousands of parameters where uncertainties are impossible or almost impossible to eliminate. Reddy [58] said that uncertainties in BEMs can be associated from these four main sources: improper input parameters, improper model assumptions, lack of robust and accurate numerical algorithms, and error in writing simulation code.

Table 2.3 Acceptance criteria for BEM

Guideline	Monthly		Hourly	
	MBE	CVRMSE	MBE	CVRMSE
ASHRAE guideline 14	5	15	10	30
IPMVP	20	-	5	20
FEMP	5	15	10	30

2.5.2.3 Current Approaches in BEM Calibration

Clarke et. al was the first to classify BEM calibration techniques [52] and these classifications were also adopted by a later review paper by Reddy et. al. [58] and Fabrizio et. al. [53] and was further expanded by Coakley et. al. [52]. These four classifications are: manual and pragmatic calibration, graphical technique of calibration, calibration based on special tests and analytical procedures, and analytical/mathematical methods of calibration.

- *Manual Calibration* – it is a trial and error approach of tuning the model parameters so that BEM outputs will match measured data without a systematic and automated

procedure. It is an ad-hoc and subjective approach that heavily relies on user's experience and engineering judgment [53]. The advantage of this approach is it is very straightforward and is simple to implement, and would be advantageous to experienced users since they will have a freedom to tune the parameters depending on their judgments, however, it would be hard if the user implementing this procedure is an inexperienced building energy modeler since it heavily depends on user expertise – the inexperienced user may end up searching for values between the ranges of possible values of lots of parameters without the guarantee that the model output will fit the measured data, knowing that not all parameters will have the same level of influence on the model output. Also, the replicability of this procedure will be an issue, since different data will be available from building to building (if applied to another building) and different judgment will be concluded from user to user (if different user will apply the procedure).

- *Graphical techniques* – it is a practice of tuning model parameters guided with data visualization techniques to know what parameters to tune. Aside from the classical time-series and scatter plots, there have been new techniques developed to advance the data visualization technique of tuning model parameters:
 - 3D Comparative Plots – it can be used for tuning time-dependent parameters by plotting in three dimensions: the difference in measured and simulated outputs, period of time in a day, and the days considered. An example of 3D comparative prepared by Fabrizio et. al [53] can be seen in Figure 2.5. With this example, you will be able to know on what specific time and dates are the most discrepancies observed, and during what time of those particular days. Your judgment on the tuning process can be referred to this plot. This will help the tuning of parameters if the uncertain parameters are time-dependent like equipment schedules, lighting schedules, etc.

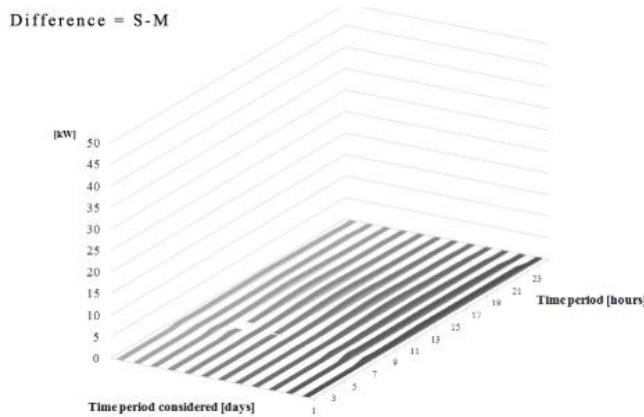


Figure 2.5 3D Comparative plot borrowed from Fabrizio et. al. [53]

- Signatures – signatures have two key types that are used together: calibration signature and characteristic signature [53].
 - Calibration signature – it is basically a scatter plot of normalized differences between measured and simulated energy consumption (either cooling or heating) calculated as $\frac{\text{Measured} - \text{Simulated}}{\text{Measured}_\text{maximum}} \times 100\%$ versus outdoor dry-bulb temperature. This means that if a model's output is a perfect fit to measured energy consumption, a flat line should be seen in the plot. It is important to remember that the energy consumption needed for this technique should be an energy consumption that has a correlation with outside temperature: i.e., cooling; heating. A sample heating calibration signature plot borrowed from Fabrizio et. al. is seen in Figure 2.6, and for the purpose of comparison, the author also prepared the same plot with energy consumption which is a combined cooling, lighting, and equipment consumptions in Figure 2.7. The trend is quite obvious in the signature plot in Figure 2.6 that around 0 degree Celsius, the energy consumption difference is minimum, but the model tends to overestimate and underestimate as the temperature goes left and right from 0, respectively. On the other hand, using total energy consumption in Figure 2.7 will not deliver a good trend between x and y variables.

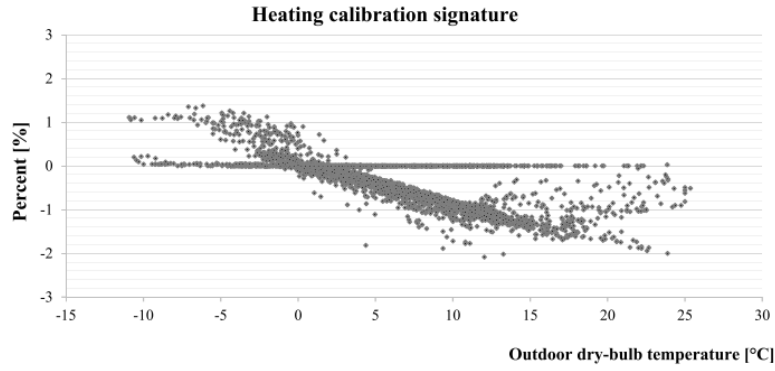


Figure 2.6 Heating calibration signature plot borrowed from Fabrizio et. al. [53]

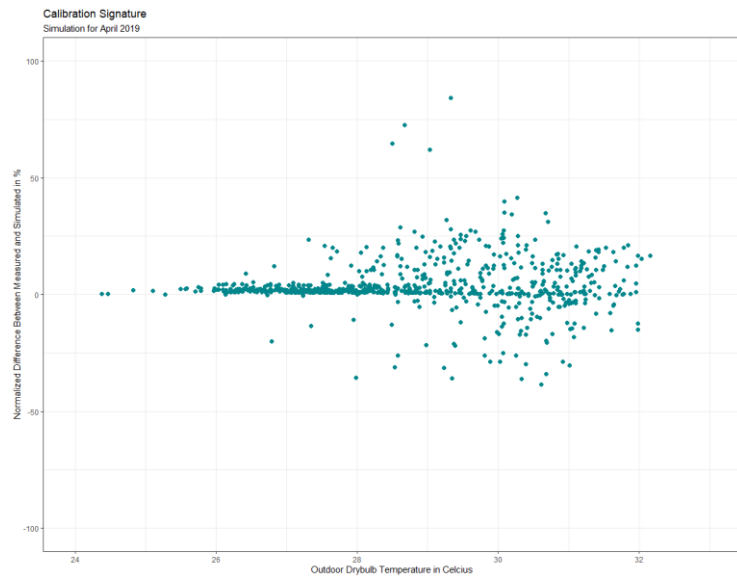


Figure 2.7 “Total energy consumption calibration signature” sample

- Characteristic signature – knowing the trend of the energy consumption versus outdoor temperature is not enough to finalize the judgement for the tuning process, another important thing to do is to assess what parameters are capable of “flattening” the trend of the calibration signature plot. That is where characteristic signature is used. Instead of plotting the difference between measured and simulated values, the normalized difference between two simulation outputs computed as $\frac{\text{change in energy consumption}}{\text{Measured_maximum}} \times 100\%$ if a certain parameter’s value is changed versus outdoor dry-bulb temperature

is plotted. A sample characteristic signature plot when cooling setpoint is changed from 27C to 15C was prepared by the author as shown in Figure 2.8. This sample plot is, again, total energy consumption (cooling + lighting + equipment) but the offset is theoretically from cooling energy consumption. It can be seen that if the setpoint is changed from 27 to 15 degrees Celsius, the energy consumption will increase with as much as 25% between 29 to 32 degree Celsius of outdoor dry-bulb temperature. If coupled with the calibration signature, the user can base his judgements from the characteristic signature on what parameters to be tuned and what value of the parameter will be applied.

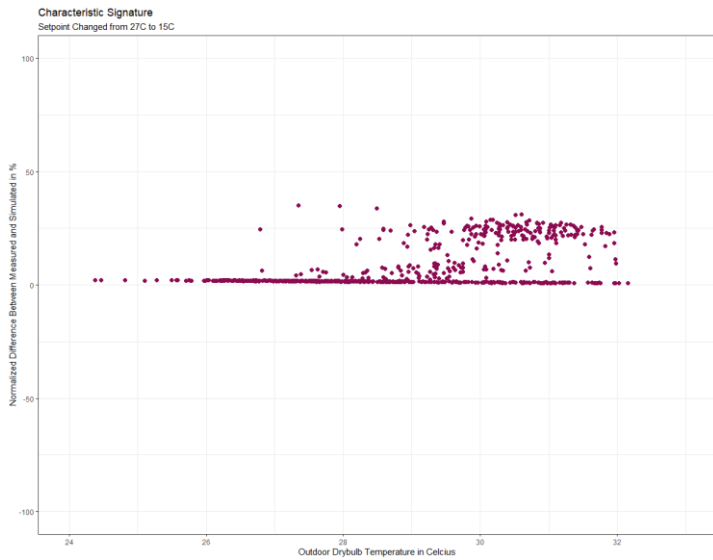


Figure 2.8 Sample characteristic signature

- *Calibration based on special tests and analytical procedures*
 - is a procedure of calibration where the user judges the tuning process from short- or long-term monitoring of building processes/activities or applying special tests to measure building properties. Some of the special tests are blower door test for measuring air infiltration/tightness or material thermal properties tests [53]. These procedures are very logical but will not always be practical especially if the building is occupied because these tests are

intrusive for the building occupants if performed. On-site inspections and short-term monitoring are common practices for calibration procedures belonging to this category. A study from Pedrini et. al. [59] showed a method on how to calibrate a building energy simulation using walkthrough audits. The preliminary modeling was aided with data purely from layout plans and documentations alone, the building was modeled without any contact with the physical building. The simulation result was then compared to measured monthly energy consumption for 1 year and a non-desirable fitment with annual difference of 114% was obtained. The next step performed was building fabric tuning using parametric analyses. After that, schedules were tuned based from hourly energy consumption provided by the utility provider. Next steps were the tuning of parameters based on walkthrough audit with hand-held meters and data loggers: the lighting level was tuned using lux meters, temperature data loggers were used to tune cooling setpoint, occupancy, and fan coil schedules (no fluctuations in temperature), and current data logger was used to tune equipment power density. Finally, the model was further tuned using separated energy consumptions (lighting, cooling, and convenience outlet) and by changing lighting and equipment power densities and switching schedules.

- Automated Calibration using Analytical/Mathematical Methods
 - All the mentioned calibration procedures above are basically manual tuning of the parameters that heavily depends on users' expertise and preferences as bases for what parameters to tune and what values of these parameters to apply. But for automated calibration using analytical/mathematical methods, the problem of calibration is somehow treated as an optimization problem with the goal of minimizing the difference between measured and simulated values. There are different mathematical/statistical tools applied in the literature: the concept of Monte Carlo simulations as applied in a study from Reddy et. al. [51] wherein they did a randomized search of

possible solutions (combination of parameter values) to fit the model to measured data. They identified first the uncertain parameters and their possible range of values, then a probability distribution is defined for each parameter and a sampling technique of Latin Hypercube Sampling was employed for the series of simulations (hundreds and thousands) to search the solution space. They were able to extract a number of plausible solutions and used 20 calibrated models for analyzing possible energy conservation measures (ECM). The main strength of using many calibrated models than using only a single calibrated model is that the prediction uncertainty is addressed since the problem of calibrating a model will not have a unique solution, so the range of variation of energy savings can be captured by this approach. Latin Hypercube Monte Carlo was also used in the study for sensitivity analysis as preparation for further tuning using *fine grid approach*. Another mathematical approach in tuning building energy simulation is meta-modelling just like what Manfren et. al. applied in their study [60] wherein they applied supervised learning for calibration and uncertainty analysis. A meta-model is a surrogate model of an original model to reduce model complexity and have a computationally faster model. For example, there is a building energy model from a simulation program (e.g., *EnergyPlus*), one should characterize first the building in the software and define the meta-model by varying inputs using sampling techniques, with this different inputs, different outputs can also be realized. These different scenarios of inputs and outputs will be the basis for the meta-model. Then model optimization will be applied to the meta-model. Another mathematical method for calibrating a building energy simulation is optimization-based methods. It is the application of common optimization algorithms (e.g., genetic algorithm) to optimize (minimize difference between measured and simulated values) the model [53].

- An important thing to do when applying automated mathematical/analytical procedures for calibration is reducing the number of uncertain parameters before tuning the parameters. This can be done using sensitivity analysis to filter out influential from non-influential parameters [61]. This is important because dealing with lots of parameters may be challenging computationally. For example, when applying the Monte Carlo simulation, having 20 uncertain parameters and 4 samples for each parameter will give $4^{20} = 1.099 \times 10^{12}$ possible combinations, while reducing the number of parameters to 19 will give $4^{19} = 2.748 \times 10^{11}$ possible combinations which is already four times less. Searching the solution space with 20 parameters may cost the user additional extra hundreds or thousands simulations compared to reducing it to 19 [51]. Sensitivity analysis techniques that are commonly used in the domain of building energy simulation are reviewed carefully in a review paper from Wei Tian [62].
- Morris Method for Sensitivity Analysis in Building Energy Simulations
 - There is no defined rule on how to perform sensitivity analysis in the field of building energy simulation [61] because each tool has their own strengths and weaknesses [62], it just really depends on the judgment of the user and for what purpose will the sensitivity analysis be used.
 - Morris method has been used for ranking the influence of parameters to model output. It has been used in other domains like in a study from the Journal of Hydrology [63] and also in studies related to building energy simulation [61]. Morris method does not need any assumptions of linearity or correlation between parameters and outputs like other tools (e.g., Regression methods). Also, there is no need for defining first the probability distribution of parameters like Monte Carlo analysis. It is an easy to implement tool which is likely to be used if exposed to a large number of uncertain parameters [61]. However, Morris method cannot exactly quantify how much uncertainty does a particular parameter contribute to the

model output unlike some more complicated tools like Variance Based method [62]. It would be useful only for ranking parameters based on their influence on the model output.

- The Morris method of sensitivity analysis by Max D. Morris [64] applies a “one-factor-at-a-time” (OAT) approach but is considered a global sensitivity analysis because the base case is changing [62]. The intuition for an OAT approach is if the parameters are changed equally relative to each other, then the parameter that causes the largest change on the model output is the most influential one. One good way to explain how Morris method differs from a classical OAT approach is from a diagram borrowed from King et. al. [63]. Figure 2.9a shows a classical OAT approach where a pair of simulations is required for each parameter to test how does the model output respond to the change of a particular parameter. Thus, a classical OAT approach requires $2k$ number of simulations for a single trial of testing where k = number of parameters. However, in Figure 2.9b, for Morris Method, the experiment is designed so that it will build a trajectory which is determined randomly that shares simulation points requiring only $k + 1$ number of simulations for a single trial of testing. The full technical details of Morris Method: how a trajectory is built, what are the indices, and other qualities of the method are carefully discussed in the Chapter 3 of this paper.

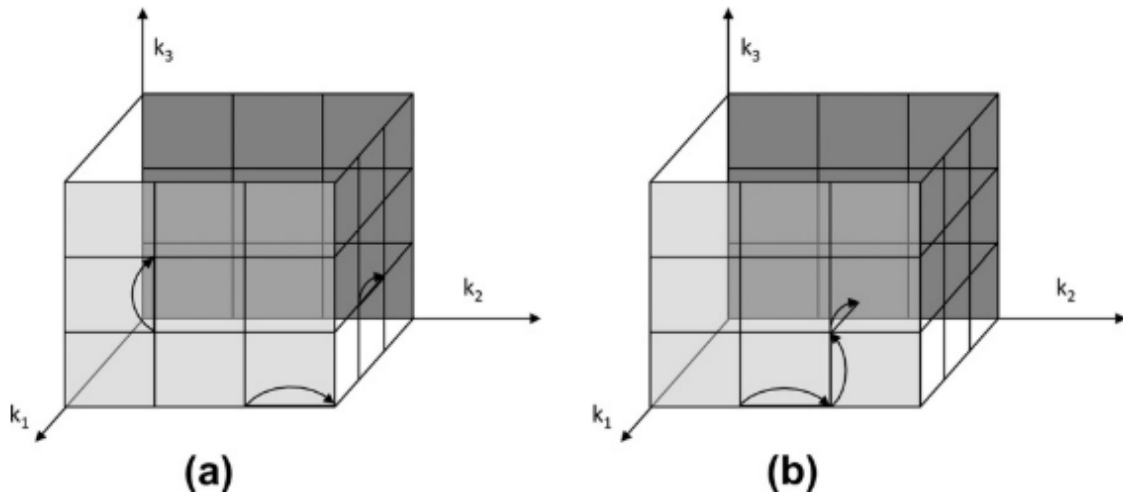


Figure 2.9 (a) Classical OAT approach (b) Morris Method [63]

- Latin Hypercube Monte Carlo for Addressing Prediction Uncertainty
 - Monte Carlo (MC) method, regardless of the type (as there are many forms of MC), is an experimental mathematics that utilizes random values to infer system response [51]. MC methods can handle both deterministic and probabilistic problems. They can be used as numerical methods of solving engineering problems by simulating different possible combinations of parameters in which each parameter takes on a random value within a pre-defined range. They are simple to implement but are computationally demanding because they may require simulations in the order of hundreds or thousands (depending on the number of parameters) which may be viewed as a drawback especially when using models that takes time to simulate. According to Reddy et. al. [51], few of the advantages of MC methods are: its simple mathematics; its applicability to variety of problems; correlation between inputs will be accounted – since parameters are changed simultaneously; and the unknown distribution of model parameters is not an issue. There are different types of MC methods that in general, only differs in the sampling strategy employed [65] [51]: *Hit and Miss* – a technique popular for estimating integrals (e.g., solving area of a circle); *Crude MC method* – the classical MC method that uses independent random sampling based from a pre-defined distribution; *Stratified MC method* – divides the whole population into subgroups or “strata” and make sure that every strata is represented by performing another random sampling within the “strata”, which means each strata follows a pre-defined distribution; and *Latin Hypercube MC method* – is a stratified sampling without replacement. The desirable feature of stratified sampling (each “strata” is represented) is also evident in LHMC without the need for defining distribution within each “strata”, this could be viewed as an advantage especially when dealing with complex models. It is more

efficient than *Crude MC* and is not as complex as *Stratified MC method* making it the most promising method to be used for complex models like building energy simulations [54]. One good example of applying LHMC in calibrating building energy simulation that considers model uncertainty is from a two-paper study from Reddy et. al. [51] [54]. They used LHMC to obtain many possible combinations of parameters that will give a good goodness-of-fit between simulation output and utility. Out from these many possible combinations, top 20 combinations that provide model predictions closest to the utility bill data are selected for energy conservation measure (ECM) analysis. The motivation of using 20 models instead of a single calibrated model is the fact that a building energy simulation has large number of parameters that makes it impossible to find a unique combination of parameter values that will fit the model output to the measured data. By using many calibrated models, many possibilities are explored, they stressed the importance of exploring these possibilities especially when the main purpose of the study is suggesting possible ECMs. An explanation how a single trial of LHMC is performed can be found in the Chapter 3 of this paper.

Chapter 3

Methodology

The present work aims to study the optimum window to wall ratio for every orientation of the SAFAD Building of the University of San Carlos in Cebu, Philippines, that could lessen its cooling and lighting energy consumption with the adequate exploitation of daylight inside the building space. To do that, the methodology was divided into three stages: Preliminary Modeling, Model Calibration, and Optimum Window Size Search. For the preliminary modeling, model parameters were identified or acquired through walkthrough audit, data from University's database, technical specification (datasheet) of building equipment, and *EnergyPlus* default values. The values are then inputted to *EnergyPlus* and a simulation was performed to obtain energy and illuminance output. Energy consumption for the whole building and illuminance for a single room were also gathered through meter and sensor installations and were compared to the simulation outputs. To further tune the model, the model went through a calibration procedure. The model was calibrated in terms of illuminance first and proceed to another calibration procedure in terms of energy afterwards. For the calibration in terms of illuminance, the visible light transmittance of the window will be tuned. For the model calibration in terms of energy, unknown or uncertain parameters along with their value ranges were identified heuristically and were then ranked depending on how influential they are to the energy output of the model using Morris Screening Method. The top seven influential parameters were then tuned using Latin Hypercube Monte Carlo with 400 trials. Five different calibrated building energy simulation obtained using LHMC were then used for the search of the optimum window size. Parametric analyses for each of the calibrated building energy simulations were performed to determine the WWR range that gives the least total energy consumption and at the same time exploit the right amount of daylight for every building orientation.

Preliminary Modeling

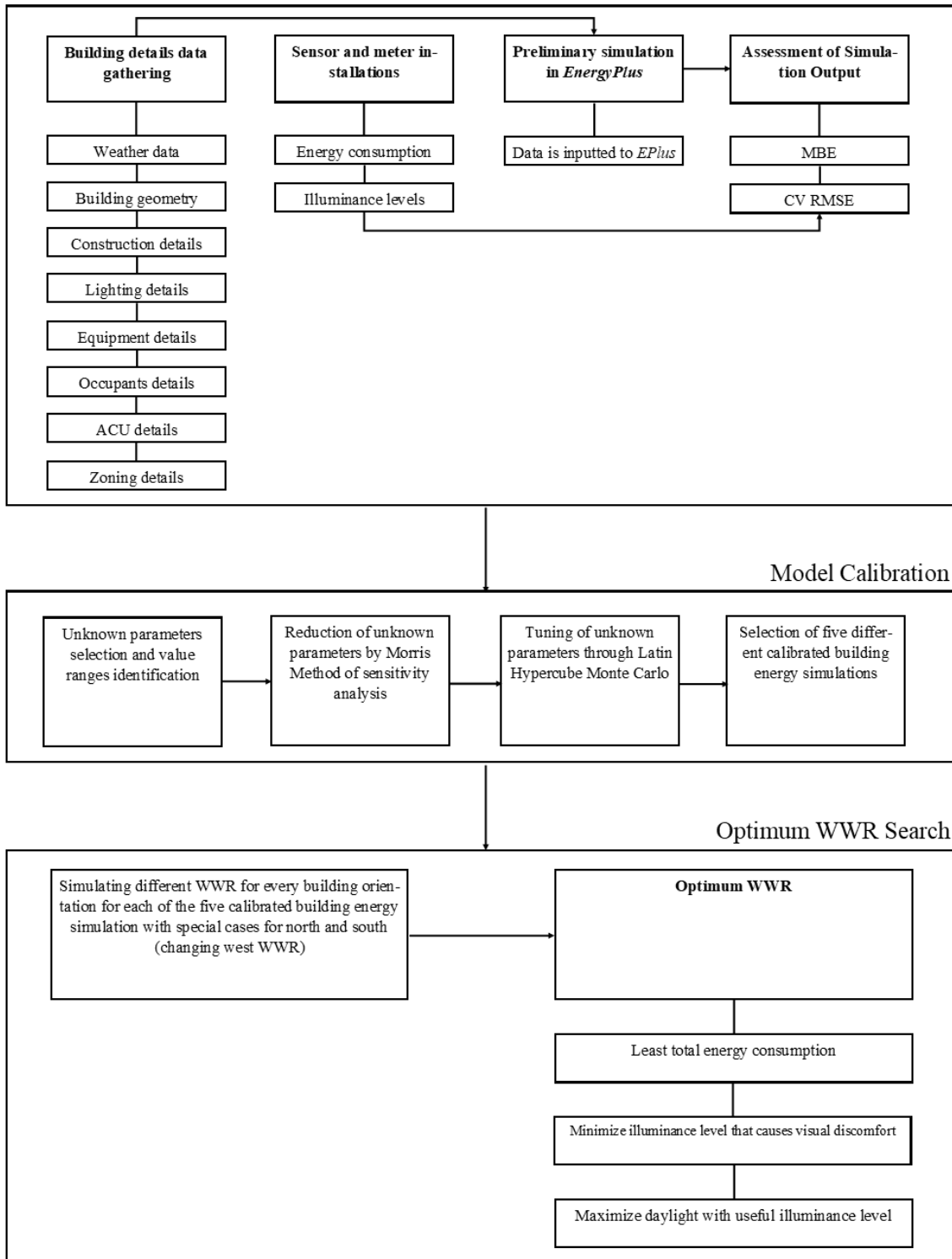


Figure 3.1 Research Workflow

3.1 Preliminary Modeling

This section discusses the details of the building parameters and inputs that were identified to define the physical characteristics of the building and its processes that will be used for the preliminary modeling.

3.1.1 Case Study Building

The building that was chosen to be the subject of the study is an existing and occupied building, the SAFAD building of the University of San Carlos. To run a building energy simulation of SAFAD in *EnergyPlus* that resembles the building's physical characteristics and internal processes as much as possible, the following data were gathered:



Figure 4.2 The SAFAD Building of University of San Carlos

- Location and Weather file
 - The building is located in Talamban, Cebu City, Philippines but the weather file used is a “typical year” weather file for Mactan, Cebu, Philippines which is provided by White Box Technologies – a recommended private source weather file

provider for simulations by EnergyPlus. “Typical year” weather file is the most representative of long-term record by concatenating twelve calendar months of different years, each month selected as the most “typical” in comparison to the long-term record for that particular month. Since *EnergyPlus* only acknowledges the location of the weather file, this means that the building is simulated to be in the location of the weather station. The location of the weather station is around 10 kilometers away from the building.

Table 3.1 Location Data

Field	Units	Value
Latitude	Degrees	10.35
Longitude	Degrees	123.91
Time Zone	Hours	8
Elevation	Meters	75

- Building geometry and construction
 - Building geometry were drawn in *SketchUp* using an extension named *Euclid* for it to be converted into an *EnergyPlus* input file. The shapes and heights of the rooms were derived from the SAFAD building’s floor plan verified and identified through walkthrough audits. Floor plan layouts can be found in the Appendix of this paper.
 - Details of the surface constructions of the building were identified which pertain to what are the materials used, what is the layering of the materials (if applicable), and what are the corresponding properties of the materials for different building surfaces – walls, roof, floor, and windows. All walls of the SAFAD building except for walls that separate two different

rooms are generally made up of concrete that has 25 cm thickness (denoted as “Outside Wall in the table”). However, walls that separate different rooms are generally made up of two 1.27 cm plyboard with air gap in between (denoted as “Inside Wall in the table”). See Table 3.2 for the summary.

- The properties (conductivity, density, specific heat) of the construction material were obtained by referring to ISO 13786: 2017 – Thermal Performance of Building Components – Dynamic Thermal Characteristics – Calculation Methods [66] while measurable property like thickness were obtained manually. Thermal absorptance, solar absorptance, and visible absorptance were all left with *EnergyPlus* default values. See Table 3.2 for the summary.
- The window material properties were obtained by referring to the available data provided by *EnergyPlus*, it can be found in the “dataset” folder inside the installation folder of the software. Windows in SAFAD are generally made up of bronze-tinted glass. Bronze 3mm found in *EnergyPlus* dataset was used. See Table 3.3 for the summary. On the other hand, window area for each room were identified through walkthrough audits and are listed in the appendix.

Table 3.2 Building Construction Data

Construction	Thickness (Meter)	Conductivity (W/m-K)	Density (Kg/m³)	Specific Heat (J/kg-K)	Thermal Resistance (m²-K/W)
Inside Walls					
Plyboard	0.0127	0.13	500	1600	
Air gap					0.18
Plyboard	0.0127	0.13	500	1600	

Outside Walls					
Concrete	0.25	1.33	2000	1000	
Roof					
Concrete	0.25	1.33	2000	1000	
Floor					
Concrete	0.25	1.33	2000	1000	

Table 3.3 Window Properties Data

Window Material	U – factor (W/m²-K)	Solar Heat Gain Coefficient	Visible Light Transmittance
Bronze 3mm	5.894	0.729	0.685

- Lighting, equipment, occupants, and ACU details
 - Data regarding artificial lighting, equipment, and air conditioners were gathered through manual inspection of all the rooms in the building. See Table 3.4 for the summary and refer to the appendix for the details of all rooms.
 - Equipment
 - Computers and projectors were assumed to be turning ON only when there are classes in the room, if there are breaks in between classes then they were turned OFF. However, fans were assumed to be turning ON from start of the class for that room until the end of last class, no breaks were scheduled. These were observed during walkthrough audits. For all equipment found in all offices, the schedules were assumed to be from 8am to 5pm. Schedules from 2nd semester of school year 2018-2019 were the bases for all schedules.

- Equipment properties like fraction latent, radiant, and lost are left with *EnergyPlus* default values.
- Lighting
 - Lightings were scheduled to be turned ON only when there is a class going on in the room.
 - No dimming control was simulated
 - Return air fraction, fraction radiant, and fraction visible are 0, 0.27, and 0.23 respectively. These values are from *EnergyPlus* "InputOutputReference" documentation.
- Air conditioners
 - ACUs are scheduled to be turning ON from the start of the first class up to the end of the last class, these were observed during walkthrough audits. Second semester of school year 2018-2019 were the bases of all schedules.
 - The ACUs are split-type air conditioners with indoor unit of Trane Model No. 4MYW5524A1 and outdoor unit of Trane Model No. 4TYK5524A1000AA. Specification sheet was obtained and was considered as the bases for the *EnergyPlus* inputs. There are rooms that use different brands of ACUs but the model mentioned were used for the simulation because it was the most common model of ACU in the building. This is to reduce the complexity of the model.
 - The cooling setpoint was fixed to 26 degrees Celsius for all air-conditioned zones throughout the operation.
- Occupants
 - The details regarding the number of occupants and their schedules for all the lecture rooms were acquired from the University's data for 2nd semester of school year 2018-2019.

However, for all offices, it was assumed to have 10 persons from 8am to 5pm.

- People activity schedule for lecture rooms and offices are assumed to be 140 watts/person throughout the day. Value is from *EnergyPlus* “InputOutputReference” which was derived from 2005 ASHRAE Handbook of Fundamentals.
- Fraction radiant and sensible heat fraction will take the values of 0.46 and 0.61 respectively. These values are from ASHRAE Handbook of Fundamentals.

Table 3.4 Lighting, Equipment, and ACU summary

Equipment Specifications		Lighting Specifications		ACU Specifications	
Equipment	Wattage	Lighting	Wattage	ACU	Specifications
PC	100 watts	T5	36 watts	Indoor Unit	Trane Model No. 4MYW5524A1
Apple Computer	200 watts	Pin light	9 watts	Outdoor Unit	Trane Model No. 4TYK5524A1000AA
Fan	60 watts				
Projector	300 watts				
Refrigerator	77 watts				
Printer (standby)	20 watts				
TV	40 watts				
Water Dispenser	300 watts				
Laptop	40 watts				

- Zoning of the building
 - Zone is where there is a uniform temperature in the air circulating. For simple understanding, each room that is served with unique air conditioning unit is considered a “zone”. Floor

plan and walkthrough audits were the bases for zoning. Refer to appendix for the complete list of zones and their details.

3.1.2 Building Energy Modelling in EnergyPlus

For the geometry, *Euclid* – an extension for *SketchUp* was used. *Euclid* will act as a bridge between *EnergyPlus* and *SketchUp* that will give you freedom in drawing geometries at the same time convert the drawing immediately into an *EnergyPlus* – readable file. This will ease the drawing of the building geometry knowing that *EnergyPlus* do not have its own graphical user interface. See Figure 3.3. On the other hand, all other model parameters mentioned above are inputted in *EnergyPlus* using *EnergyPlus* IDF editor. *EnergyPlus* version 8.7.0 was used in this study. See Figures 3.4 and 3.5.

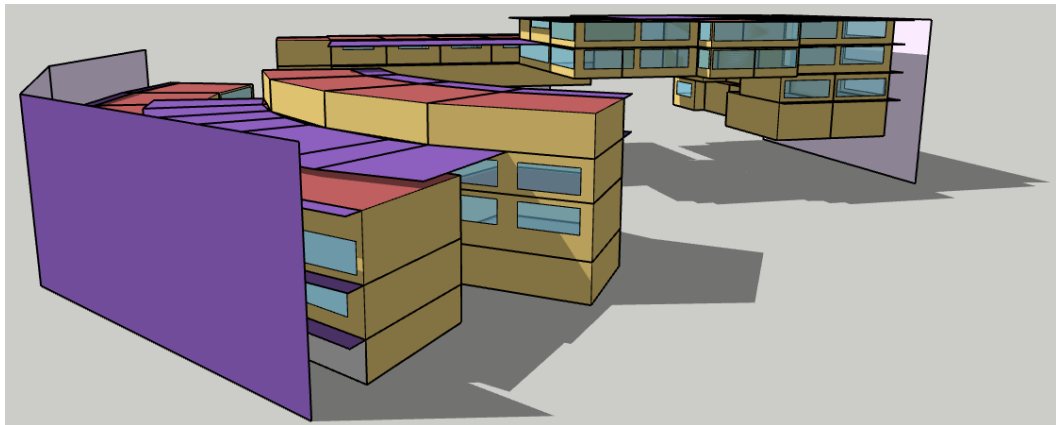


Figure 3.3 The Case Study Building drawn in SketchUp using Euclid Plugin

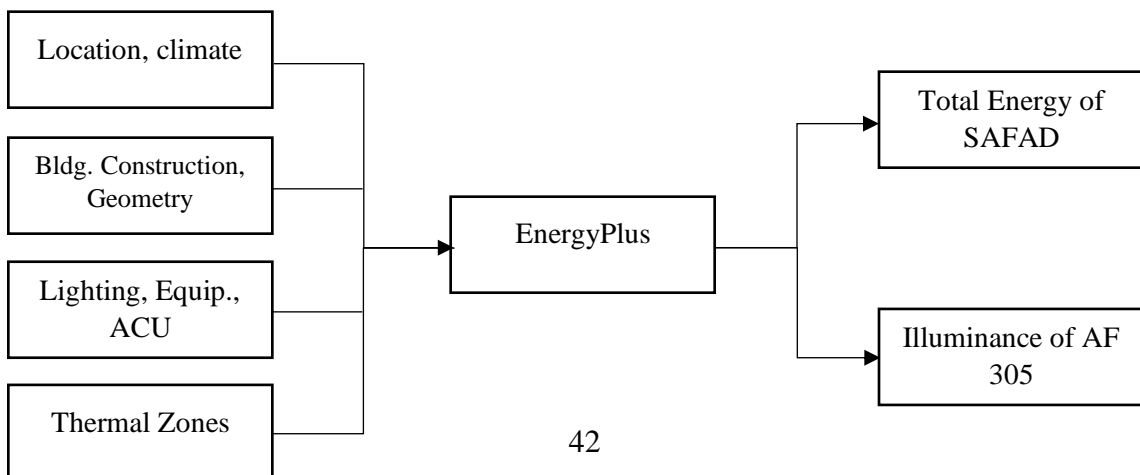


Figure 3.4 Modelling structure in EnergyPlus

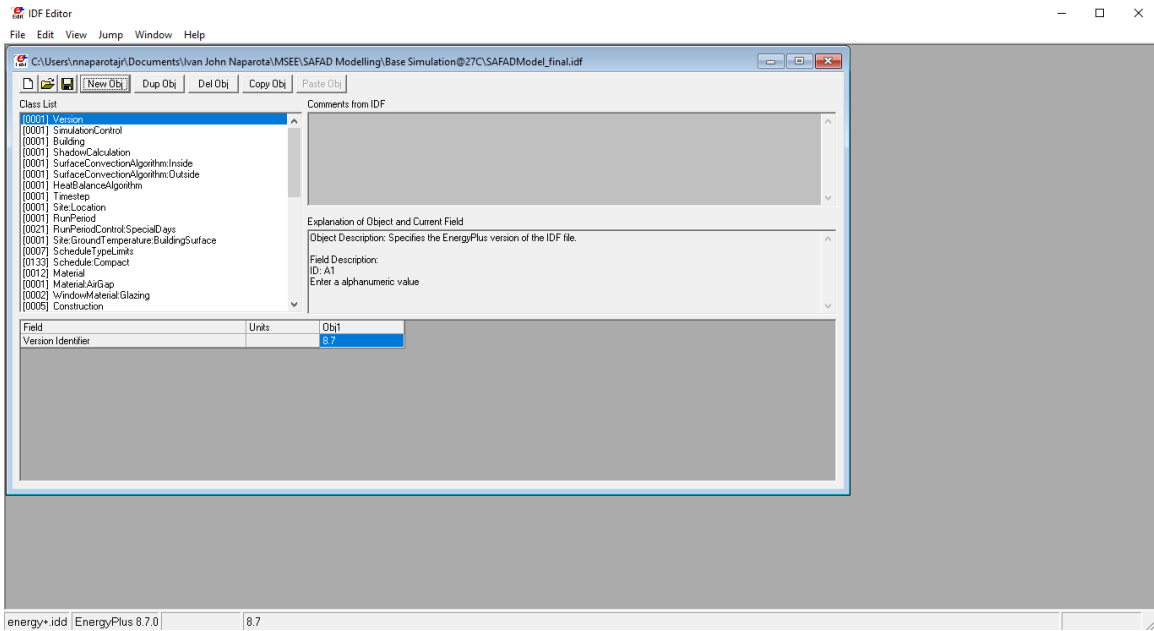


Figure 3.5 *EnergyPlus* IDF Editor where model parameters are inputted

The energy consumption utilized from the *EnergyPlus* simulation was the total energy consumption for the whole building for the month of April. For the illuminance, AF 305 was the only subject room and illuminance values for the whole October were extracted. Two reference points were simulated in room AF305. The first reference point is 4 meters away from the window and the next reference point is 8.26 meters away from the window. Both the reference points are 1.2 meters above the floor. Figure 3.6 shows the details of the placement of reference points. The placements of the reference points were referred from a study by Ochoa et. al [33] – one reference point is near and the other is far from the window which are both in the center line of the room. AF 305 was the chosen room for the data gathering of illuminance values because it was the most unshaded room from the entire building. All rooms from east, south, and west sides of the building were basically shaded with trees and only in the north side of the building are rooms with minimal shading from trees can be found. Out from the rooms in the north, AF 305 was the

farthest from any shading coming from trees. It has an existing window to wall ratio of 70%.

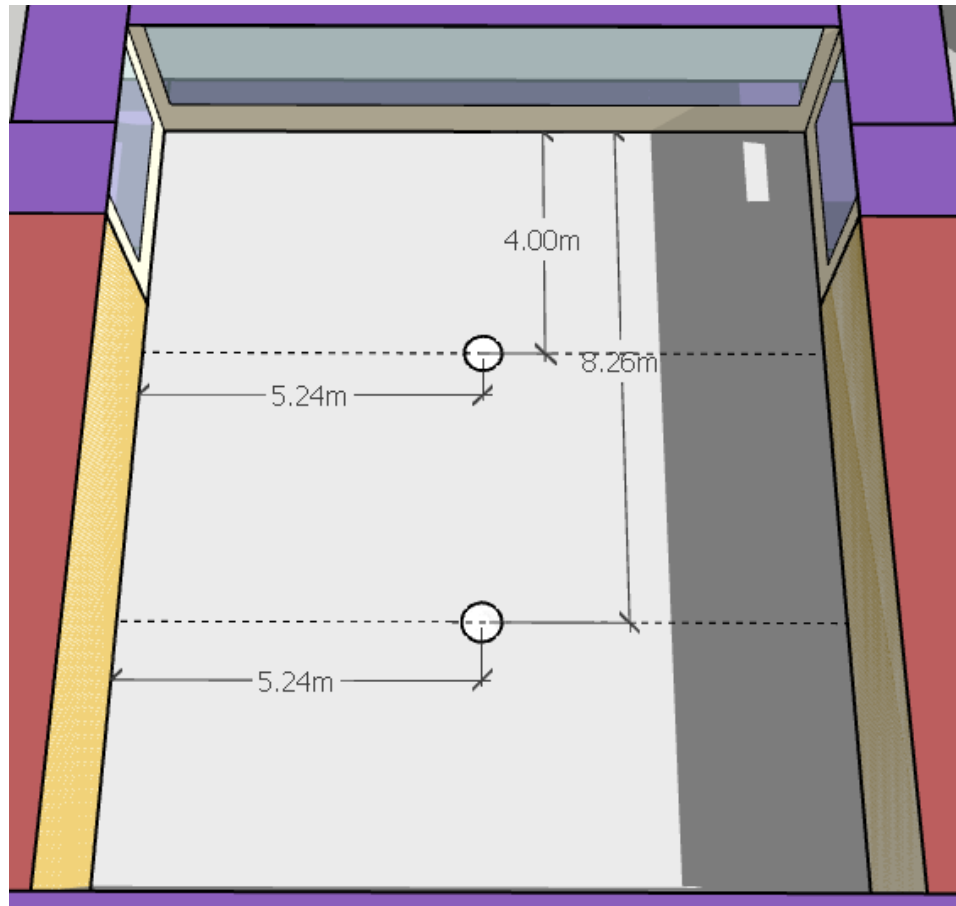


Figure 3.6 Reference Points in AF305

3.1.3 Simulation Results

After drawing the building geometry and inputting model parameters in *EnergyPlus*, a simulation was performed, then simulation outputs were extracted.

- Hourly total energy consumption
 - Hourly total energy demand of the whole building from 9AM to 9PM from April 1 to April 30 was extracted. There was a total of 390 datapoints. Since this simulated energy output will be used for calibrating the model, 9AM to 9PM were the only datapoints considered every day because the school

building only operates during this time. Energy consumption that will be measured by the energy meter not within this timeframe are subject to large uncertainties; e.g., appliances that are accidentally left open, usage that are unscheduled, etc. By doing this, calibration of the model with respect to some uncertain or variable energy usage can be avoided.

- Illuminance values
 - Hourly illuminance values from the two reference points were extracted from 9AM to 5PM every day for the whole month of October and were averaged hourly. As a result, there were only 9 datapoints in total for illuminance output.

3.1.4 Measuring Total Energy Consumption and Illuminance

- Total Energy Consumption
 - The building's total energy consumption from April 1 to April 30, 2019 were gathered by installing an energy meter that is capable of logging energy consumption of the building. The meter used was a three-phase meter with model EDMI MK10A, it was already calibrated by the distributor and has Energy Regulatory Commission (ERC) verification before it was acquired by the researcher of this study, so no further calibration was made.



Figure 3.7 Energy meter installed in the SAFAD Building

- Illuminance Values
 - Illuminance values were manually gathered from 9AM to 5PM starting from October 23 to October 26, 2019 using a digital lux meter. The reference points for the manual gathering of illuminance values were the same as the simulated reference points.
 - The digital lux meter used was BENETECH GM1020 and was calibrated by Micro Precision Calibration Cebu, Inc. The certificate of calibration and calibration report can be found in the appendix.



Figure 3.8 Illuminance Data Gathering

3.1.5 Comparison Between Simulated and Measured Energy and Illuminance

- Total Energy Consumption
 - The simulated hourly energy consumption of the building was compared to that of the measured energy consumption using Mean Bias Error (MBE) and Coefficient of Variation of the Root Mean Square (CV RMSE).

$$\text{▪ MBE} = \frac{\sum_{i=1}^n (m_i - s_i)}{\sum_{i=1}^n (m_i)}$$

Where: m_i and s_i are the measured and simulated total energy consumption for every datapoint (hourly from 9 AM to 9PM for the whole April was used for this study) and n is the number of data points (9AM to 9PM for thirty days equates to 390 datapoints all in all were considered in this study)

$$\text{▪ CV RMSE} = \sqrt{\frac{\sum_{i=1}^n (m_i - s_i)^2}{\frac{n}{\bar{m}}}}$$

Where: m_i and s_i are the measured and simulated total energy consumption for every instance (hourly from 9 AM to 9PM for the whole April was used for this study); n is the number

of data points (9AM to 9PM for thirty days equates to 390 datapoints all in all were considered in this study); and \bar{m} is the average of the measured data points.

- Goodness-of-fit criteria: maximum of 10% for MBE and maximum of 30% for CV RMSE. This is the threshold suggested by ASHRAE [55].
- Illuminance Values
 - It was mentioned in Chapter 2 of this paper that unlike energy outputs of building energy simulations, there are no existing indices on how to validate a simulation's environmental outputs like illuminance. But since MBE and CV RMSE are common statistical indices used for comparing simulation results to measured data, and were also used in some research papers for assessing simulated illuminance values [44], MBE and CV RMSE were still used for comparing measured and simulated illuminance values in this study. The same formulas were applied but the observations were hourly average illuminance values from 9AM to 5PM only, meaning, there were only 9 datapoints. There were no thresholds set for the two statistical indices, but the lesser MBE and CV RMSE means a better fit to the simulation.

3.2 Model Calibration

The second stage of this study is the model calibration. The building energy model made during the preliminary modeling will undergo a calibration procedure by tuning the uncertain parameters. The model parameters used in the preliminary modeling are only the parameters that are measurable and attainable given the available resources. But using a model that is based from first principles like *EnergyPlus* to model a system that is as complex as a building requires lots of parameters for it to compute its output. Aside from the fact that these parameters are a lot to measure, some of these parameters are hard to identify (e.g., air infiltration, equipment fraction radiant, ACU COP, etc.) and are very intrusive to the building occupants/activities when measured. That is why it is very hard to

measure everything to have a “perfect” representation of the system. If the building energy model will be used for studies suggesting possible improvements for a particular building, not taking into consideration the issue of uncertainties, then it will give a negative notion on the output of the study. That is why, model calibration has been a common practice not only in the field of building energy simulation, but also in other disciplines that uses computer simulations [51]. In the context of building energy simulations, model calibration can be seen as the tuning of model parameters so that the simulated outputs will have a good fit to measured data. The common approaches in model calibration found in the literature are carefully discussed in the Chapter 2 of this paper.

So far, there are no consensus guidelines set on how to calibrate a building energy simulation. The calibration procedure applied in this study does not necessarily mean that the real-world system and processes happening in the case study building will be replicated. But the calibration procedure performed in this study aims to provide a robust prediction and at the same time reduce uncertainty regarding the output of the study while staying methodical, rational, and computationally efficient. The calibration procedure applied in this study can be sequenced into: (1) tuning the visible light transmittance of windows to have a good illuminance reading (2) identifying uncertain parameters that are easy to manipulate in the building energy simulation program and their range of possible values; (3) reducing the number of uncertain parameters by choosing only the most influential ones with the use of Morris Method of screening parameters; (4) performing Monte Carlo simulation with an efficient sampling method using the most influential parameters to search for a number of solutions that will pass the goodness-of-fit criteria; (5) ranking all the solutions that passed the goodness-of-fit criteria and selecting a number of solutions that will be used for the search for optimum window to wall ratio.

3.2.1 Calibrating in terms of Illuminance

The model was tuned first so that it will give illuminance values that are close to measured values. This was performed by tuning the visible light transmittance of the windows. Visible light transmittance was the model parameter selected for tuning because

it will affect the amount of light that will enter a particular zone. There are other factors that can affect the illuminance calculation: the sky model used by *EnergyPlus*, the numerical method of computation underneath the software, the window orientation, the window size, and the window properties. Out from these factors, the window orientation, window size, and window properties are the only accessible parameters to tune, but out from these parameters, window properties are the only rational choice for tuning. Altering the window orientation and size to compensate for the difference in measured and simulated illuminance values will affect the reliability of the output of the study – optimum window size for every building orientation. Furthermore, out from all window properties, visible light transmittance is the only property that accounts for the amount of light to pass through a window. Therefore, the said parameter was the chosen parameter to tune. The value for this parameter is from 0 – 0.9 and was varied in a step of 0.1. The visible light transmittance value which will give the lowest MBE and CV RMSE will be applied in the model.

3.2.2 Calibrating in terms of Energy Consumption

After tuning the model in terms of illuminance, the calibrated model will further undergo a calibration procedure in terms of energy consumption. The parameters used in the calibration of model in terms of energy were parameters that do not have an impact on the illuminance calculation of the software. The procedure performed was carefully discussed in the following sections.

3.2.2.1 Uncertain Parameters and their Value Ranges

Model parameters that were not measured during the preliminary modeling and their possible range of values are identified heuristically. Some of these parameters were left with the default *EnergyPlus* values during the preliminary modeling; i.e., material thermal and solar absorptance, air gap thermal resistance, and equipment fraction radiant. Some are referred from ASHRAE Handbook of Fundamentals; i.e., people fraction radiant and activities, and light fraction radiant. Some are “wild” guesses; i.e., air infiltration, fan total efficiency, and pressure rise. While the COP is solved analytically using the air conditioner

datasheet.

Referring to Table 3.5, the “base” column contains the values for these parameters during the preliminary modeling. The “upper” and “lower” columns contain the maximum and minimum possible values for each parameter, these ranges are defined by *EnergyPlus*. Most likely, the “actual” values for each parameter are between these ranges which will theoretically, give the model a good fit to the measured data.

Table 3.5 Uncertain Parameters and their Values

	Uncertain Parameters	<i>Lower</i>	<i>Base</i>	<i>Upper</i>
X1	Concrete thermal absorptance	0.001	0.9	0.999
X2	Concrete solar absorptance	0	0.7	1
X3	Plywood thermal absorptance	0.001	0.9	0.999
X4	Plywood solar absorptance	0	0.7	1
X5	Air gap thermal resistance	0.001	0.18	1
X6	People fraction radiant	0	0.46	1
X7	People activity level computer lab	100	140	150
X8	People activity level offices	100	140	150
X9	People activity level lecture rooms	100	140	150
X10	Light fraction radiant	0	0.27	1
X11	Equipment fraction radiant	0	0	1
X12	Air Infiltration air changes/hour	0.1	1	6
X13	Fan total efficiency	0.3	0.5	0.9
X14	Pressure rise	30	75	120
X15	DXCoolingCoil COP	1	3	5

3.2.2.2 Morris Method of Ranking Parameters

The Morris Method of ranking parameters was employed in this study to reduce the number of uncertain parameters to be used for calibrating the model and was done by selecting only the parameters that are most influential to the model output. Since the calibration method to be used is a variant of Monte Carlo methods, having many parameters for tuning the model will result to a need for many simulations (could be in order of thousands) before having a “good” number of possible solutions as there will be a large number of total possible combinations. Seven parameters were chosen arbitrarily. For the

sake of comparison, considering 5 samples for each parameter, 7 parameters would equate to $5^7 = 78125$ total possible combinations, and for 15 parameters, there will be $5^{15} = 3.05 \times 10^{10}$ total possible combinations. That is 390,625 times as many total possible combinations of model parameters.

Though a package in R called “sensitivity” (*morris* function) was used in this study, the following section shows how the Morris method of ranking parameters was computed.

Considering k numbers of model parameters and scalar output Y .

$$Y = f(X_1, X_2, \dots, X_k)$$

The standardized effect of a positive or negative change (or step) denoted as Δ of a single parameter to the model output is calculated using Eq.1. This effect is called by Morris, Elementary Effect (EE) [64].

$$EE_i(X) = [y(X_1, X_2, \dots, X_{i-1}, X_i + \Delta, X_{i+1}, \dots, X_k) - y(X)] / \Delta \quad Eq. 1$$

Where Δ is the magnitude of step that is a multiple of $1/(p - 1)$; p is the number of “levels”, or is simply the number of possible samples for each parameter. One *EE* for each parameter needs one trajectory that translates to $k + 1$ number of simulation points that can easily be understood using Figure 2.7b in Chapter 2 of this paper. The number of *EE* denoted as r for each model parameter depends on the analyst and in the domain of building energy simulation, is mostly between 5-15 [61]. The total number of simulations will be equal to $(k + 1) * r$. The finite distribution of r *EE* for each parameter is denoted as F_i .

3.2.2.2.1 Morris Method Indices

Each F_i for each model parameter that contains r number of *EE* will be used to compute the indices. The original Morris method [64] suggests two indices: mean (μ_i) and standard deviation (σ_i) of r *EE*. The μ_i is the measure of sensitivity between i -th model parameter and model output which is associated to the model parameter’s effect [63], this can be computed using Eq.2.

$$\mu_i = \frac{\sum_{n=1}^r EE_n}{r} \quad \text{Eq. 2}$$

The greater the μ of a parameter, the higher its influence on the model output since this is the average of the standardized effects of a particular parameter on the model output. On the other hand, σ_i is the measure of the spread of $r EE$ for each parameter that can be computed using Eq.3., this measures possible interaction between model parameters or if a parameter has non-linear effect on the model output.

$$\sigma_i = \sqrt{\frac{1}{r} \sum_{n=1}^r (EE_n - \bar{u}_i)^2} \quad \text{Eq. 3}$$

For ranking influential parameters in monotonic models, μ_i may be enough, however, for non-monotonic models, the two indices should be carefully considered [67]. This is because, for these models, the distribution of F_i may contain negative and positive EE and may yield to a low value of μ even if the parameter is in fact influential or has large magnitudes of EE (regardless if its positive or negative). Furthermore, since Morris Method does not assume linearity, μ_i and σ_i should be both considered in preparation for possibility that the model is non-monotonic – a model parameter with negative and positive signs of EE may have a low value of μ but large value of σ [67].

But for the purpose of this study, an “improved” index denoted as (μ_i^*) suggested by Campolongo et. al. [67] was used and was computed using Eq. 4.

$$\mu_i^* = \frac{\sum_{n=1}^r |EE_n|}{r} \quad \text{Eq. 4}$$

Unlike μ_i , μ_i^* takes the absolute values of $r EE$, with this approach, the index will be free from any cancelation effects (negative output cancels positive and vice versa) which the original index, μ_i may experience. This index alone, is enough to rank the influence of model parameters to the model output which was the main purpose of employing this method in this study. The motivation of Campolongo et. al. in improving the index μ is the efficiency of considering both indices when dealing with complex models that has many

inputs and many outputs.

3.2.2.2.2 Building a Trajectory

Considering a model with k number of model parameters, the region of experimentation, ω , is a regular k -dimensional p -level grid. Again, the level, p , is the number of possible values from the set: $\mathbf{x} = \{0, 1/(p - 1), 2/(p - 1), 3/(p - 1), \dots, (p - 2)/(p - 1), 1\}$ that can be sampled from each model parameter. The magnitude of step, Δ , is a multiple of $1/(p - 1)$. A trajectory starts from a base point or the base values denoted as \mathbf{x}^* for k model parameters. For each parameter, its value is randomly chosen from the set of values, \mathbf{x} , but should only be from the range of 0 to $(1 - \Delta)$. This range is necessary so that if a magnitude of step, Δ , is added to \mathbf{x}^* , the next sample point will not be outside the region of experimentation, ω . The final matrix, \mathbf{B}^* , that defines the trajectory is defined by Morris [64] as:

$$\mathbf{B}^* = (\mathbf{J}_{m,1}\mathbf{x}^* + (\Delta) \left(\frac{1}{2}\right) [(2\mathbf{B} - \mathbf{J}_{m,k})\mathbf{D}^* + \mathbf{J}_{m,k}])\mathbf{P}^* \quad \text{Eq. 5}$$

The $\frac{1}{2} [(2\mathbf{B} - \mathbf{J}_{m,k})\mathbf{D}^* + \mathbf{J}_{m,k}]$ part of the equation defines the random direction of the trajectory (negative or positive) [63]. \mathbf{D}^* is k -dimensional diagonal matrix in which each element in the diagonal have equal probability of taking a value of either positive or negative 1; $\mathbf{J}_{m,k}$ is an $(m \times k)$ dimensional matrix of 1's, where $m = k + 1$; \mathbf{B} is an $(m \times k)$ dimensional sampling matrix containing only 0's and 1's and is arranged that it forms a lower triangular matrix in the lower left; \mathbf{P}^* is a permutation matrix that has exactly one entry of 1 for each row and each column. This permutes the columns of the matrix defined by $(\mathbf{J}_{m,1}\mathbf{x}^* + (\Delta) \left(\frac{1}{2}\right) [(2\mathbf{B} - \mathbf{J}_{m,k})\mathbf{D}^* + \mathbf{J}_{m,k}])$ since matrix \mathbf{P}^* is post-multiplied to it, this shuffles the perturbations across all model parameters. *Note: the randomization of values for each element of \mathbf{D}^* , \mathbf{x}^* , and \mathbf{P}^* is independent from other elements.* The final matrix that defines the trajectory, \mathbf{B}^* , should be an $(m \times k)$ dimensional matrix wherein each row represents the combination of values for all model parameters for a single simulation. Furthermore, \mathbf{B}^* matrix is used to compute one *EE* for each model parameter as defined in Eq. 1. Finally, the design matrix, \mathbf{X} , is composed of r \mathbf{B}^* matrices which are constructed

independently that will result in r number of EE for each parameter that will be used to solve the index defined in Eq. 4.

3.2.2.3 Latin Hypercube Monte Carlo

After screening the most influential parameters using Morris sensitivity analysis, the values for each influential parameter was searched randomly within its range using a variant of Monte Carlo methods which is Latin Hypercube Monte Carlo. R, a software for statistical computing was used in performing Latin Hypercube Monte Carlo.

Latin Hypercube Monte Carlo (LHMC) was employed in this study to produce multiple calibrated models as there are many possible combinations of values of the parameters that could make the model perform well. It was the aim of the calibration procedure to produce multiple calibrated models and be used in the optimization process to provide a robust conclusion on the optimum window to wall ratio. Instead of using one calibrated model, 5 different calibrated simulations were used to know the optimum window to wall ratio which is common to all models. There were only 5 calibrated simulations considered, as this study does not aim to quantify a range of variability, rather, it is viewed as a problem of “is the optimum window to wall ratio consistent even with different model parameters?”.

LHMC is a form of stratified sampling without replacement and without the necessity for pre-defining probability distribution in each “strata”. Considering k number of model parameters, $x = [x_1, x_2, x_3, \dots, x_k]$, a sample size n for each parameter needs to be determined. The range of possible values for each parameter, x_i , is then divided into n non-overlapping “strata” with equal probability, $1/n$. One value for each “strata” is then selected randomly with respect to the probability density function in that “strata”. Therefore, n number of values are obtained for each x_i . The n values obtained for x_1 are paired in random with the n values of x_2 , this pair of values are again paired in random with the n values of x_3 and so on until n k -tuples is formed.

The type of distribution for each parameter depends on the user. Reddy et. al. [54]

suggested to apply triangular distribution if the user have a best guess value of the parameter and is confident about it. But if the only certain thing is the range of possible values, then uniform distribution (which is easier to apply than triangular) would suffice.

3.3 Optimum Window to Wall Ratio Search

The final stage of this study is to determine the window to wall ratio for every building orientation that will result to the least cooling and lighting energy consumption, at the same time exploit the right amount of daylight.

During the optimization process, the building was first divided into four sections which represent one building orientation each (building north, east, south, and west). Figure 3.9 shows the sectioning of the building for the optimization process. To avoid misconceptions, note that the SAFAD building is 15 degrees East of true North, therefore, the North in the Figure is really 15 degrees shifted to the East from the true North. The building was not shifted to align to the true North so that the result of this study will be highly relevant to the building being studied. The rooms selected were rooms in the building that really have windows facing to the specified orientation. The rooms that belong to the East section (yellow x-mark) were the rooms used to find the optimum window to wall ratio for building East, the rooms belonging to North section (pink x-mark) for North, and so on. Also, the figure is a top view image, so there are rooms not captured in the image but were used for the optimization.

Looking at the Figure, aside from the East-facing rooms, there were rooms that have windows facing two different directions (South and West, North and West), concerns may arise if the window facing the other direction has an effect on the optimum window to wall ratio for the other orientation; for example, is the optimum window to wall ratio for the building North still the same if the size of the windows facing the building West was changed? To consider this concern, North, South, and West were optimized differently compared to East. The succeeding sections explain this in full details.

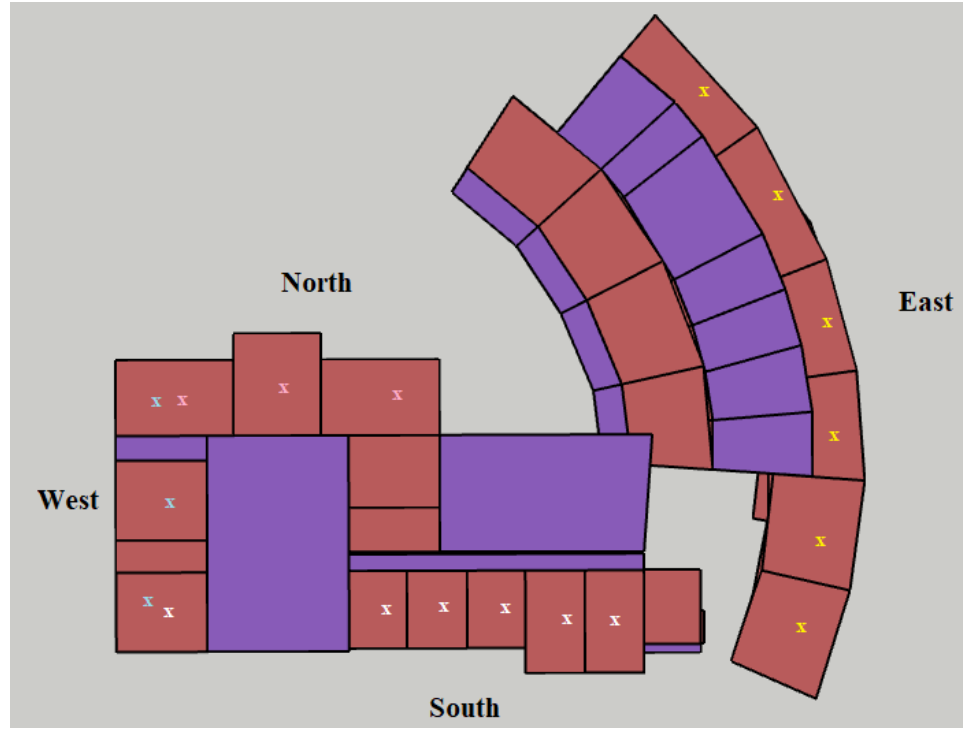


Figure 3.9 Sectioning of the Building

3.3.1 East-Facing Windows

There were five different window to wall ratios (WWR) simulated – 20%, 35%, 50%, 65%, and 80%. Each WWR corresponds to a single simulation, thus, there were 5 simulations in total for each model (as there were 5 calibrated models considered). Aside from the WWR, other important conditions for each simulation were:

- ✓ Electric lighting control system (continuous off dimming control) was simulated in *EnergyPlus* to know how much electrical energy for lighting was needed to compensate for the difference between the daylight illuminance level and the illuminance setpoint. The illuminance setpoint was set to 500 lux.
- ✓ Illuminance reference point was set 4 meters from the center of the window (this was the same distance applied in the calibration of model in terms of illuminance) and 0.8 meters above the floor. Note: only one reference point was considered because of the problem of *EnergyPlus* when dealing with reference points far from windows.

- ✓ Run period was set to January 1 to December 31 to have one-year worth of observations.
- ✓ The output of the simulation was set to return cooling energy consumptions and illuminance values for all rooms analyzed.

After each simulation, three performance indicators were computed:

- Total energy consumption for all rooms, E_{TOT} , which was computed using Eq. 6.

$$E_{TOT} = E_{LIGHTING} + E_{COOLING} \quad \text{Eq. 6}$$

Where: $E_{LIGHTING}$ is the total lighting energy consumption and $E_{COOLING}$ is the total cooling energy consumption.

- Useful Daylight Illuminance 500-2000lux, $UDI_{500-2000}$ was computed using Eq. 7.

$$UDI_{500-2000} = \frac{\text{No.of hours in 1 year Illuminance is within } 500\text{--}2000\text{lux}}{\text{Number of daylighting hours in 1 year}} \quad \text{Eq. 7}$$

- Useful Daylight Illuminance >2000lux, $UDI_{>2000}$ was computed using Eq. 8.

$$UDI_{>2000} = \frac{\text{No.of hours in 1 year Illuminance is beyond } 2000\text{lux}}{\text{Number of daylighting hours in 1 year}} \quad \text{Eq. 8}$$

For both UDI computations, since there were many rooms considered, the illuminance levels considered were average of the hourly illuminance levels of all the rooms. In addition, simulating only 5 different WWR values gives only 5 discrete values of the three metrics and the WWR values within the 15% step were not covered. As an answer to this, cubic spline interpolation was performed for the three functions: E_{TOT} (WWR); $UDI_{500-2000}$ (WWR); and $UDI_{>2000}$ (WWR) using *spline* function in R Software.

3.3.1.1 Rooms Analyzed and Computing WWR

The rooms analyzed for the east facing windows were: AF1B12F; AF1B12E; AF1B12D; AF1B12C; AF1B12B; AF1B12A; CB1; CB2; CB3; and CB4. The room details were already given in the Chapter 2 of this paper.

WWR was defined in this study as the ratio of transparent area to gross exterior

wall area – gross exterior wall area is simply the “length*width” area of the wall. Figures 3.10 – 3.14 provide screenshots on how WWR were computed for each simulation and how windows were placed in the walls.

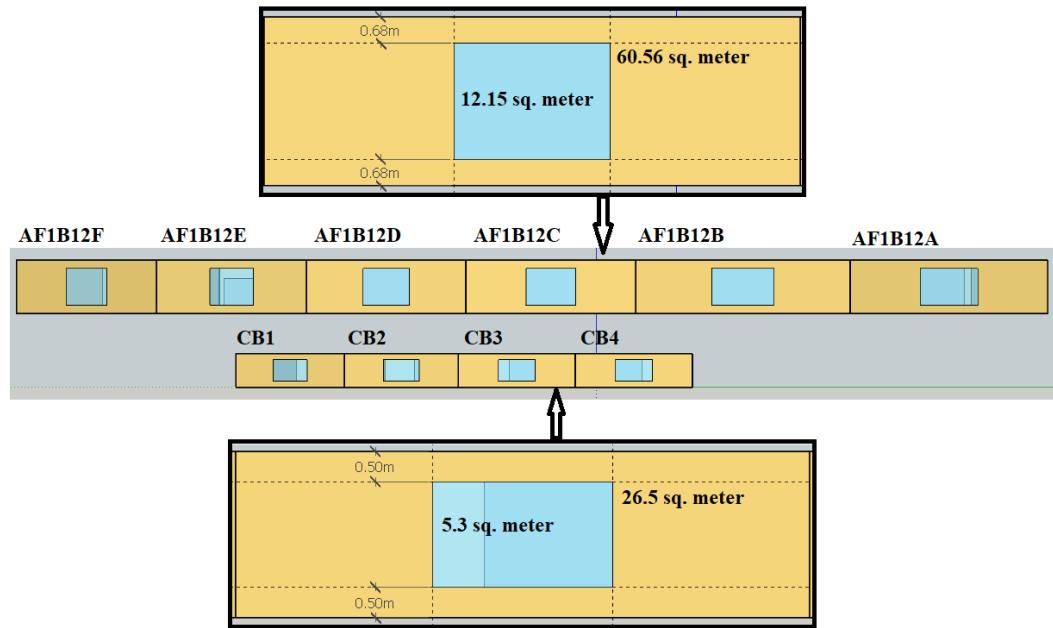


Figure 3.10 20% WWR for East

Figure 3.10 shows how 20% WWR for each room was achieved. For AF1B12F to AF1B12A, the windows were placed 0.68 meters above the floor and 0.68 meters below the ceiling. For rooms CB1 to CB4, the windows were placed 0.50 meters below the ceiling and 0.50 meters above the floor. The widths of all windows depend on the area of the wall to achieve WWR of 20%. Each window was placed in the center of each wall’s side edges.

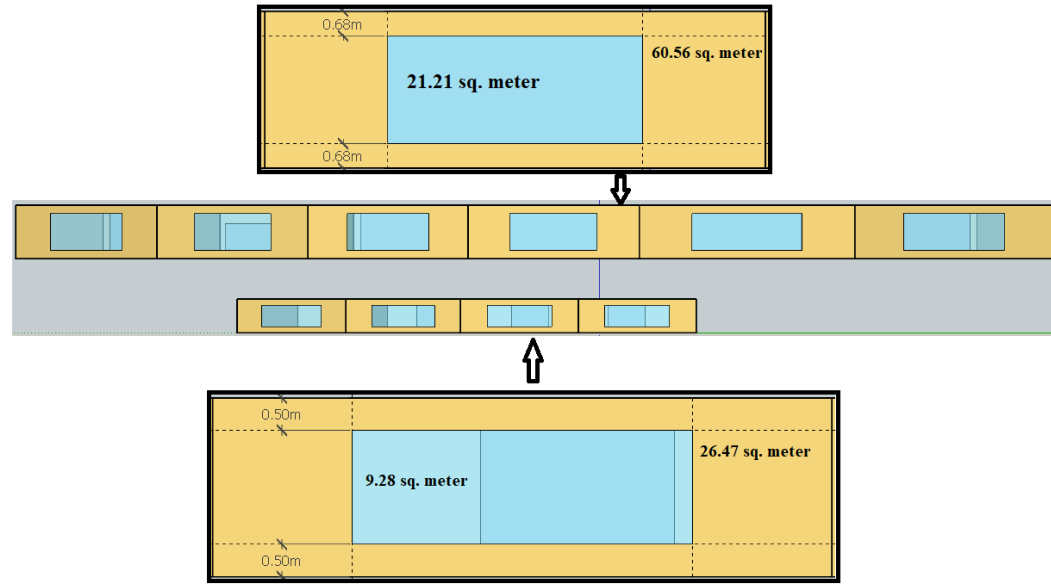


Figure 3.11 35% WWR for East

Same way for 35% WWR as shown in Figure 3.11, the windows for AF1B12F to AF1B12A were placed 0.68 meters below the ceiling and above the floor, and for CB1 to CB4, the windows were placed 0.5 meters below the ceiling and above the floor. The width depends on the wall area to achieve 35% WWR. Each window was placed in the center of each wall's side edges.

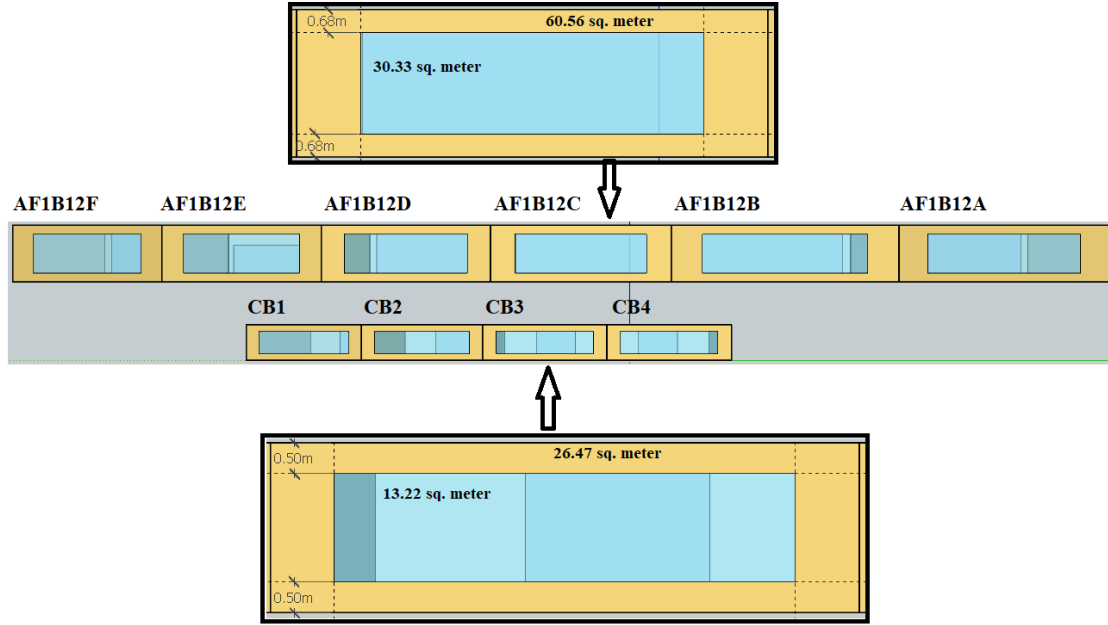


Figure 3.12 50% WWR for East

The same way for 50% WWR as shown in Figure 3.12, the windows for AF1B12F to AF1B12A were placed 0.68 meters below the ceiling and above the floor, and for CB1 to CB4, the windows were placed 0.5 meters below the ceiling and above the floor. The width depends on the wall area to achieve 50% WWR. Each window was placed in the center of each wall's side edges.

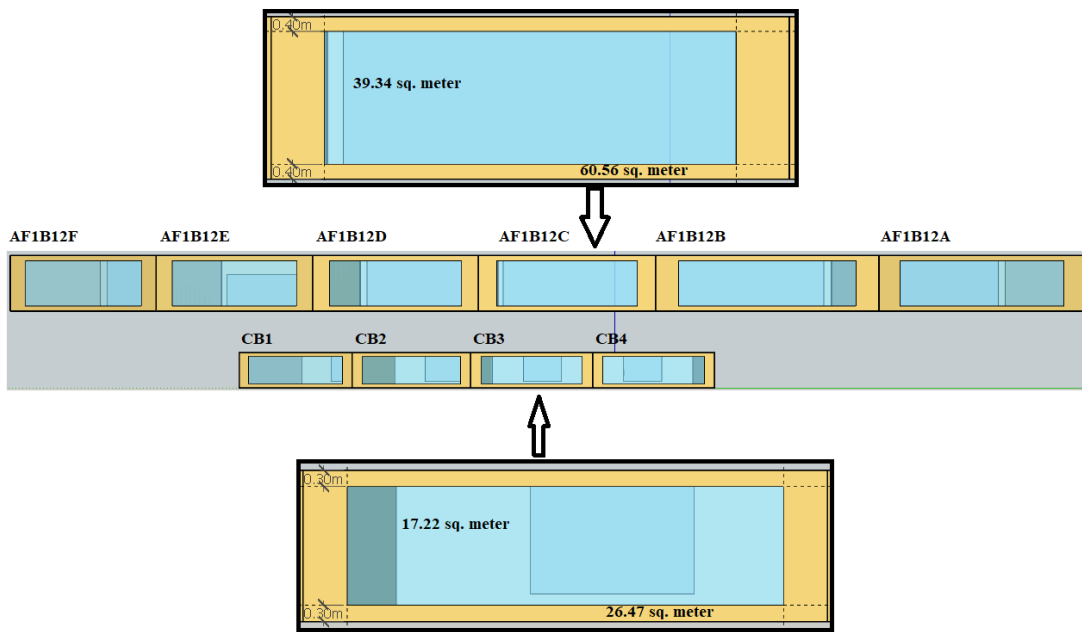


Figure 3.13 65% WWR for East

Figure 3.13 shows how 65% of WWRs for all rooms were achieved. For rooms AF1B12F to AF1B12A, the windows were placed 0.4 meter below the ceiling and above the floor. For rooms CB1 to CB4, windows were placed 0.3 meter below the ceiling and above the floor. The widths for the windows were computed to have 65% WWR for each room. Each window was placed in the center of each wall's side edges.

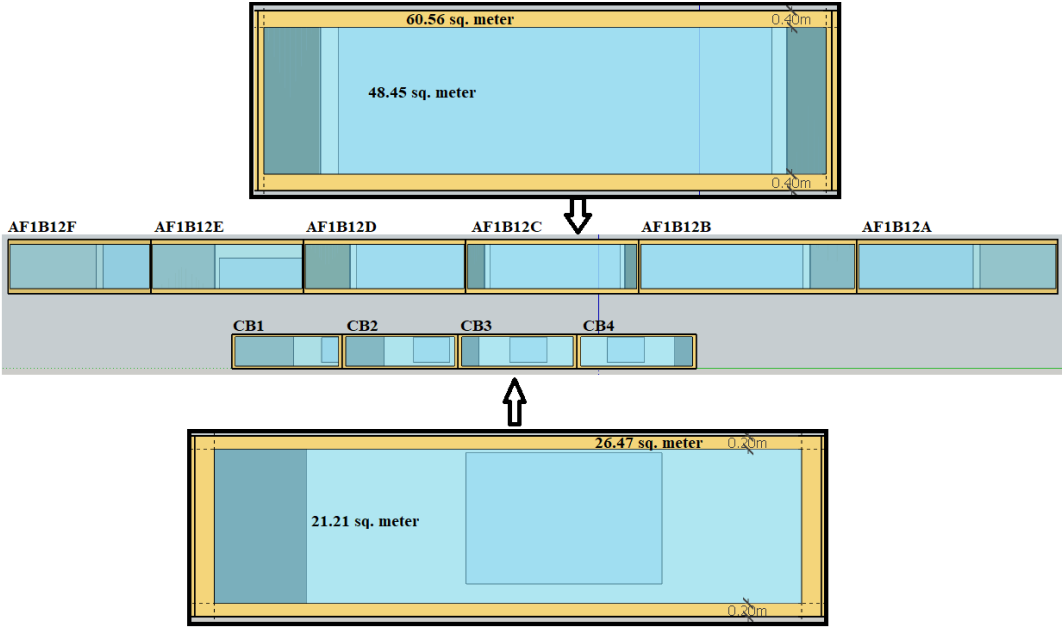


Figure 3.14 80% WWR for East

Finally, Figure 3.14 shows how 80% WWR was simulated. For AF1B12F to AF1B12A, the windows were placed 0.4 meter above the floor and 0.4 meter below the ceiling. For rooms CB1 to CB4, the windows were placed 0.2 meter above the floor and 0.2 meter below the ceiling. The widths were determined depending on the area of each wall to have 80% WWR. Each window was placed in the center of each wall's side edges.

3.3.1.2 Choosing the Optimum WWR

Three metrics were viewed in the assessment of the different WWR: E_{TOT} , which was computed using Eq. 6; $UDI_{500-2000}$, which was computed using Eq. 7; and $UDI_{>2000}$, which was computed using Eq. 8.

To be considered optimum, these criteria were needed to be met:

Criteria 1: Total energy consumption, E_{TOT} , should be minimized for the five different calibrated models while;

Criteria 2: $UDI_{500-2000}$ should be maximized; and

Criteria 3: $UDI_{>2000}$ should be less than or equal to 20%

There should be an agreement among the five different models used on the WWR that gave the least total energy consumption, E_{TOT} , to test the robustness of the optimum WWR. The consistency of UDIs was not tested since all five different models differ only in parameters that have effects on the energy consumption and not in illuminance.

Furthermore, though thresholds for UDI are not standardized, it is understandable that $UDI_{500-2000}$ should be at a higher percentage since this would mean that daylight was exploited properly. On the other hand, since $UDI_{>2000}$ is the measure of illuminance level over 2000 lux, this should be minimized to not cause visual discomfort in the building occupants. Goia et. al. [14] suggests a threshold of at least 50% for $UDI_{500-2000}$ and at most 20% for $UDI_{>2000}$. The threshold of at most 20% for $UDI_{>2000}$ suggested by the mentioned researcher above was applied in this study. However, setting an exact minimum percentage for $UDI_{500-2000}$ may not be a logical thing to do when studying an existing building since the amount of daylight that will enter the building space highly depends on the positioning of the real building and the existing material of the windows present in the real building.

3.3.2 North and South-Facing Windows

The optimization process performed for north and south-facing windows was generally the same for east-facing windows, the only difference is the number of simulations performed. Again, there were five WWR values simulated with the same simulation conditions and the same outputs computed. But this time, the WWR of west-facing windows were changed for every set of the five WWR of south and north, this translates to a total of 125 simulations for north and the same number of simulations for south – 5 west WWR * 5 south/north WWR * 5 calibrated models. This was done because there are rooms that have both south and west-facing windows and also north and west-facing windows, there is a possibility that the optimum WWR for south and north-facing windows is affected with the WWR of the connected west-facing windows.

The same conditions for each simulation was followed, the same outputs were

computed for each simulation, and the same metrics were considered in concluding to the optimum WWR

3.3.2.1 Rooms Considered and WWR Computations for North

The rooms used for analyzing north facing windows were AF 306, Architecture Faculty Room, Architecture Department, Dean's Office, SAFAD Conference Room, AF 304, Auxiliary Offices, AF 101, and AF 102. All rooms have a total floor area of 884.51 sq. meter, and all were air conditioned. Again, WWR was computed as the ratio between the transparent area and the gross exterior wall area. Figures 3.15 to 3.19 present the placements of the windows for each WWR in north.

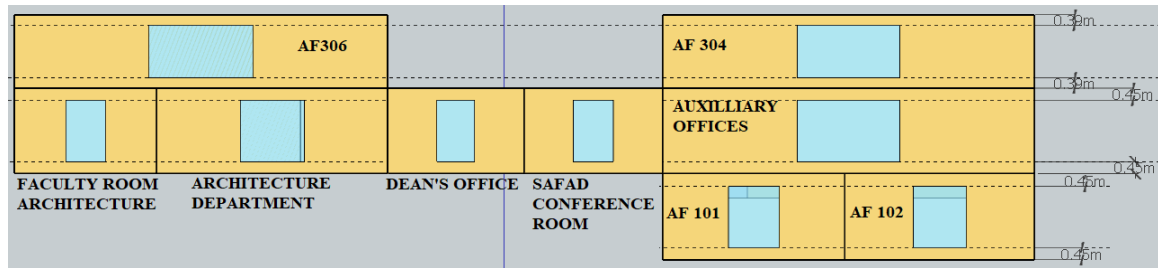


Figure 3.15 20% WWR for North

For 20% WWR, windows for AF 306 and AF 304 were placed 0.39 meter below the ceiling and above the floor, then each width was at the center of the wall width computed to have a WWR of 20%. For the rest of the rooms, their windows were placed 0.45 meter below the ceiling and above the floor, then each window width was at the center of the wall width computed to have a WWR of 20%. Refer to Figure 3.15.

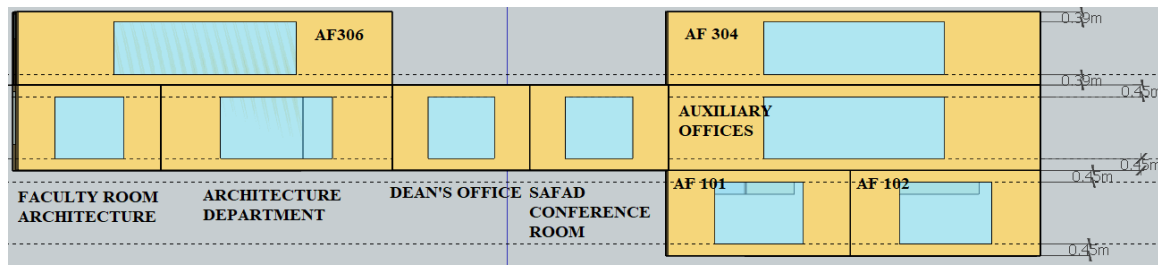


Figure 3.16 35% WWR for North

The same distances from the ceilings and floors were followed for 35% WWR, only

each window's width was different, which was computed to have 35% WWR. See Figure 3.16.

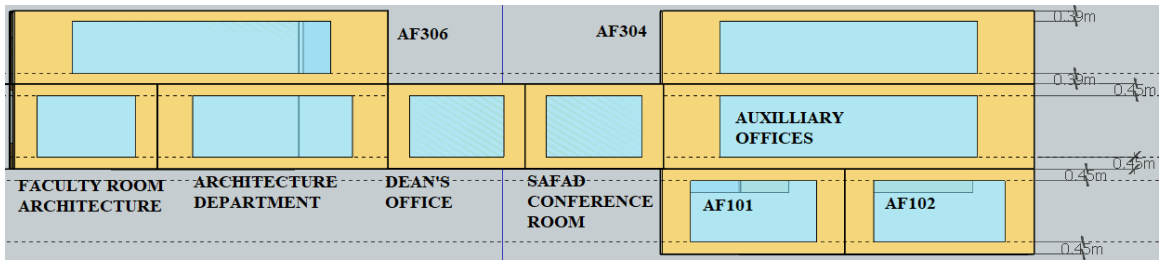


Figure 3.17 50% WWR for North

The same distances from the ceilings and floors were followed for 50% WWR, only each window's width was different, which was computed to have 50% WWR. See Figure 3.17.

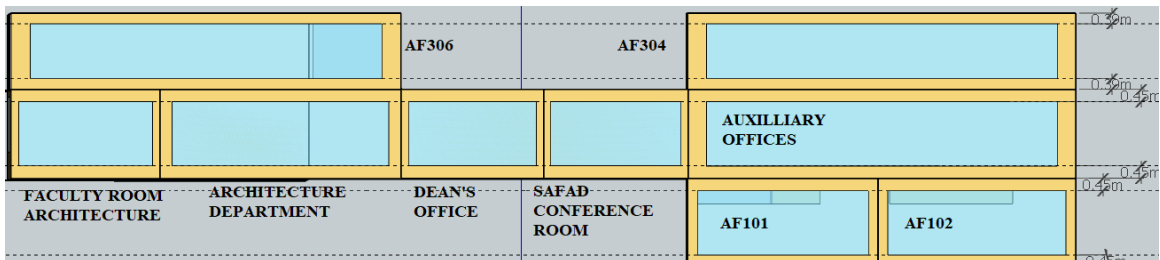


Figure 3.18 65% WWR for North

The same distances from the ceilings and floors were followed for 65% WWR, only each window's width was different, which was computed to have 65% WWR. See Figure 3.18.

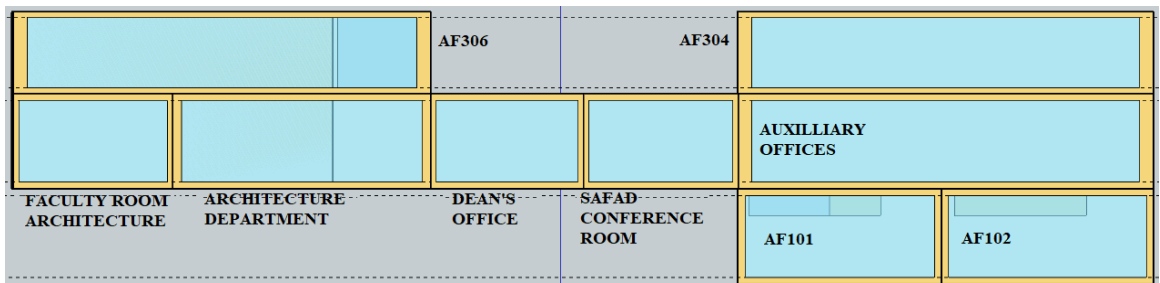


Figure 3.19 80% WWR for North

For 80% WWR, windows for AF 306 and AF 304 were placed 0.20 meter below the ceiling and above the floor, then each width was at the center of the wall width computed to have a WWR of 80%. For the rest of the rooms, their windows were placed 0.23 meter below the ceiling and above the floor, then each window width was at the center of the wall width computed to have a WWR of 80%. Refer to Figure 3.19.

3.3.2.2 Rooms Considered and WWR Computations for South

The rooms used for analyzing south-facing windows were IPD, Fine Arts Department, Guidance Office, Guidance Counselor, AF 207, AF 208, AF 209, AF 210, and AF 211. All rooms have a total floor area of 685.7 sq. meter and were air conditioned. The WWR was also computed as the ratio between the transparent area and the gross exterior wall area. Figures 3.20 to 3.24 present the placements of the windows for each WWR in south.

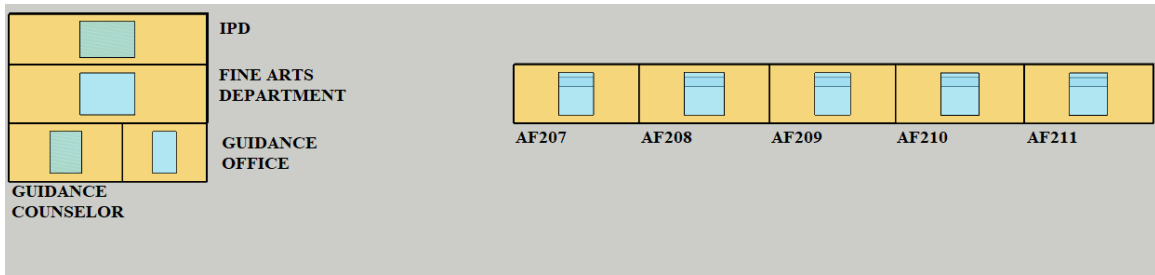


Figure 3.20 20% WWR for South

For 20% WWR, windows for AF 207, AF 208, AF 209, AF 210, AF 211, Fine Arts Department, Guidance Office, and Office of the Guidance Counselor were placed 0.45 meter below the ceiling and above the floor, then each width was at the center of the wall width computed to have a WWR of 20%. For IPD, its window was placed 0.39 meter below the ceiling and above the floor, then the window width was at the center of the wall width computed to have a WWR of 20%. Refer to Figure 3.20.



Figure 3.21 35% WWR for South

The same distances from the ceilings and floors were followed for 35% WWR, only each window's width was different, which was computed to have 35% WWR. See Figure 3.21.

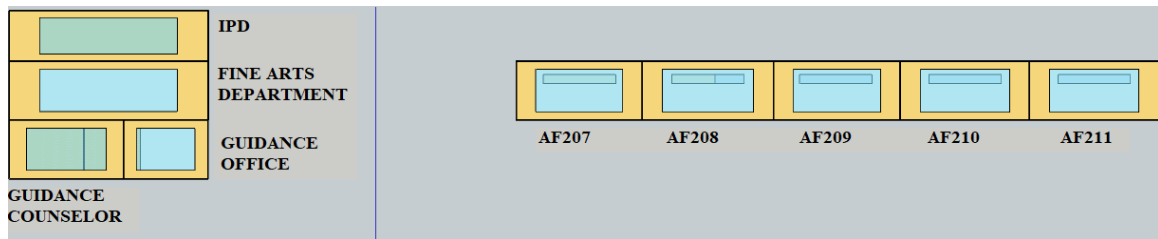


Figure 3.22 50% WWR for South

The same distances from the ceilings and floors were also followed for 50% WWR, only each window's width was different, which was computed to have 50% WWR. See Figure 3.22.

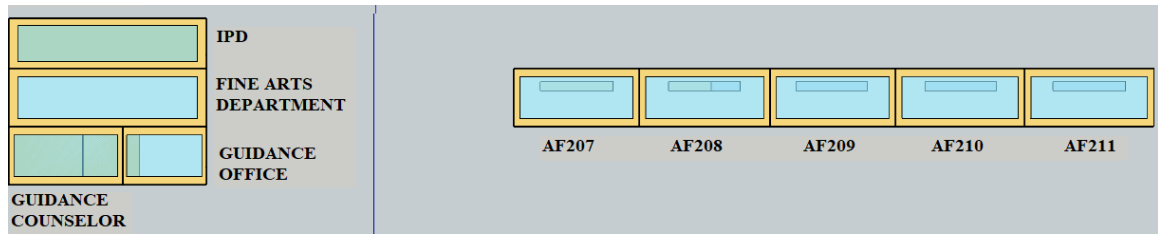


Figure 3.23 65% WWR for South

The same distances from the ceilings and floors were also followed for 65% WWR, only each window's width was different, which was computed to have 65% WWR. See Figure 3.23.

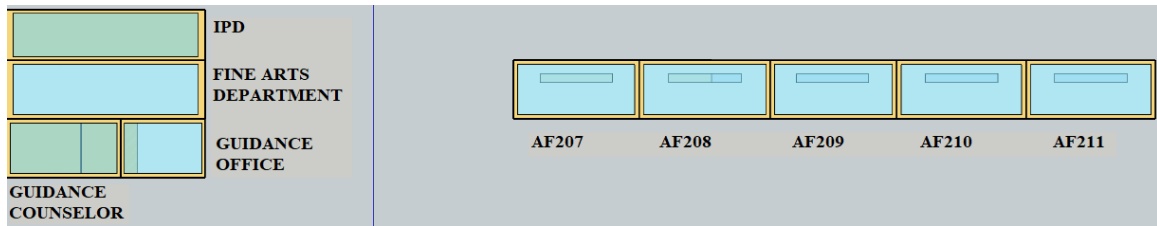


Figure 3.24 80% WWR for South

For 80% WWR, windows for AF 207, AF 208, AF 209, AF 210, AF 211, Fine Arts Department, Guidance Office, and Office of the Guidance Counselor were placed 0.23 meter below the ceiling and above the floor, then each width was at the center of the wall width computed to have a WWR of 80%. For IPD, its window was placed 0.20 meter below the ceiling and above the floor, then the window width was at the center of the wall width computed to have a WWR of 80%. Refer to Figure 3.24.

3.3.3 West Facing Windows

Since there are rooms that have both west and south/north facing windows, the WWR for south and north facing windows should be carefully selected during the optimization process for west-facing windows. This is because there is a possibility that the optimum WWR for west will depend on what WWR were applied for south and north since there are zones that connect west and north/south windows. In this study, the WWR for south and north were set to their most optimum WWR during the optimization process of west-facing windows. This was done to minimize the number of simulations during the optimization of west-facing windows. Exploring all possible combinations of west, north, and south will equate to a total of 625 possible combinations which is equal to the number of simulations since there are 5 different models used (5 west WWR * 5 south WWR * 5 north WWR * 5 models). The approach applied in this study may not be enough when trying to draw a general conclusion of the most optimum WWR of west-facing windows which could be applicable to many different buildings in the Philippines, but this is believed to be enough for the purpose of this study since this study is contextualized for the case study building. And the priority of this study is to optimize the WWR of the case study building.

As mentioned, the WWR for south and north were fixed to their most optimum WWR. And five WWR for west-facing windows were simulated: 20%, 35%, 50%, 65%, and 80%. The same conditions for the simulations applied during the optimization of other building orientations were applied, the same outputs were computed, and the same metrics were used to conclude to the optimum WWR. The computation of WWR are presented below.

3.3.3.4 Rooms Considered and WWR Computations for West

The rooms used for optimizing west-facing windows were AF 304, Auxiliary Office, AF 102, VPPF, Fine Arts Faculty Room, AF 103, AF 104, Office of the Guidance Counselor, Fine Arts Department, and IPD. All rooms were air conditioned. The WWR was computed as the ratio between the transparent area and the gross exterior wall area. Figures 3.25 to 3.29 present the placements of the windows for each WWR in west.

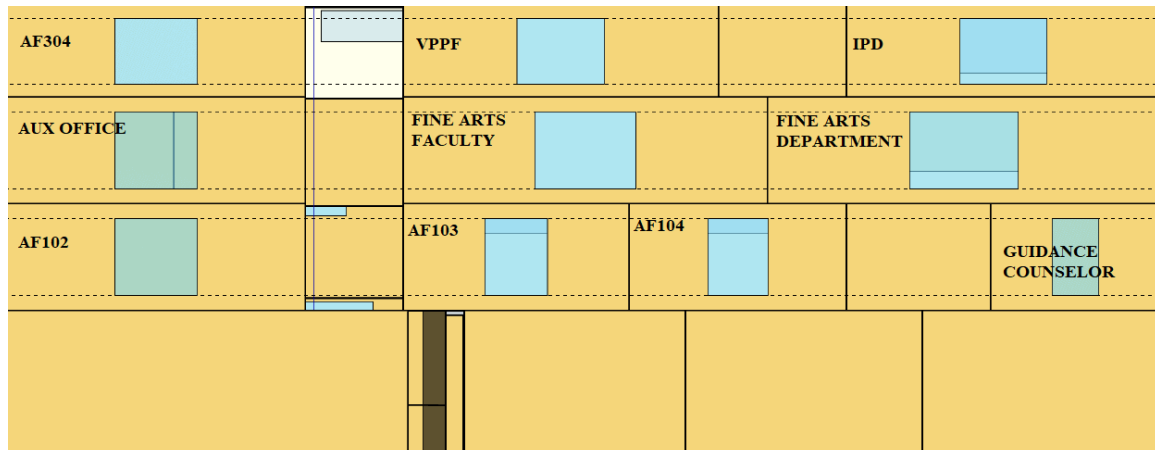


Figure 3.25 20% WWR for West

For 20% WWR, windows for AF 304, VPPF, and IPD were placed 0.39 meter below the ceiling and above the floor, then each width was at the center of the wall width computed to have a WWR of 20%. For the rest of the rooms, the windows were placed 0.45 meter below the ceiling and above the floor, then the window width was at the center of the wall width computed to have a WWR of 20%. Refer to Figure 3.25.

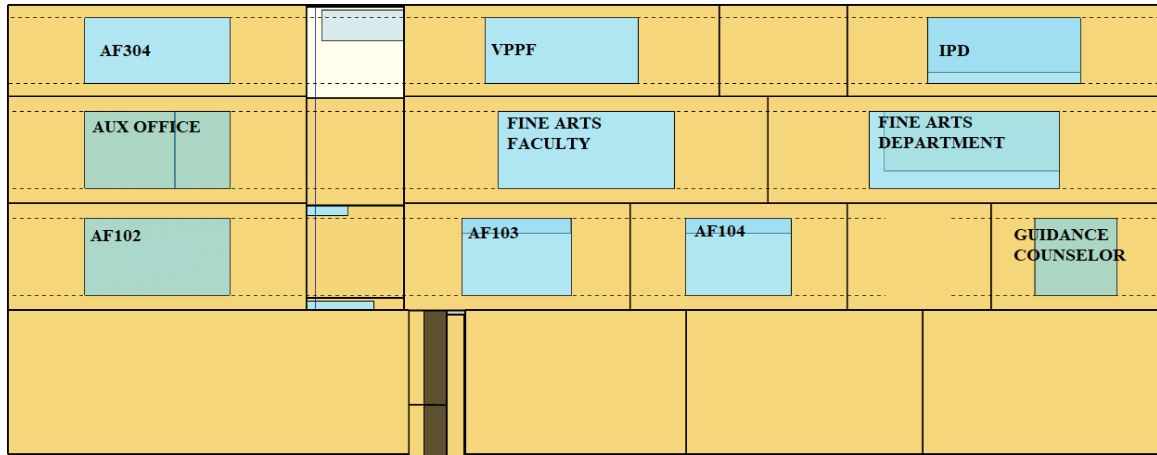


Figure 3.26 35% WWR for West

The same distances from the ceilings and floors were followed for 35% WWR, only each window's width was different, which was computed to have 35% WWR. See Figure 3.26.

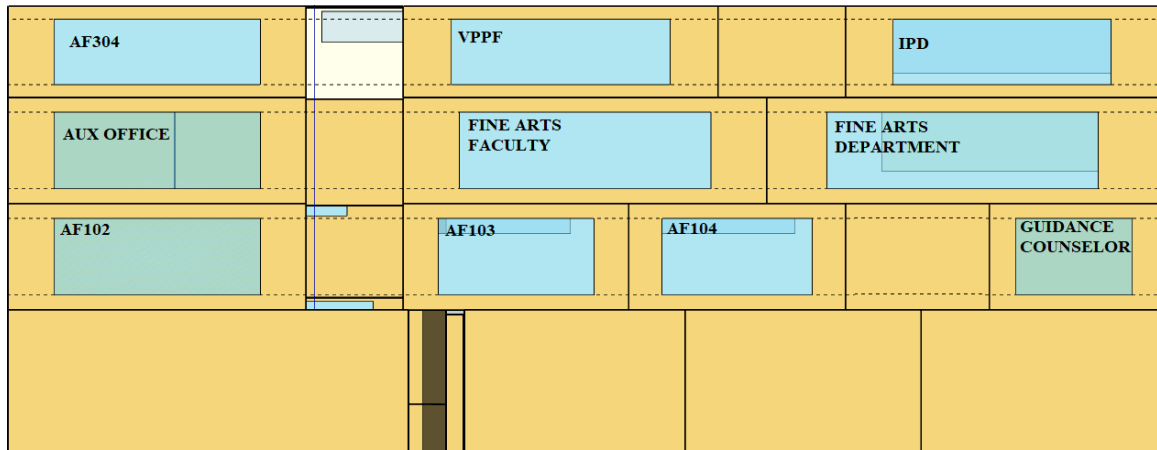


Figure 3.27 50% WWR for West

The same distances from the ceilings and floors were also followed for 50% WWR, only each window's width was different, which was computed to have 50% WWR. See Figure 3.27.

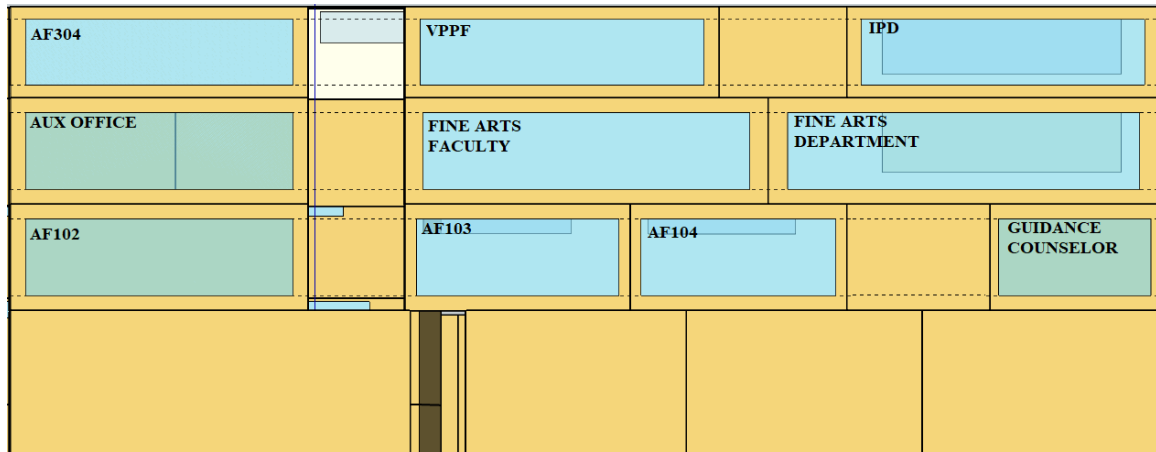


Figure 3.28 65% WWR for West

The same distances from the ceilings and floors were also followed for 65% WWR, only each window's width was different, which was computed to have 65% WWR. See Figure 3.28.

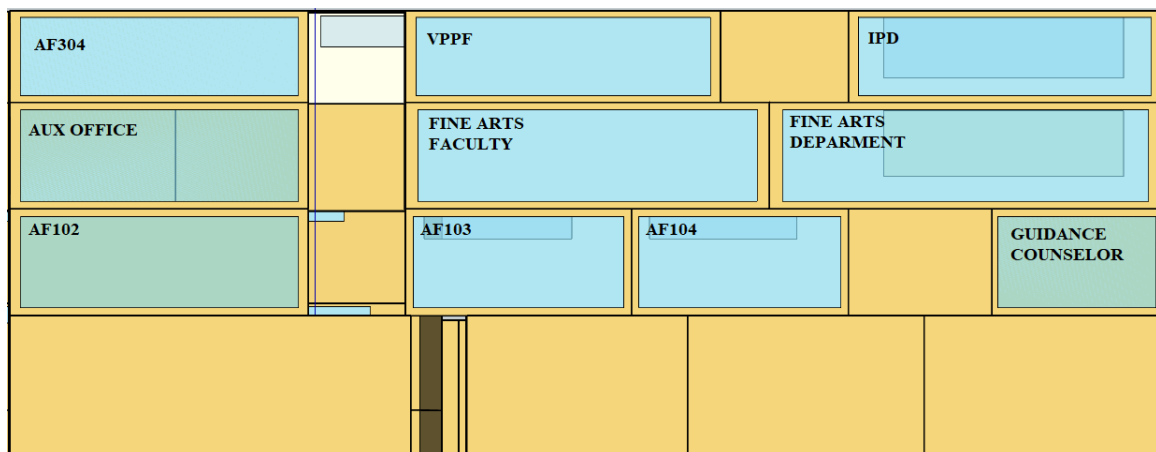


Figure 3.29 80% WWR for West

For 80% WWR, windows for AF 304, VPPF, and IPD were placed 0.39 meter below the ceiling and above the floor, then each width was at the center of the wall width computed to have a WWR of 20%. For the rest of the rooms, the windows were placed 0.45 meter below the ceiling and above the floor, then the window width was at the center of the wall width computed to have a WWR of 80%. Refer to Figure 3.29.

Chapter 4

Results and Discussions

To accomplish the objectives of the study, the methodology was divided into three: (1) Preliminary Modeling, (2) Model Calibration, and (3) Optimum Window Size Search. The following sections present the results for each part of the methodology.

4.1 Preliminary Modeling

As stated in Chapter 3, a preliminary modeling was performed after acquiring data about the SAFAD building's weather, building geometry, materials and construction, lighting density and schedules, equipment density and schedules, occupant schedules, air conditioning systems details, and zoning. The details of the data acquired can be found in Chapter 3 and in the Appendix of this paper.

4.1.1 Modeling Process

The building geometry and physical features of the SAFAD building were defined first using *Euclid*. The entire process was basically a drawing process of the building to replicate its features – shapes of rooms, height of each rooms, dimensions of windows, shading features, and vegetation around the building. Also, the building was geo-located to define the orientation of the building. The output file of *Euclid* is already in “.idf” format which is an *EnergyPlus* input file. **Figure 4.1** shows the finished drawing of the SAFAD building rendered in terms of building surface types, the different colors represent the different surfaces: purple for shading objects, brown for walls, maroon for roofs, and a transparent blue for windows. The large shading objects around the building represent the trees around the building.

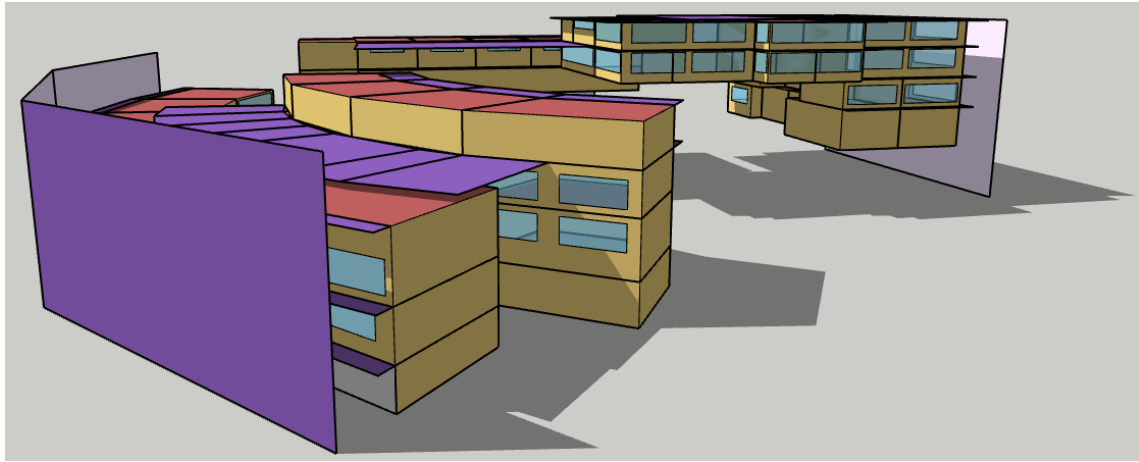


Figure 4.1 Drawing of Building in Euclid

The outside boundary conditions were also defined. Outside boundary conditions will determine what is outside a particular surface (e.g., outdoors, ground, etc.). It was assumed that there is no heat transfer between rooms, theoretically, this assumption will not have a significant effect on the simulation output since the cooling setpoint will also be uniformed later on for all zones. The walls between rooms were set to “adiabatic” outside boundary condition and all other surfaces were set to “outdoors” (wind exposed and/or sun exposed depending on the placement of the surface in the real building). **Figure 4.2** shows the model rendered in terms of outside boundary conditions. The different colors represent different outside boundary conditions – pink for adiabatic and blue for outdoors. Outside boundary conditions for windows and shading objects don’t need to be defined.

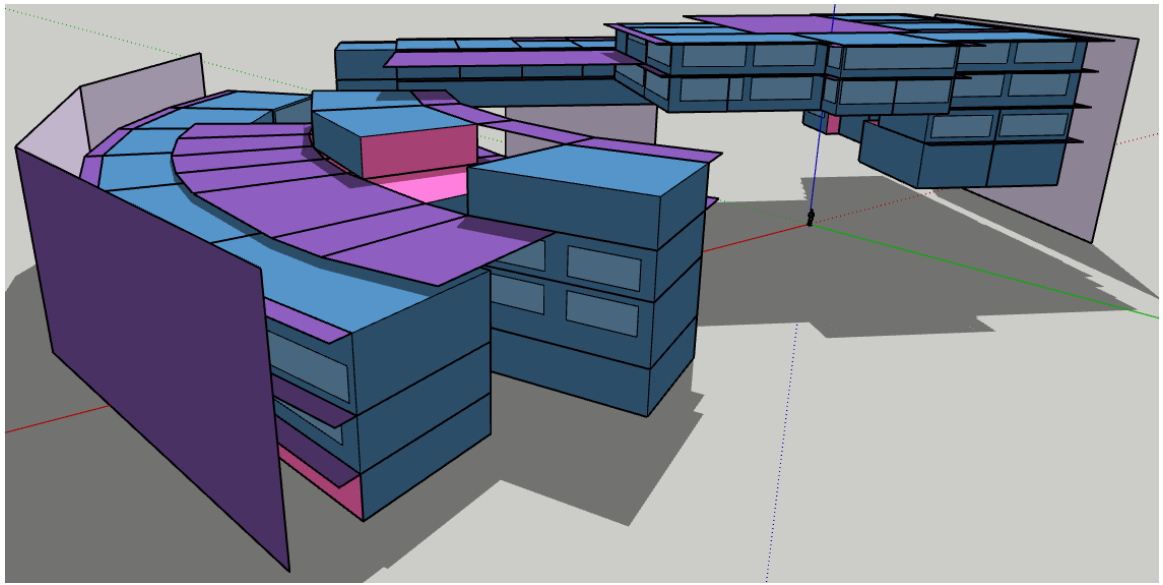


Figure 4.2 Model Rendered in terms of Outside Boundary Conditions

The orientation of the building was also defined in *Euclid*, since *Euclid* is an extension of *SketchUp*, the “geo-location” feature of *SketchUp* can be used. **Figure 4.3** shows that the model building was aligned to the orientation of the real building using geo-location. The green or Y-axis of *SketchUp* represents the true North. The building is 15 degrees East of North as shown in **Figure 4.4**.

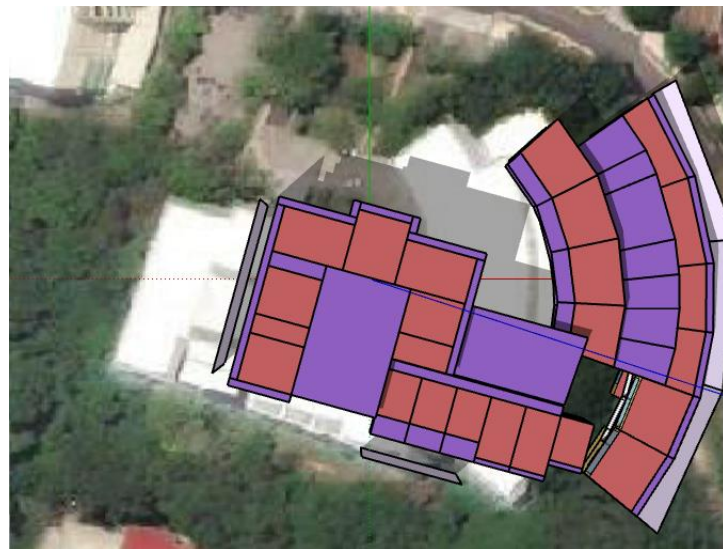


Figure 4.3 Defining the Orientation of the Building in Euclid



Figure 4.4 Orientation of the Case Study Building

After setting all the physical features of the building in *Euclid*, the output file of *Euclid* with a file extension of “.idf” was extracted.

The “.idf” file format extracted from *Euclid* was then opened in *EnergyPlus* IDF editor so that the details of the building regarding its materials and construction, lighting density and schedules, equipment density and schedules, occupant schedules, and air conditioning systems details can be defined carefully. The weather file selected for the simulation was a weather file for Mactan, Cebu acquired from a weather file provider mentioned in Chapter 3. All the details about the details of the building can be viewed in Chapter 3 and in the Appendix of this paper.

After defining all the building details in *EnergyPlus* IDF editor (see Figure 4.5 for a screenshot of IDF editor), it was set that the simulation will output hourly energy consumption for the whole building and hourly illuminance values for AF 305. The setting of reference points for the illuminance values in AF 305 was explained in Chapter 3 of this paper. After setting the outputs, a simulation was performed (see Figure 4.6).

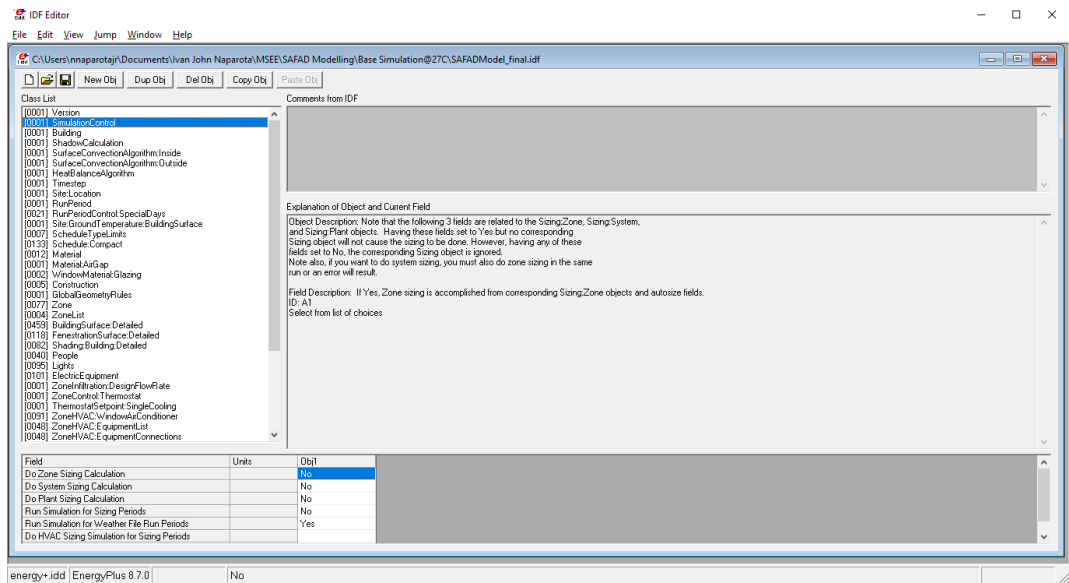


Figure 4.5 Screenshot of *EnergyPlus* IDF editor

```
0001 - EnergyPlus Process
C:\Users\nnaparotajr\Documents\Ivan John Naparota\MSEE\SAFAD Modelling\Base Simulation@27C\EPTEMP-00000001>IF EXIST eplu
smap.tab DEL eplusmap.tab

C:\Users\nnaparotajr\Documents\Ivan John Naparota\MSEE\SAFAD Modelling\Base Simulation@27C\EPTEMP-00000001>IF EXIST eplu
stbl.csv DEL eplustbl.csv

C:\Users\nnaparotajr\Documents\Ivan John Naparota\MSEE\SAFAD Modelling\Base Simulation@27C\EPTEMP-00000001>IF EXIST eplu
stbl.txt DEL eplustbl.txt

C:\Users\nnaparotajr\Documents\Ivan John Naparota\MSEE\SAFAD Modelling\Base Simulation@27C\EPTEMP-00000001>IF EXIST eplu
stbl.tab DEL eplustbl.tab

C:\Users\nnaparotajr\Documents\Ivan John Naparota\MSEE\SAFAD Modelling\Base Simulation@27C\EPTEMP-00000001>IF EXIST eplu
stbl.htm DEL eplustbl.htm

C:\Users\nnaparotajr\Documents\Ivan John Naparota\MSEE\SAFAD Modelling\Base Simulation@27C\EPTEMP-00000001>IF EXIST eplu
stbl.xml DEL eplustbl.xml

C:\Users\nnaparotajr\Documents\Ivan John Naparota\MSEE\SAFAD Modelling\Base Simulation@27C\EPTEMP-00000001>IF EXIST eplu
sout.log DEL eplusout.log

C:\Users\nnaparotajr\Documents\Ivan John Naparota\MSEE\SAFAD Modelling\Base Simulation@27C\EPTEMP-00000001>IF EXIST eplu
sout.svg DEL eplusout.svg

C:\Users\nnaparotajr\Documents\Ivan John Naparota\MSEE\SAFAD Modelling\Base Simulation@27C\EPTEMP-00000001>IF EXIST eplu
sout.shd DEL eplusout.shd

C:\Users\nnaparotajr\Documents\Ivan John Naparota\MSEE\SAFAD Modelling\Base Simulation@27C\EPTEMP-00000001>IF EXIST eplu
sout.wnl
```

Figure 4.6 Performing Single Simulation

4.1.2 Simulated Energy Compared to Measured Energy

This section compares the simulated and measured hourly energy consumption. The indices used for the comparison were Mean Bias Error (MBE) and Coefficient of Variation of the Root Mean Square (CV RMSE). As mentioned in the Chapter 2 of this paper,

currently, a model is an “acceptable” model if it will comply to the guidelines set by ASHRAE [55]. For a building energy simulation with hourly energy output, ASHRAE requires MBE and CV RMSE to not exceed 10% and 30%, respectively. Figure 4.7 shows the plot of average measured and simulated hourly energy consumption from 9AM to 9PM for the whole month of October.

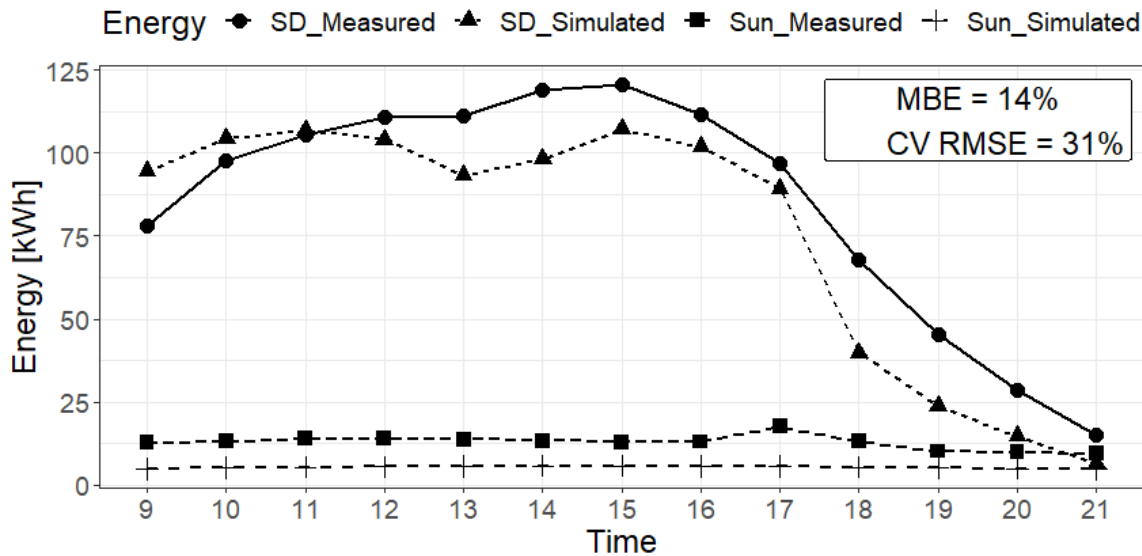


Figure 4.7 Measured vs Simulated Hourly Energy Consumption

The plot was grouped into school days (i.e., SD_measured, SD_simulated) and Sundays (i.e., Sun_measured, Sun_simulated) to see how the model performs during both operating hours and non-operating hours. Both for school days and Sundays, the model does not show a perfect fit to measured values. For school days, the model undercalculates for the most part of the day specifically past 11 AM, but it overestimates from 9AM to around 9:30 AM. For Sundays, the simulated and measured energy consumptions almost follow a flat line trend since no activities that will cause surges in the consumption were expected to happen in the building. However, both the model and simulation do not perfectly have zero energy consumption even though ideally, no activities were happening during Sundays. According to the SAFAD building technician, the non-zero energy consumption of the measured data could be caused by the load that were intentionally left running: water pumps, internet connection, air conditioner in the server room and film

room, and refrigerators. Consequently, this mentioned equipment were also inputted to the simulation but still did not give a precise prediction. A discrepancy of around 5kWh can be observed for all hours. The “real” reasons for this were uncertain; it is possible that there were still other equipment left turned ON that were unaccounted, or the internet connection energy consumption was not represented carefully as this kind of usage is hard to measure. It is also possible that the air conditioning units were not properly modeled in the simulation software since the modeling of the air conditioning units were based from datasheet and no special tests were performed to determine details about the units (e.g., the theoretical COP of ACU is different from “real-world” COP), or it is caused by all of the mentioned possibilities and there may still be other possibilities causing these discrepancies. As it is impossible to represent all of these precisely without performing costly tests, the researcher performed further calibration of the model to account for these uncertainties and to further improve the model performance.

Furthermore, the MBE and CV RMSE of the model were 14 and 31%, respectively. Both indices did not pass the guidelines set by ASHRAE. However, the model showed a great performance for a preliminary simulation especially knowing that it was compared to hourly measured data with 390 datapoints, it was 4% and 1% shy for MBE and CV RMSE to be deemed “calibrated” by ASHRAE. When compared to a preliminary simulation like from a simulation from Pedrini et. al [59], their preliminary model reported a 114% annual difference on measured energy consumption, their preliminary model was made just by documentations alone and no physical contact with the building, this shows that performing walkthrough audits for defining a model’s parameters will certainly reduce the uncertainties of the model and will provide a better model performance compared to relying solely on documentations. They also improved their model using walkthrough audits and special tests.

4.1.3 Simulated Illuminance Compared to Measured Illuminance

This section compares the measured and simulated illuminance of two reference points in AF 305. Figure 4.8 shows the average hourly simulated and measured illuminance

values. One reference point is near the window (N_{measured} , $N_{\text{simulated}}$) and one reference point far from the window ($F_{\text{simulated}}$, F_{measured}). To have a basis for comparison, same indices used in comparing energy were used – MBE and CV RMSE. Unlike the energy output of a building energy simulation, no guidelines were set to assess the performance of a model in terms of its environmental outputs (e.g., illuminance, temperature, etc.). But MBE and CV RMSE are two common statistical indices to assess models in general. Also, these indices were used by Ramos et. al [44] to test the performance of *EnergyPlus* program in calculating illuminance.

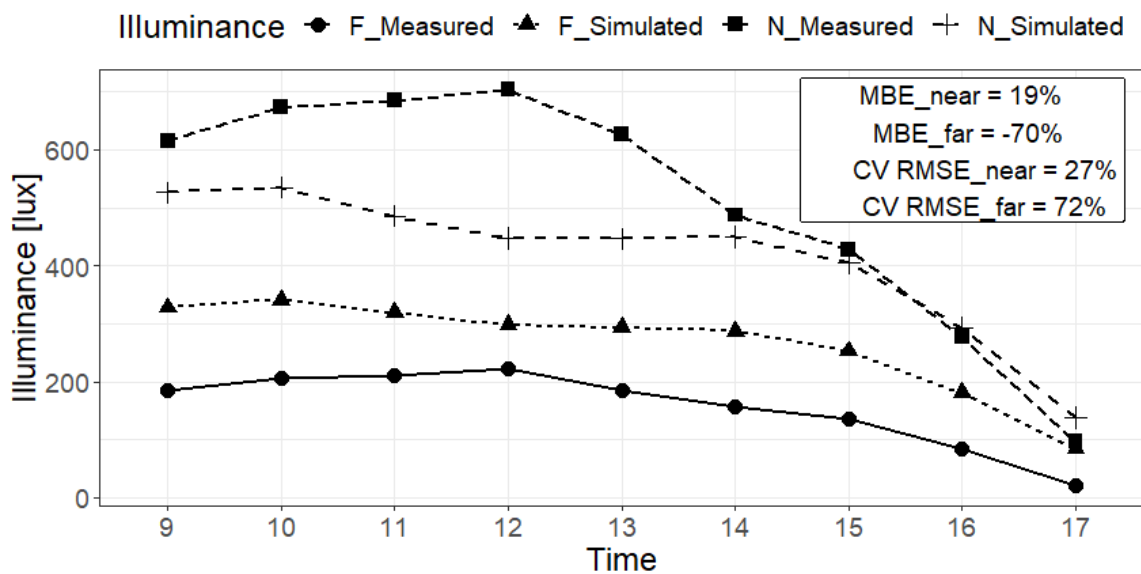


Figure 4.8 Measured vs Simulated Illuminance from Two Points in AF 305

Referring to Figure 4.8, it can be observed that *EnergyPlus* does not calculate the illuminance values very precisely. For the reference point near the window, *EnergyPlus* undercalculates the illuminance values from 9AM to around 2PM and the highest difference can be observed at around 12PM. The measured values for both reference points followed the same trend – the illuminance values continue to rise from 9AM to 12PM and gradually drops until 5PM. However, for the simulated illuminance values in the two reference points, the upward trend stops at around 10AM and the trend sags at around 12PM and slowly rises up to around 2PM before declining continuously. This trend of the

simulated illuminance values appears to be the same for a study conducted by Ramos et. al. [44] in a tropical country like the Philippines, Brazil.

The MBE for “far” and “near” reference points were -70% and 19%, respectively. On the other hand, the CV RMSE for “far” and “near” were 72% and 27%, respectively. With these values, it can be pointed out that the reference point farther from the window experienced the larger discrepancy. Again, this result can also be observed from the same study by Ramos et. al. They reported that when using *EnergyPlus* in computing space illuminance, the farther the reference point to the window, the more overcalculated the illuminance values in the reference point will be. They reported that these overestimations maybe due to the sky model used by *EnergyPlus* which was a model developed by Perez et. al [45].

With these results, since *EnergyPlus* has a problem on computing reference points farther from the window, only one reference point was considered in the assessment of daylighting for different window sizes which has the same distance from the window as the “near” reference point. Also, the visible light transmittance of windows was tuned to bring the simulated illuminance values closer to the measured values – have a lesser MBE and CV RMSE.

4.2 Model Calibration

To further improve the model in predicting energy and illuminance, the model went through a calibration process. The model was first calibrated in terms of illuminance before it was calibrated in terms of energy.

4.2.1 Calibration Considering Illuminance Output

To bring the simulated illuminance to measured values, the visible light transmittance (TVis) of windows was altered from 0 to 0.9 in a step of 0.1 {0.1, 0.2, . . . , 0.9} and the MBE and CV RMSE were calculated that corresponds to each TVis value. To have a single index that considers both MBE and CV RMSE, another index denoted as “GOF_Total” or total goodness-of-fit which was introduced by Reddy et. al. [54] was used.

GOF_Total can be computed using Eq. 4.1.

$$\text{GOF_Total} = \frac{W_{CV}^2(CV\ RMSE^2) + W_{MBE}^2(MBE^2)}{W_{CV}^2 + W_{MBE}^2} \quad \text{Eq. 4.1 ; } w \text{ is the weight assigned to each index.}$$

Reddy et. al. suggested 1:3 of $w_{cv}:w_{mbe}$ ratio of the weight. Though this ratio was applied when they were calibrating model in terms of energy, this was still applied because giving more weight to MBE would be a rational choice – MBE is the “overall” measure of the difference of measured and simulated values. Furthermore, tuning only a single parameter that will carry a continuous value throughout the day like TVis which works as a factor will not affect the trend pattern of the illuminance values, but will most likely just “offset” the trend – above or below the baseline. So, giving a greater weight to MBE than CV RMSE was a rational choice.

Table 4.1 The results of changing the TVis values from 0.1 – 0.9.

TVIS	NEAR		FAR		GOF_Tot	
	MBE	CVRMSE	MBE	CVRMSE	NEAR	FAR
0.1	88.32489	95.26359	75.66245	82.77843	89.0431	76.40387
0.2	76.64978	83.31222	51.32489	57.96954	77.34186	52.02756
0.3	64.97468	71.42614	26.98734	33.99589	65.64836	27.76791
0.4	53.29957	59.64439	2.649781	15.42813	53.96763	5.488344
0.5	41.62446	48.04377	-21.6878	24.64522	42.31024	22.00142
0.6	29.94935	36.796	-46.0253	47.5794	30.7028	46.18309
0.7	17.12121	25.38861	-73.7985	75.67135	18.11851	73.98791
0.8	5.281381	17.51412	-98.6268	101.1965	7.468476	98.88682
0.9	-6.55845	16.50143	-123.455	126.8655	8.120445	123.8005
BASE	18.89718	26.85935	-70.0742	71.86446	19.83773	70.25531

As shown in Table 4.1, the TVis values that brought the simulated illuminance closest to the measured illuminance were TVis = 0.8 and TVis = 0.4 for near and far reference points, respectively. These values were highlighted in the table. For the near reference point, it can be observed that this TVis value is close to the baseline TVis value which is 0.685. On the other hand, for the far reference point, this TVis value is far from

the baseline value. Furthermore, it was evident that the GOF_Total of near and far reference points are contradicting – good GOF_Total (less value) for near reference point will cause bad GOF_Total (large value) for far reference point.

Since it was observed in the preliminary modeling that *EnergyPlus* has a problem calculating illuminance values from the reference point far from the window and was also observed by another research study by Ramos et. al. [44], the near reference point will be given priority and the model that was concluded as the calibrated one is the model with TVis = 0.8. Because of these situations, only one reference point was considered during the daylighting assessment of different window sizes.

4.2.2 Calibration Considering Energy Output

Carrying the TVis value, which is equal to 0.8, the model went through another calibration process, but now in terms of energy consumption. This calibration procedure can be sequenced into: (1) reducing the number of parameters by weeding out the most influential ones; (2) random searching of the values for each influential parameter that brought the simulated energy consumption closest to the measured energy consumption; and (3) selecting few calibrated simulations to be used for the window optimization process.

4.2.2.1 Ranking of Uncertain Parameters using Morris Method

Model parameters that were not measured during the preliminary modeling and their possible range of values were identified heuristically. Some of these parameters were left with the default *EnergyPlus* values during the preliminary modeling; i.e., material thermal and solar absorptance, air gap thermal resistance, and equipment fraction radiant. Some were referred from ASHRAE Handbook of Fundamentals; i.e., people fraction radiant and activities, and light fraction radiant. Some were “wild” guesses; i.e., air infiltration, fan total efficiency, and pressure rise. While the COP was computed using the air conditioner datasheet.

Referring to Table 4.2, the “base” column contains the values for these parameters

during the preliminary modeling. The “upper” and “lower” columns contain the maximum and minimum possible values for each parameter, these ranges were defined using *EnergyPlus*. Most likely, the “actual” values for each parameter are between these ranges which will theoretically, give the model a good fit to the measured data.

Table 4.2 Uncertain Parameters and their Values

	Uncertain Parameters	<i>Lower</i>	<i>Base</i>	<i>Upper</i>
X1	Concrete thermal absorptance	0.001	0.9	0.999
X2	Concrete solar absorptance	0	0.7	1
X3	Plywood thermal absorptance	0.001	0.9	0.999
X4	Plywood solar absorptance	0	0.7	1
X5	Air gap thermal resistance	0.001	0.18	1
X6	People fraction radiant	0	0.46	1
X7	People activity level computer lab	100	140	150
X8	People activity level offices	100	140	150
X9	People activity level lecture rooms	100	140	150
X10	Light fraction radiant	0	0.27	1
X11	Equipment fraction radiant	0	0	1
X12	Air Infiltration air changes/hour	0.1	1	6
X13	Fan total efficiency	0.3	0.5	0.9
X14	Pressure rise	30	75	120
X15	DXCoolingCoil COP	1	3	5

Using these 15 uncertain parameters and their value ranges, Morris Method of sensitivity analysis was performed to rank the parameters in terms of their influence to the energy consumption. The function can be written as:

$$Energy = f(X_1, X_2, \dots, X_k) \quad ; \text{where } k \text{ is the number of uncertain parameters, 15.}$$

The details on the computations for Morris Method were explained in the Chapter 3 of this paper. The design matrix, \mathbf{X} , was obtained using *R Software* with the package *sensitivity* and the function *morris*, provided the following conditions: the number of elementary effects for each parameter, r , is 5; number of levels or samples for each parameter, p , is 4; and the magnitude of step, Δ , is $\frac{1}{1-p} = \frac{1}{3}$. The computation cost was $(k + 1)*r = 80$.

Meaning, there were 80 simulations performed to complete the sensitivity analysis. Thus, the design matrix, \mathbf{X} , is an 80x15 matrix. The design matrix, \mathbf{X} , is in the Appendix of this paper.

After performing all 80 simulations, the 80 total energy consumption values were used to compute the index, μ^* , which is the measure of influence of each parameter to the energy consumption. The results of the 80 simulations is in the Appendix of this paper. The greater μ^* , the more influential a parameter.

Table 4.3 Ranking of the Parameters

Parameter	ID	μ^*
DXCoolingCoil COP	X ₁₅	94665.78
Air Infiltration air changes/hour	X ₁₂	30005.45
Concrete solar absorptance	X ₂	7819.038
Concrete thermal absorptance	X ₁	2674.26
People fraction radiant	X ₆	2534.742
Fan total efficiency	X ₁₃	1599.306
Equipment fraction radiant	X ₁₁	1294.878
Pressure rise	X ₁₄	1088.784
People activity level lecture rooms	X ₉	1050.27
Light fraction radiant	X ₁₀	968.808
Plywood thermal absorptance	X ₃	931.104
Plywood solar absorptance	X ₄	564.924
People activity level offices	X ₈	489.552
People activity level computer lab	X ₇	109.194
Air gap thermal resistance	X ₅	33.156

Table 4.3 ranks the parameters from the most influential at the top to the least influential at the bottom. The result show that the coefficient of performance (COP) is indeed the most influential parameter out of the 15 parameters to the energy consumption, then followed by air infiltration, concrete solar absorptance, and so on.

4.2.2.3 Tuning of Parameters Using Latin Hypercube Monte Carlo

Out from the 15 uncertain parameters, only the top 7 most influential parameters determined by the sensitivity analysis performed above were calibrated and the remaining 8 parameters were left with values from the preliminary modeling. The highlighted parameters in Table 4.3 were the top 7 most influential parameters.

The calibration method used was a variant of Monte Carlo methods which is Latin Hypercube Monte Carlo (LHMC). The design matrix for the computer experiment was constructed using *R Software* with the package *LHS* and the function *randomLHS*, with the conditions: number of samples for each parameter, n , is 5; number of parameters, k , is 7. The design matrix can be found in the Appendix. As explained in the Chapter 3 of this paper, for a single LHMC trial, there are n combinations of k number of values. In other words, there are 5 combinations of values of the 7 parameters, which also translates to 5 *EnergyPlus* simulations. There were 80 trials of LHMC performed in this calibration procedure that translates to 400 simulations. Out from the 400 simulations, the simulations that passed the threshold set for the Mean Bias Error (MBE) and Coefficient of Variation of the Root Mean Square (CV RMSE) were weeded out – maximum of 10% and 30% for MBE and CV RMSE, respectively.

After weeding out the simulations that passed the two indices, the simulations were then ranked from “best” to “worst” goodness-of-fit which was measured using a modified index from Reddy et. al. [54]. The index was denoted as GOF_Total and computed using Eq. 4.2. This index combines the CV RMSE and MBE to have only one index for ranking the simulations. A weight for MBE and CV RMSE needs to be defined for this index.

$$\text{GOF_Total} = \frac{W_{CV}^2(CV\ RMSE^2) + W_{MBE}^2(MBE^2)}{W_{CV}^2 + W_{MBE}^2} \quad \text{Eq. 4.2 ; } w \text{ is the weight assigned to each index.}$$

Reddy et. al. suggested 1:3 of $w_{cv}:w_{mbe}$ ratio of the weight. They said that it is more practical for a calibration procedure to capture the mean more precisely than the variation for each time step – which in this case, hourly.

Out from the 400 simulations, there were 77 simulations that passed both the MBE and CV RMSE. These 77 simulations that passed the indices were then ranked according to their GOF_Total and hereby presented in Table 4.4.

Table 4.4 Ranking of Simulations that Passed MBE and CV RMSE

Run	MBE	CVRMSE	GOF_Total	Rank
330	0.46	29.42	9.31	1
92	0.33	29.47	9.32	2
75	1.76	29.09	9.35	3
395	2.43	28.98	9.45	4
163	2.33	29.09	9.46	5
353	0.52	29.95	9.48	6
99	-0.05	30.00	9.49	7
329	1.47	29.74	9.51	8
172	-0.30	30.16	9.54	9
343	-0.29	30.22	9.56	10
342	2.50	29.35	9.58	11
128	-0.03	30.33	9.59	12
236	-0.97	30.20	9.59	13
87	1.92	29.80	9.60	14
6	3.28	28.94	9.67	15
189	-1.63	30.19	9.67	16
212	2.51	30.19	9.84	17
298	3.87	28.88	9.84	18
279	-1.67	30.74	9.85	19
245	-2.13	30.83	9.96	20
4	4.20	28.88	9.97	21
370	-2.16	30.87	9.97	22
295	4.24	28.88	9.98	23
251	-2.66	30.66	10.02	24
106	4.49	28.74	10.03	25
322	4.43	29.04	10.10	26
226	4.43	29.08	10.11	27
234	-3.11	30.64	10.13	28
351	4.92	28.76	10.22	29
348	5.02	28.86	10.29	30
371	4.84	29.26	10.33	31
36	5.14	28.95	10.37	32

103	4.16	30.45	10.41	33
139	5.43	28.83	10.47	34
319	5.49	28.77	10.48	35
8	4.79	30.15	10.56	36
391	5.36	29.32	10.57	37
188	5.22	29.59	10.59	38
26	4.53	30.68	10.61	39
331	5.50	29.44	10.67	40
22	5.60	29.37	10.70	41
23	6.41	28.64	10.91	42
41	5.81	30.36	11.07	43
382	6.71	28.90	11.14	44
148	6.98	28.60	11.21	45
201	6.86	28.95	11.23	46
60	7.20	28.63	11.34	47
327	7.15	28.83	11.36	48
69	7.43	28.82	11.52	49
144	7.29	29.19	11.53	50
44	7.44	28.99	11.57	51
248	7.57	28.81	11.60	52
143	6.68	30.77	11.61	53
202	7.32	29.52	11.63	54
190	7.77	28.78	11.71	55
13	7.60	29.51	11.79	56
166	8.02	28.70	11.84	57
241	8.21	28.75	11.97	58
142	8.45	28.78	12.13	59
105	8.43	29.15	12.20	60
272	8.66	29.15	12.35	61
289	9.01	28.91	12.52	62
204	9.18	28.85	12.61	63
359	9.25	28.97	12.69	64
210	9.33	29.24	12.80	65
56	9.07	30.02	12.81	66
55	9.44	29.30	12.89	67
285	9.57	29.14	12.94	68
335	9.61	29.11	12.96	69
118	9.72	29.06	13.02	70
58	9.76	29.32	13.10	71

182	9.68	29.63	13.12	72
181	10.09	29.23	13.31	73
361	10.19	29.13	13.36	74
350	10.42	29.15	13.52	75
228	10.55	29.26	13.63	76
120	10.10	30.99	13.71	77

The CV RMSE and MBE for all of the 77 calibrated models are presented in Figure 4.9. It may be observed that there are CV RMSE values slightly higher than 30%, these models even though have CV RMSE slightly higher than 30% which is not more than 1%, still have a good GOF_Total. Furthermore, it can be observed in the plot that the ranking is more determined by the value of the MBE – the higher MBE, the farther the model is in the ranking. This is because MBE was given a greater weight in the formula for GOF_Total.

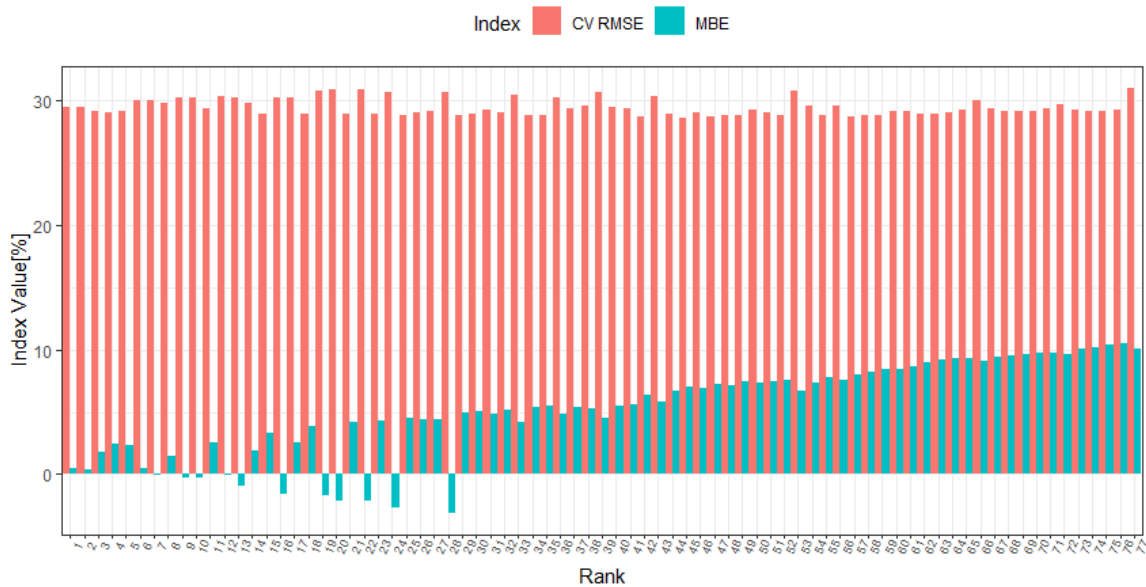


Figure 4.9 MBE and CV RMSE of the 77 Calibrated Models

4.2.2.4 Selection of Five Calibrated Simulations

From the 77 simulations that passed the MBE and CV RMSE, 5 simulations were selected for the optimization of window size. Instead of picking the top 5 simulations based

on their GOF_Total, the simulations selected were: Rank 1, Rank 20, Rank 60, and Rank 77. The reason for this is to have different models with very diverse parameter values and also having different performances in terms of MBE and CV RMSE. As the entire calibration procedure was tailored for this goal – to have different models to test if the optimum window size is consistent. Figures 4.10 – 4.14 present the simulated vs measured energy consumption of the 5 different models and Table 4.5 presents the values of each parameter for the five different models.

Table 4.5 Model parameters for each of the five different models

Parameter	Rank 1	Rank 20	Rank 40	Rank 60	Rank 77
COP	3.882489276	3.296928042	3.46064	3.986092421	2.585057919
Air Changes/hr	4.507065057	2.237562878	1.80943	3.944809677	1.217115479
Concrete solar absorptance	0.729820897	0.848350281	0.5546	0.372937439	0.101913969
Concrete thermal absorptance	0.405240505	0.347479767	0.03769	0.107584907	0.67292642
People fraction radiant	0.290288177	0.021541746	0.49644	0.999956257	0.770640245
Fan total efficiency	0.436408543	0.585882242	0.49253	0.746425989	0.871926015
Equipment fraction radiant	0.689550723	0.527220737	0.12065	0.500183614	0.213235706
MBE	0.46	-2.13	5.5	8.43	10.10
CV RMSE	29.42	30.83	29.44	29.15	30.99

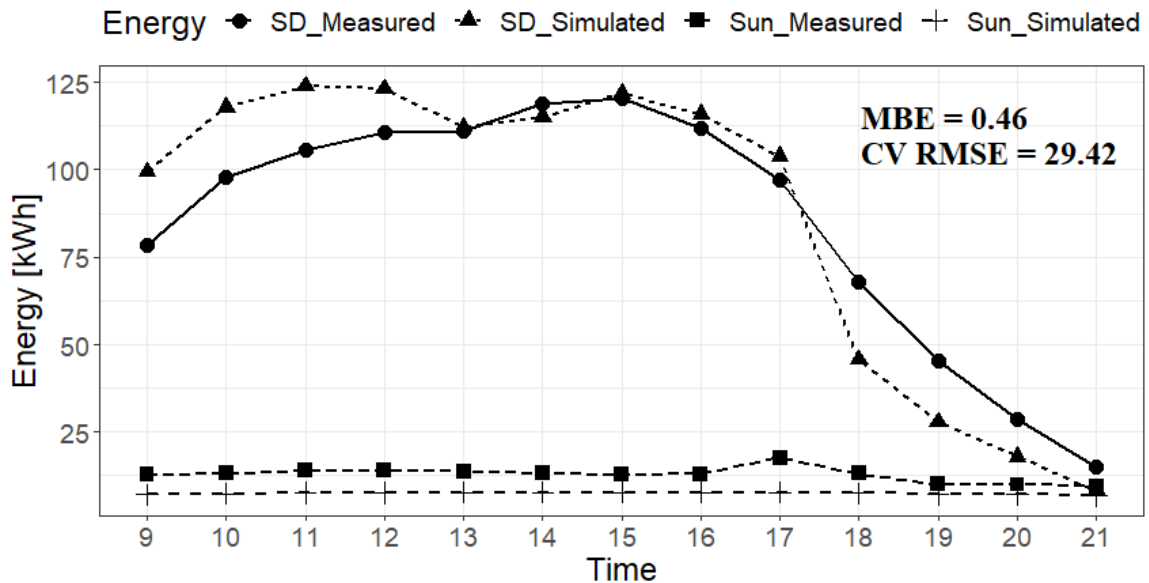


Figure 4.10 Measured vs Simulated Energy Consumption for Rank 1 Model

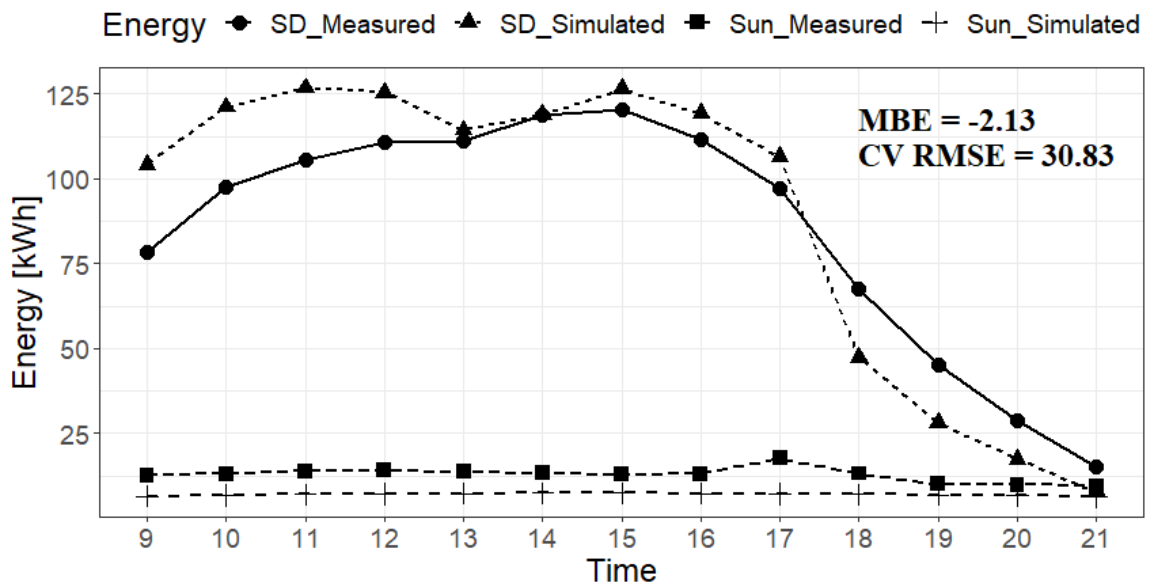


Figure 4.11 Measured vs Simulated Energy Consumption for Rank 20 Model

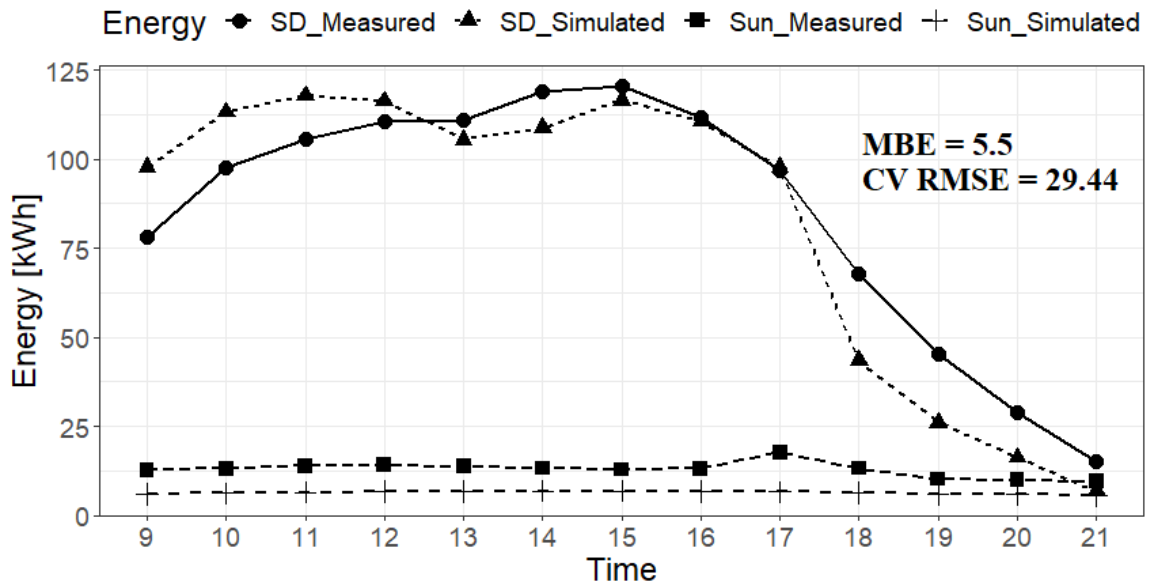


Figure 4.12 Measured vs Simulated Energy Consumption for Rank 40 Model

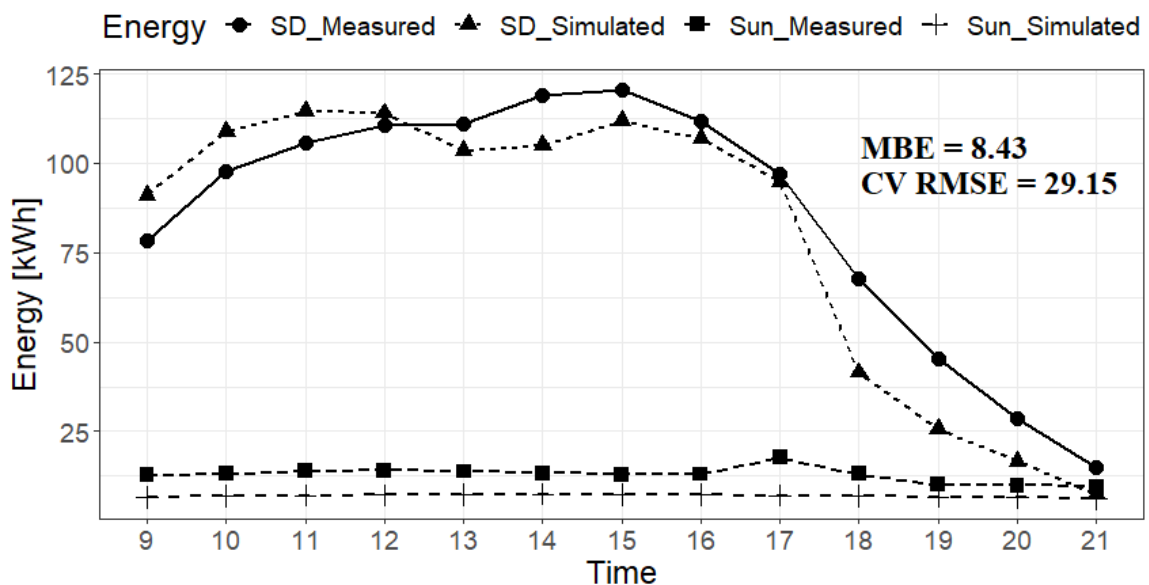


Figure 4.13 Measured vs Simulated Energy Consumption for Rank 60 Model

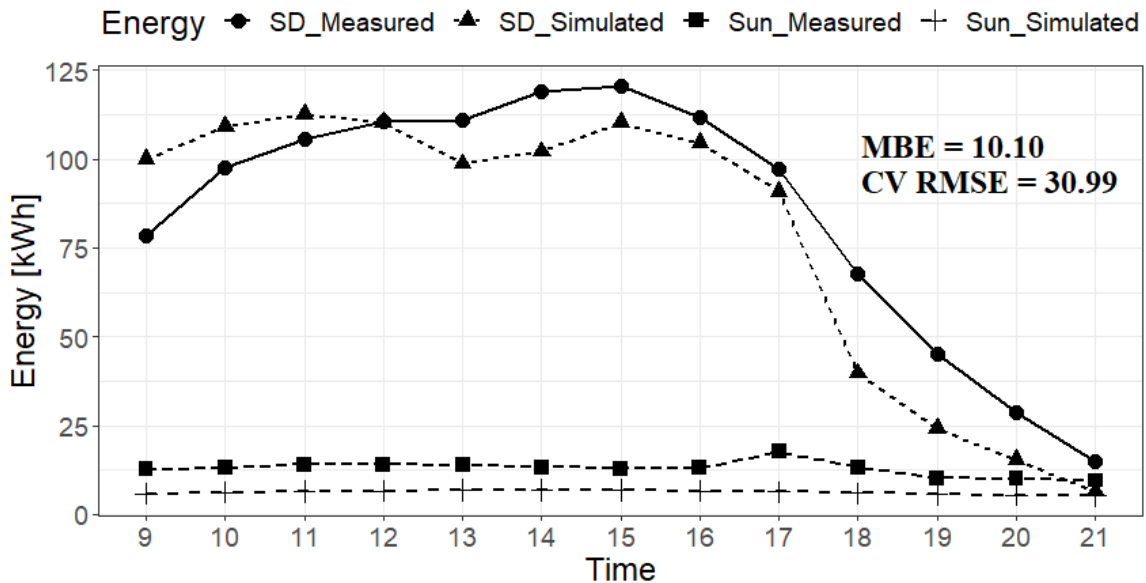


Figure 4.14 Measured vs Simulated Energy Consumption for Rank 77 Model

For all five different models, it can be seen that the hour-to-hour variation of the energy consumption does not fit very precisely, which affirms the CV RMSE of all models that is close to the threshold value. There are ways to improve this and find simulations that have very good fit of the hourly variations of energy consumption: increasing the number of trials of LHMC to further search the solution space; applying *fine grid search*; or applying optimization algorithms (e.g., genetic algorithm, etc.). However, a study from Reddy et. al. [51] that used also an actual building as a case study did not find a strong correlation between goodness-of-fit and prediction accuracy of models if used for suggesting possible Energy Conservation Measures (ECM). Thus, increasing the number of trials of LHMC or applying further optimizations is not certain to improve the outcome of the study (optimum window size) considering that building energy simulation is time consuming, not to mention the data processing needed afterwards.

The next sections present how these five models were used to find the optimum window size for each building orientation.

4.3 Optimum Window Size Search

The final stage of this study was to determine the window to wall ratio for every building orientation that will result to the least cooling and lighting energy consumption, at the same time exploit the right amount of daylight.

4.3.1 East-Facing Windows

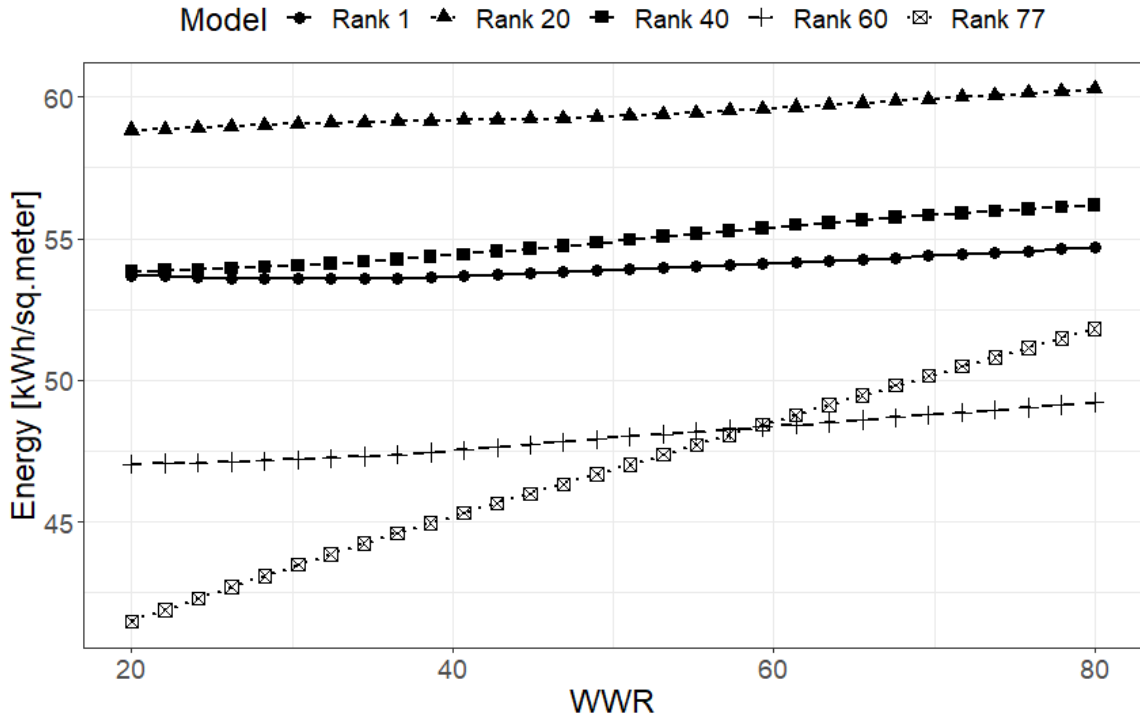


Figure 4.15 Energy consumption for different WWR for east-facing windows

4.3.1.1 Total Energy Consumption

Figure 4.15 shows the total energy consumption normalized with the total floor area of all the rooms for different WWR values. Each curve represents each of the five different calibrated models used. Just by examining at the graph, it can be observed that for the most part, total energy consumption increases as WWR also increases. However, the difference in the total energy consumption is not that large except for model Rank 77. The difference between the best and the worst WWR configurations is 2% for model Rank 1; 2% for model

Rank 20; 4% for model Rank 40; 4% for model Rank 60; and 25% for model Rank 77. The least total energy consumption is common for models Rank 20, 40, 60, and 77 to be at 20% WWR and only Rank 1 differs which is at 32% WWR. However, the difference in total energy consumption for Rank 1's 20% and 32% WWR values is only 0.23%.

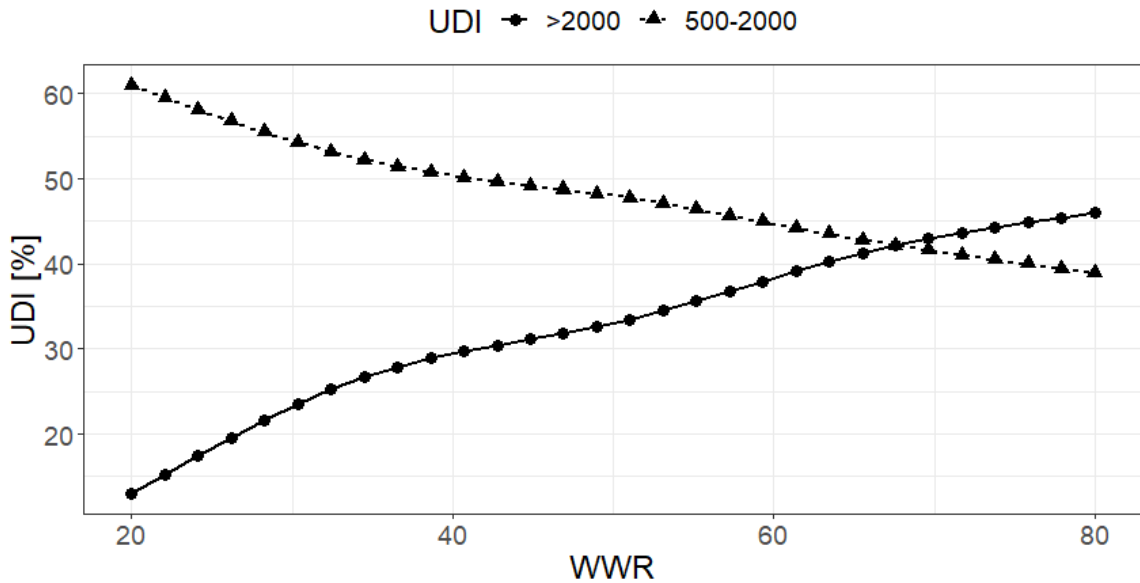


Figure 4.16 Useful Daylight Illuminance for different WWR for east-facing windows

4.3.1.2 Daylighting Assessment

Figure 4.16 shows the UDI in percent of the different WWR values. This is only for a single model because the five models only differ in parameters that have effect on the energy consumption and not on the illuminance. As the WWR gets bigger, the UDI₅₀₀₋₂₀₀₀ gets lesser while the UDI_{>2000} gets larger. Looking at UDI 500-2000, it can be seen that useful daylight is maximized when the WWR is minimized. 20% WWR showed the largest UDI 500-2000 which is at around 60% and 80% WWR showed the least which is at around 40%. Referring to UDI >2000, it can be said that visual discomfort is only a concern when WWR is at 27% and increasing the WWR further will also increase the concern for visual discomfort. At 27% WWR, around 20% of UDI >2000 was achieved which is the maximum allowable percentage as suggested by some researchers [34].

4.3.1.3 Optimum WWR

It is evident that the lesser the WWR, the lesser also is the energy consumption for rooms with east-facing windows and useful daylight (500lux to 2000lux) is maximized. On the other hand, visual discomfort starts to become an issue starting from 27% WWR up to the largest WWR. Based from all of these results, the optimum WWR that could minimize the total energy consumption, maximize useful daylighting, and minimize the concern for visual discomfort is at 20% to 27% WWR and the smaller the better.

4.3.2 North-Facing Windows

The results in the optimization of north-facing windows are presented below.

4.3.2.1 Total Energy Consumption

Figures 4.17 to 4.21 present the total energy consumption as a function of WWR for north-facing windows of the five different calibrated models and five different values of west WWR.

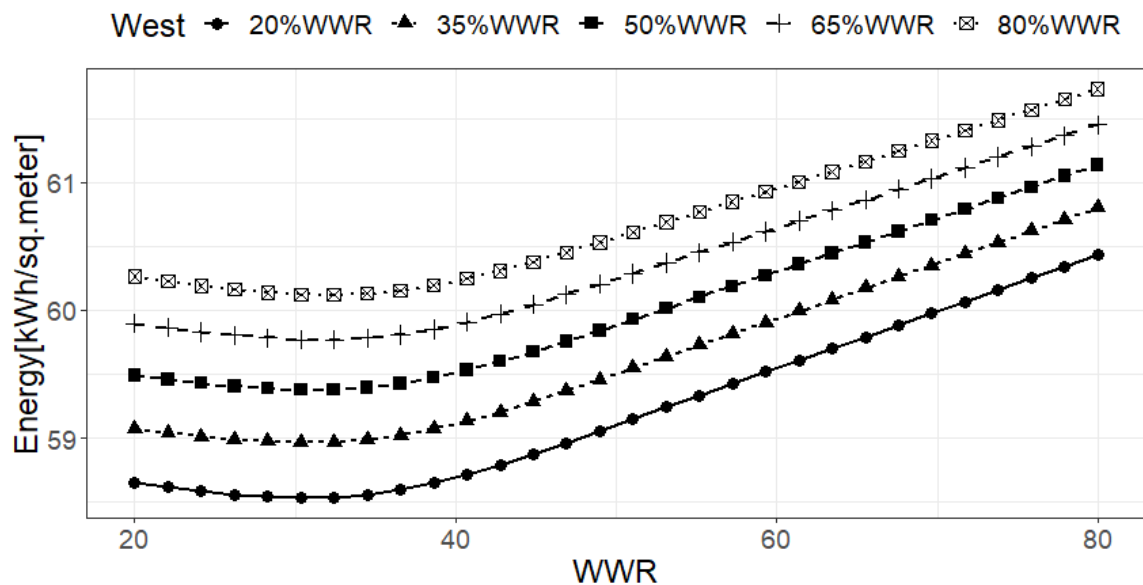


Figure 4.17 Total Energy Consumption for different WWR of Rank 1 Model for north-facing windows

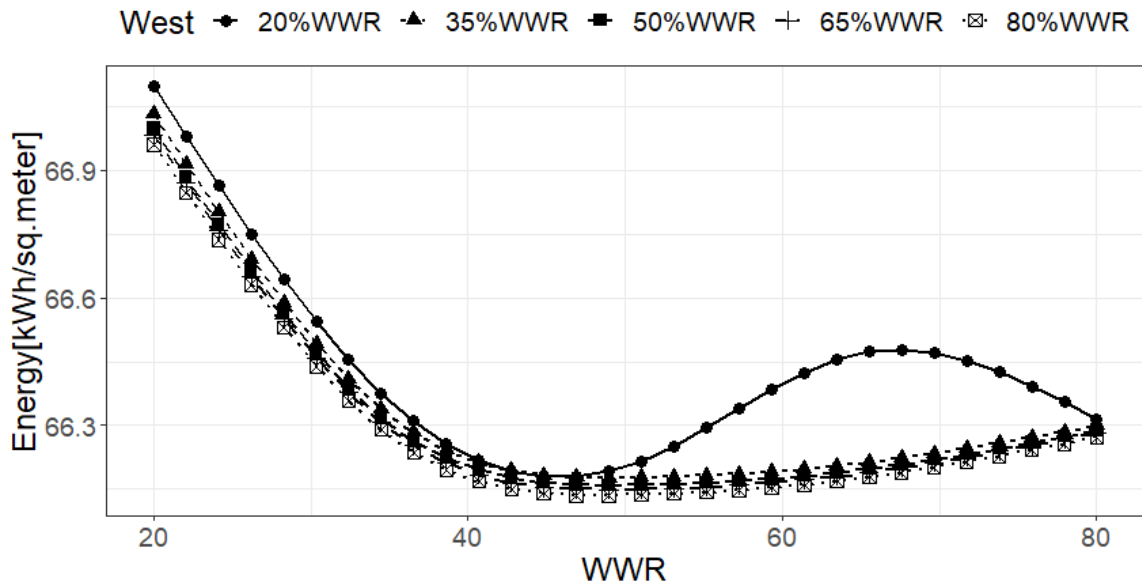


Figure 4.18 Total Energy Consumption for different WWR of Rank 20 Model for north-facing windows

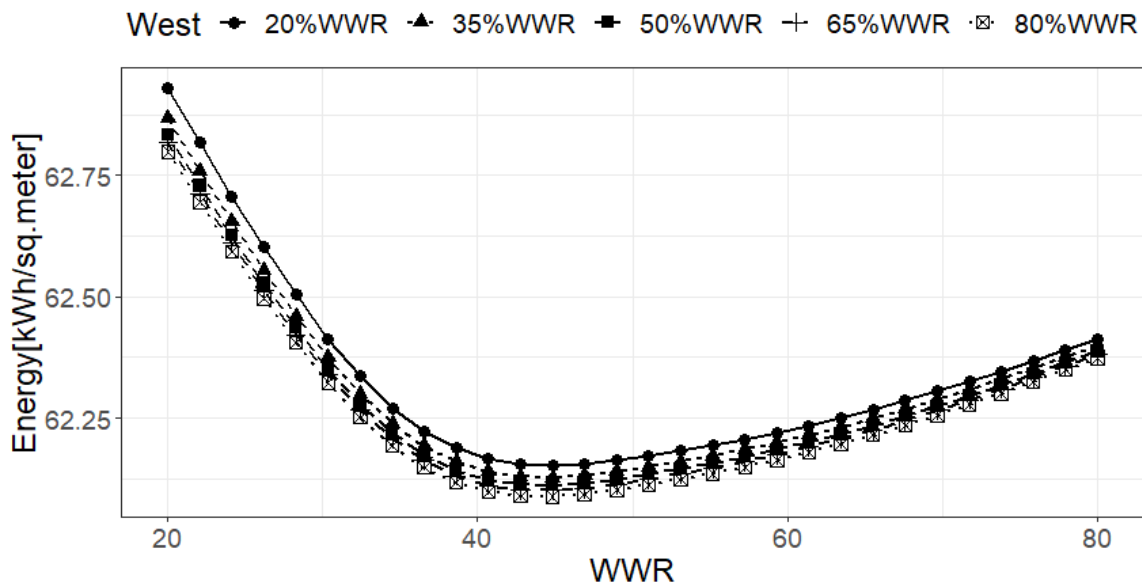


Figure 4.19 Total Energy Consumption for different WWR of Rank 40 Model for north-facing windows

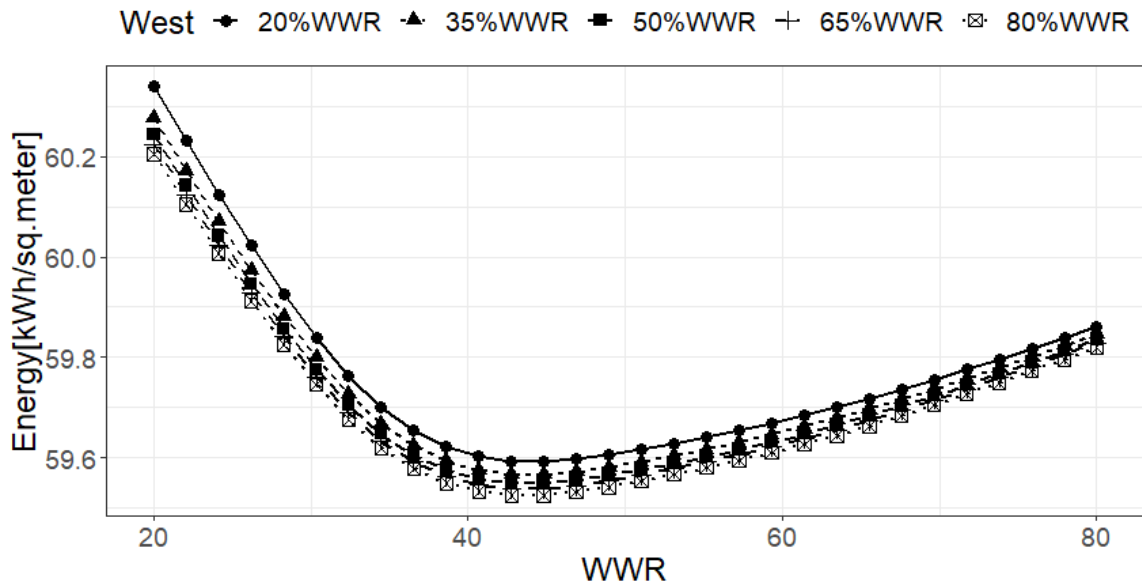


Figure 4.20 Total Energy Consumption for different WWR of Rank 60 Model for north-facing windows

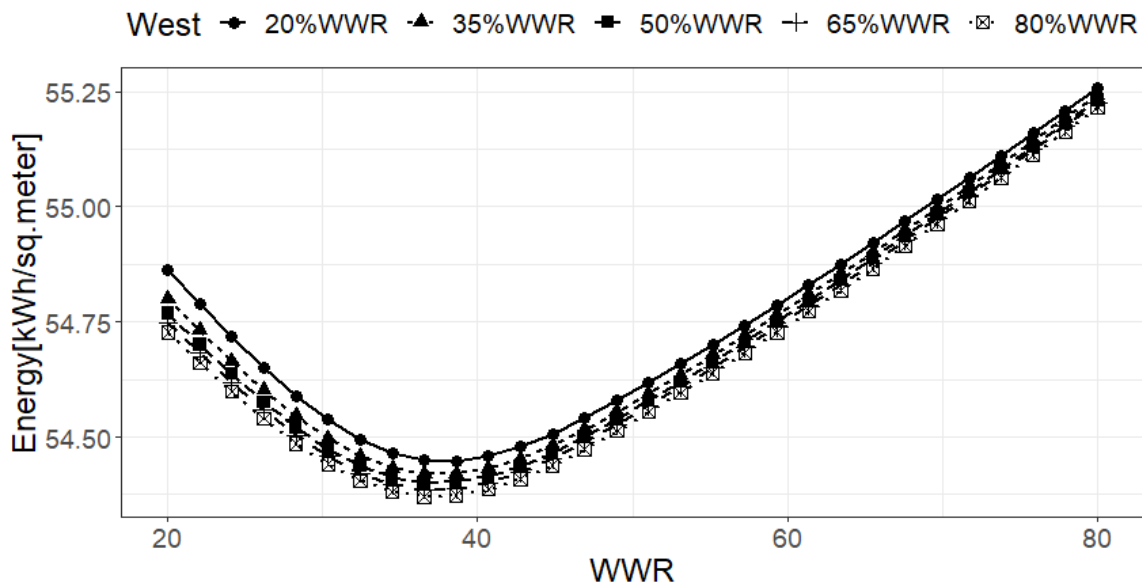


Figure 4.21 Total Energy Consumption for different WWR of Rank 77 Model for north-facing windows

Effect of Using Different Models

It can be seen that only Rank 1 model suggests different WWR that will give the least total energy consumption, all the rest suggest around 40% WWR to have the least total energy consumption. For Rank 1 model, it is around 30% WWR. However, it can be seen in Rank 1 model that the curve is almost flat from 20% WWR to 40% WWR, meaning, the difference between total energy consumptions across this range of WWR is not very large. On that regard, for different models, the difference between the best and the worst WWR configuration is not that large: around 3.4% for Rank 1 model; around 1.36% for Rank 20; around 1.2% for Rank 40; around 1.17% for Rank 60; and around 1.8% for Rank 77.

Effect of Using Different WWR for West

It can be seen that WWR of west facing windows do not have a strong effect on the optimum WWR for north-facing windows. This is because the trends of the curves are the same. Except for Rank 20 model, the 20% WWR of west causes the curve to offset from other curves, but it is worth noting that the peak difference which happened at around 65% north WWR is only around .38% to make the curve behave the same as the others. This increase in energy consumption could possibly be caused by the lighting energy consumption, since west WWR is only at 20%, the supply of daylight from west is not very high which requires supplementation from artificial lighting. This can be affirmed by looking at Figures 4.22 and 4.23. Looking at Figure 4.22, it can be said that from 50% to 60% WWR of north and 20% WWR of west, the least UDI 500-2000 was experienced. And looking at Figure 4.23 it can be said that around 60% to 80% of north WWR and 20% west WWR, the least UDI >2000 was experienced. These observations mean that around 50% to 80% WWR of north and 20% WWR of west, the dominant illuminance level is below 500 lux. Since the illuminance setpoint was set to 500 lux, then artificial lighting was required more during this WWR range. But it is hard to tell why this behavior only happened in model Rank 20. However, it is safe to assume that this is caused by the difference in model parameters among the five models. Overall, this behavior needs to be

considered in optimizing WWR in west facing windows.

4.3.2.2 Daylighting Assessment

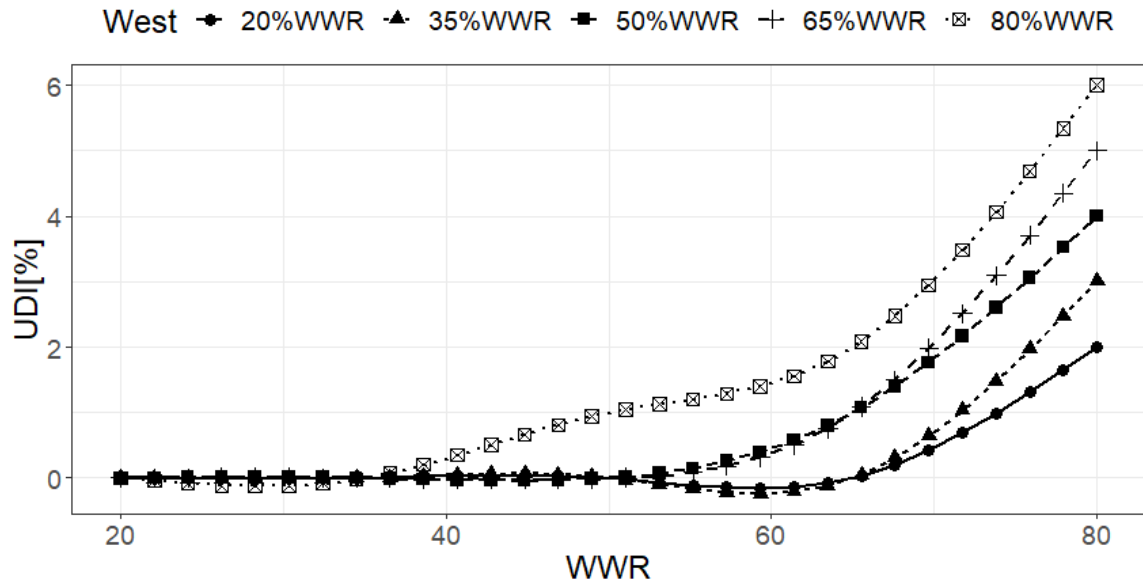


Figure 4.22 UDI >2000 for north-facing windows

It can be seen in Figure 4.22 that for any WWR of north, and any WWR of west, the concern for too much illuminance level is not an issue. When in fact the largest $UDI_{>2000}$ percentage at 80% WWR north and 80% WWR west is only 6% - far from the suggested threshold of at most 20%.

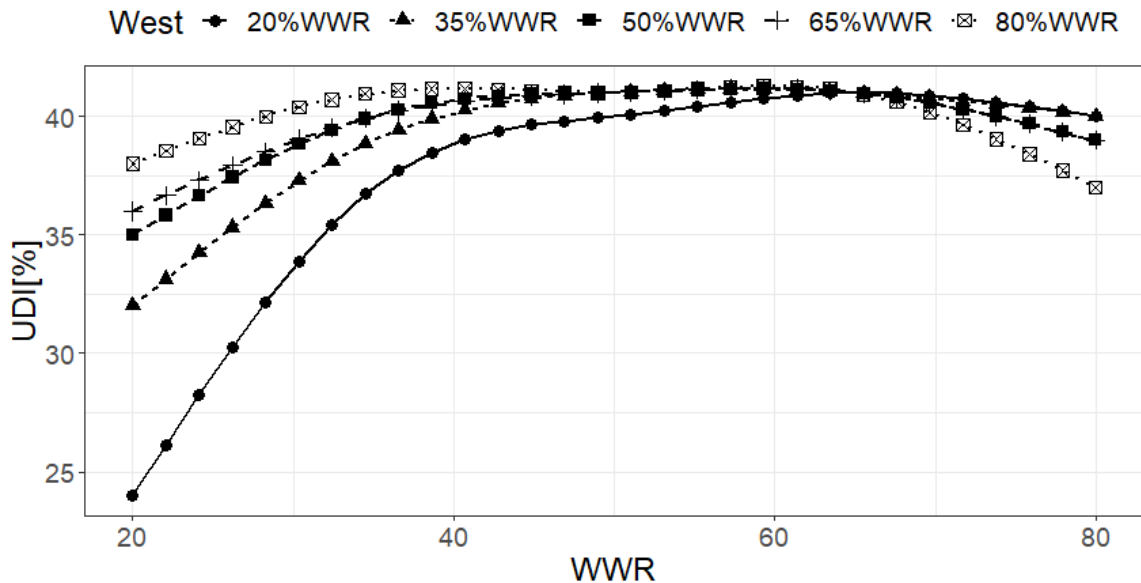


Figure 4.23 UDI 500-2000 for north-facing windows

On the other hand, looking at Figure 4.23, it can be observed that daylighting can be maximized from 40% to 80% of north WWR, which is consistent even if west WWR was changed.

4.3.2.3 Optimum WWR

Considering all criteria: total energy consumption; UDI>2000; and UDI 500-2000, it can be observed that WWR between 40% to 50% is a good choice for north facing windows. In this range, there is a balance between maximizing daylighting and minimizing total energy consumption. Around 37.5% to 40% of UDI₅₀₀₋₂₀₀₀ can be achieved, meaning, 37.5% to 40% of the total daylighting hours in a year can be supplemented by just daylighting alone, given that the preferred illuminance level of occupants is at 500-2000 lux. Also, visual discomfort due to exaggerated daylight illuminance level is not an issue for north facing windows as seen in Figure 4.21.

4.3.3 South Facing Windows

The results for the south facing windows are presented below.

4.3.3.1 Total Energy Consumption

Figures 4.24 to 4.28 present the total energy consumption as a function of WWR for south facing windows of the five different calibrated models and five different values of west WWR.

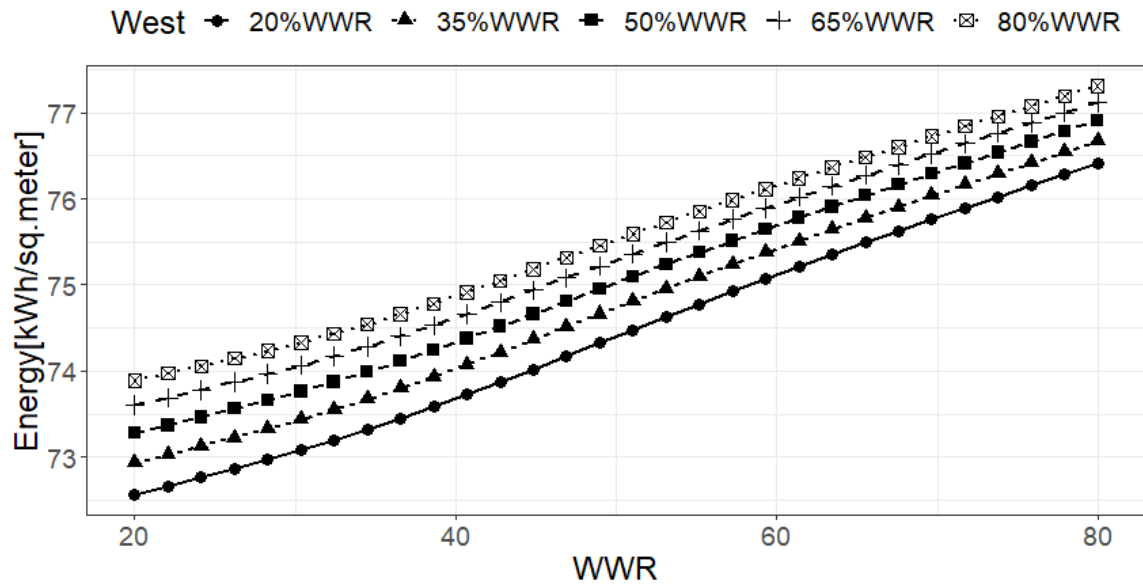


Figure 4.24 Total Energy Consumption for different WWR of Rank 1 Model for south-facing windows

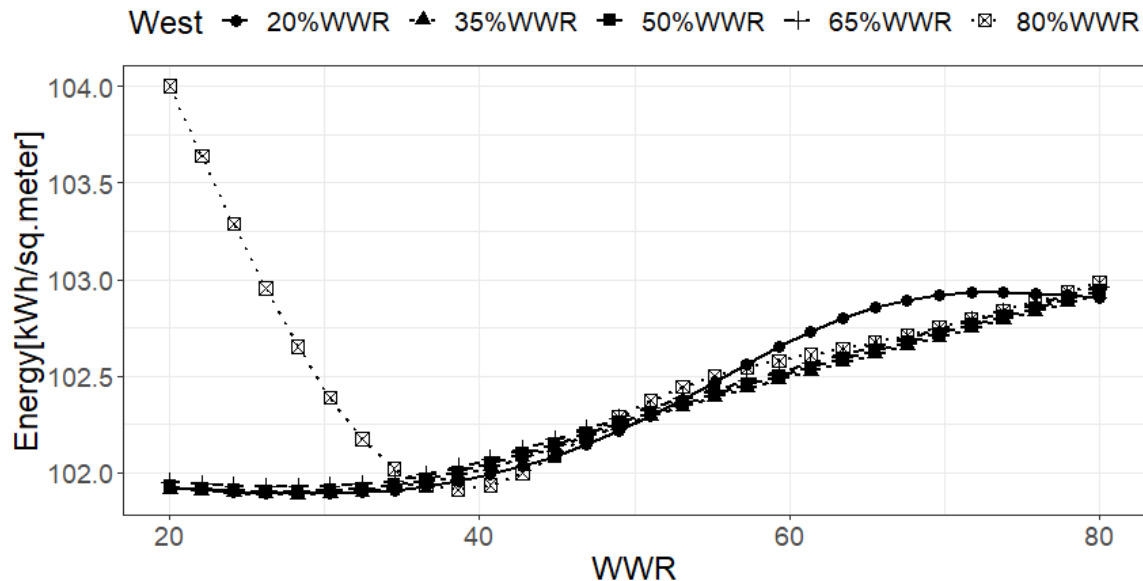


Figure 4.25 Total Energy Consumption for different WWR of Rank 20 Model for south-facing windows

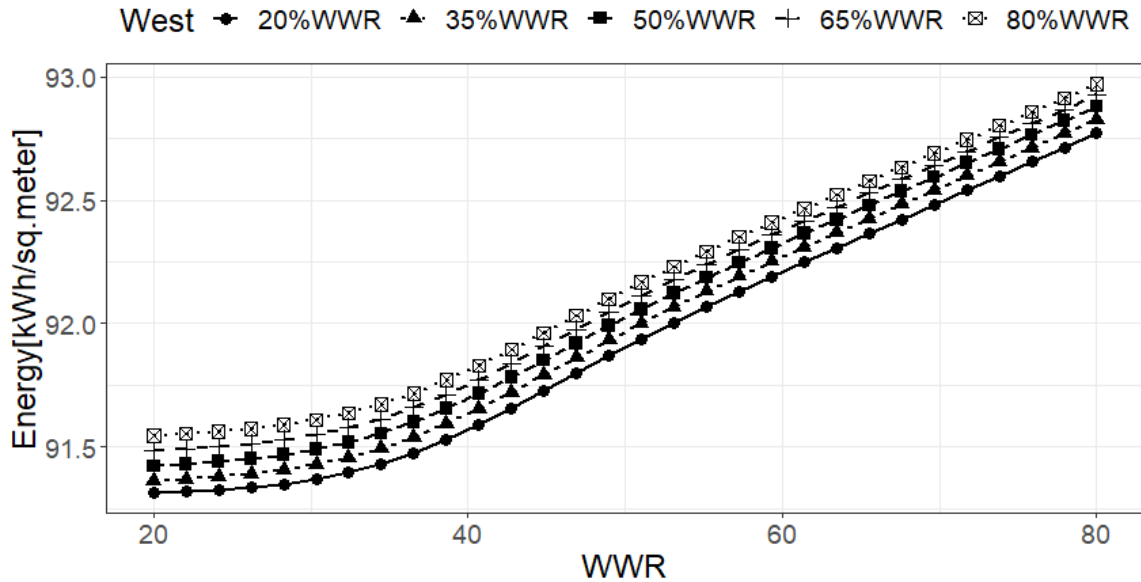


Figure 4.26 Total Energy Consumption for different WWR of Rank 40 Model for south-facing windows

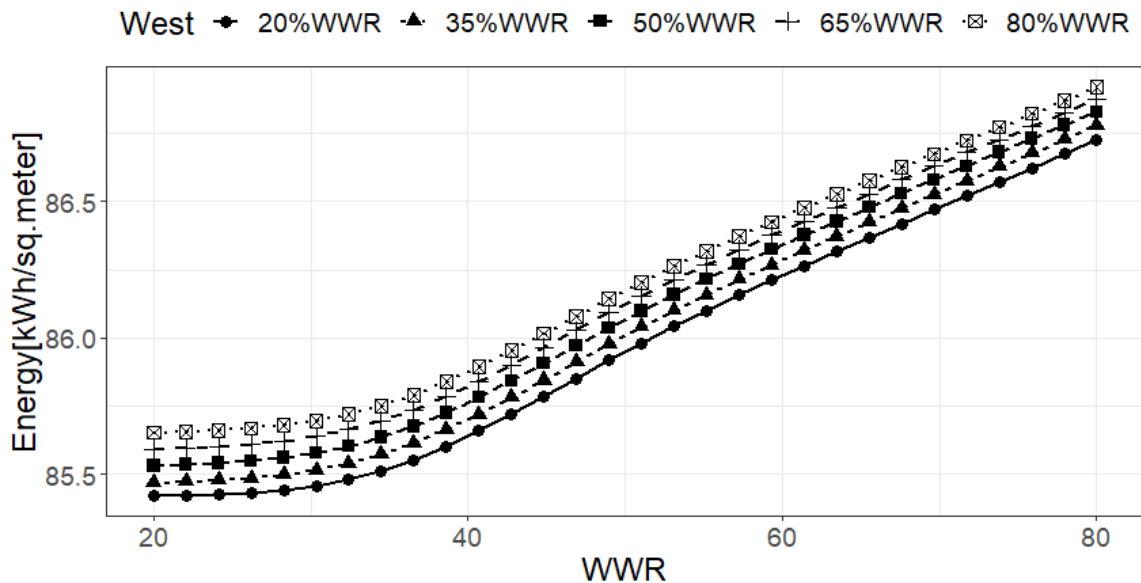


Figure 4.27 Total Energy Consumption for different WWR of Rank 60 Model for south-facing windows

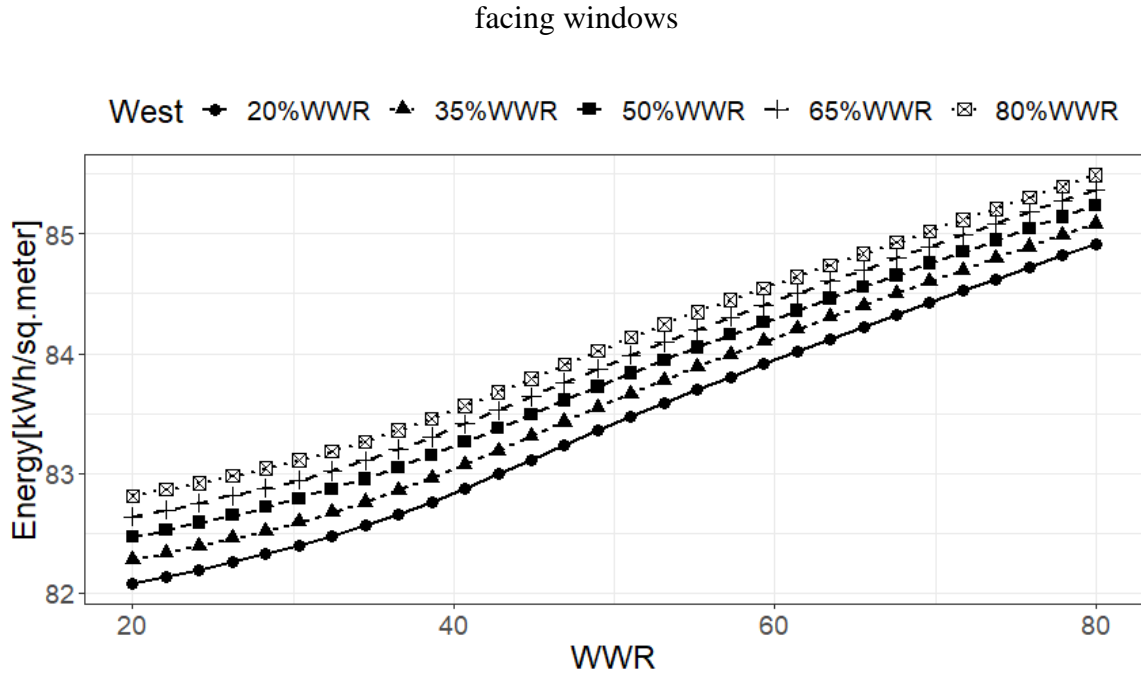


Figure 4.28 Total Energy Consumption for different WWR of Rank 77 Model for south-facing windows

Effect of Using Different Models

Referring to the Figures above, it can be observed that it is consistent for the five different models that as the WWR increases, the total energy consumption also increases. This means that the lesser the size of the south facing windows, the lesser also is the total energy consumption. However, model Rank 20 has a different trend for 80% west WWR. The total energy consumption spikes at 20% south WWR and can be observed to be at the highest. This may be caused by the increase in cooling load since the WWR in west is very large. However, among the five different models, only model Rank 20 displays a different behavior. The parameter that caused this is hard to point out since there were 7 different parameters for the model. This behavior needs to be considered in the optimization of west facing windows if the optimum WWR is at the higher value. For the most part, the percent difference between the best and worst WWR configuration is: 4.8% for Rank 1 model, 1% for Rank 20 model, 1.64% for model Rank 40, 1.52% for model Rank 60, and 3.7% for

model Rank 77.

Effect of Using Different WWR for West

Again, only model Rank 20 shows a “strange” behavior. All other four models show that the WWR in west does not affect the relationship between south WWR and total energy consumption. For model Rank 20, the total energy consumption behaves different at 20% to around 40% south WWR when the west WWR is at 80%. Also, the total energy consumption during around 60% to 75% south WWR behaves differently among others when west WWR is at 20%. This only means that there should be parameter or parameters in model Rank 20 that caused these spikes in total energy consumption. Due to uncertainties in model parameters, this behavior needs to be considered in the optimization of WWR in west – that giving either the smallest (20%) or largest (80%) WWR for west may increase the total energy consumption in rooms that both have south and west facing windows.

4.3.3.2 Daylighting Assessment

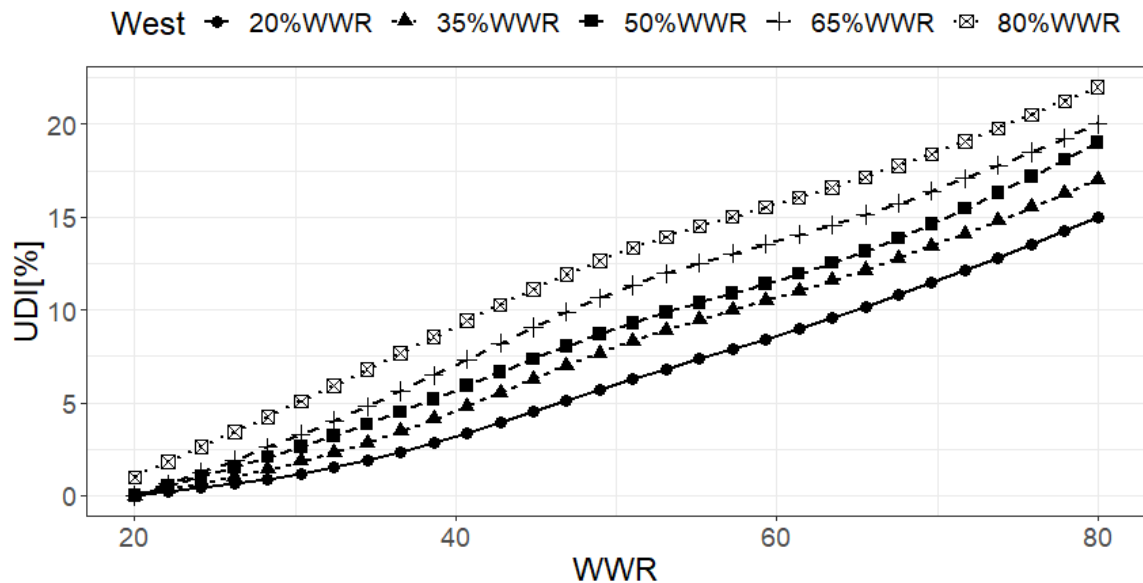


Figure 4.29 UDI >2000 for south-facing windows

It can be seen in Figure 4.29 that visual discomfort would only be an issue if both

west and south WWR is at largest (80% WWR). Referring to the figure, UDI >2000 may go up to 25% if given the said conditions. This is slightly above on what was considered by some researchers to be “tolerable” [34] [14] which is at 20%.

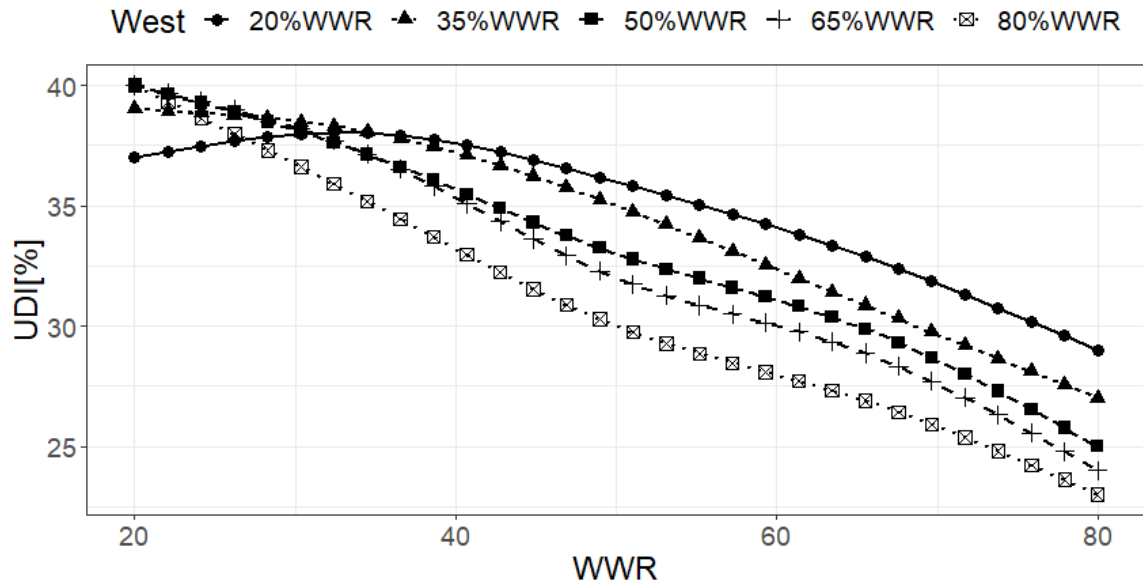


Figure 4.30 UDI 500-2000 for south-facing windows

On the other hand, looking at Figure 4.30, it can be observed that the lesser the WWR in south, the more maximized is the useful daylight illuminance. From the figure, for any WWR in west, the useful daylight illuminance can be maximized at around 20% to 30% south WWR.

4.3.3.3 Optimum WWR

Referring from above results for total energy consumption and useful daylight illuminance, 20% to 30% WWR in south is a good choice to optimize the window size – the smaller the better. Around this range, the least total energy consumption is minimized, and the daylighting is maximized. Around 37.5% to 40% of total daylighting hours can be supplied by daylight alone given that that the building occupants prefer an illuminance level of 500 to 2000 lux.

4.3.4 West Facing Windows

The results of the optimization process for south-facing windows are presented below.

4.3.4.1 Total Energy Consumption

Figure 4.31 present the total energy consumption as a function of WWR for west-facing windows of the five different calibrated models when south WWR is set to 20% and north WWR is set to 40%.

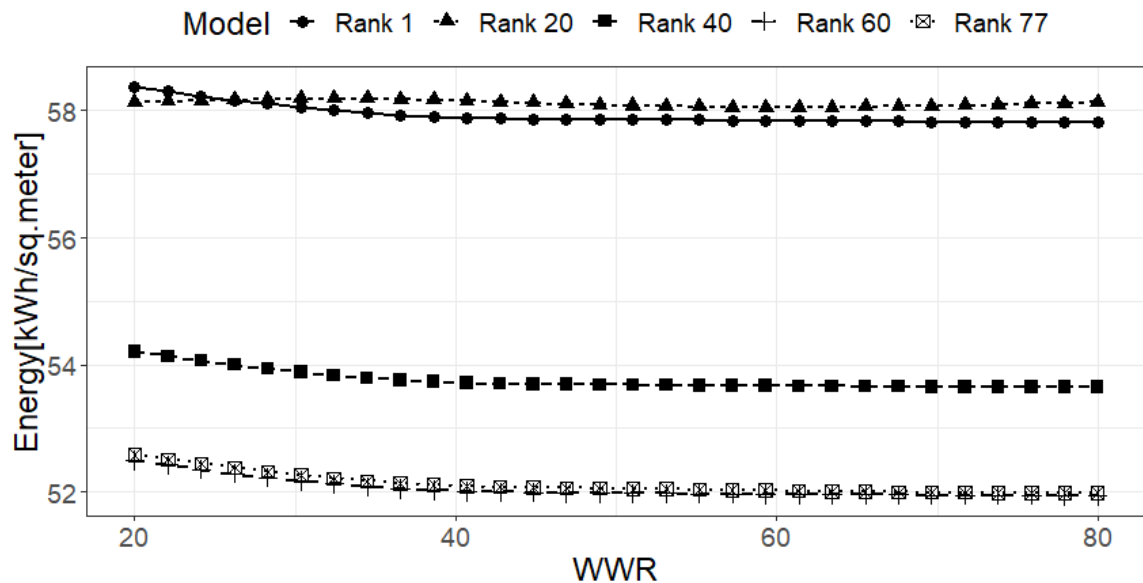


Figure 4.31 Total Energy Consumption for different WWR of the Five Models for west-facing windows

Looking at Figure 4.31, it can be observed that the WWR of west-facing windows does not have a strong effect on the energy consumption of the rooms. For all models used, it can be seen that the total energy consumption does not really change that much along with the change in WWR. Model Rank 20 almost gives a flat trend of total energy consumption as a function of WWR while all others lean towards around 40% to 80% WWR to be the most optimum. However, the change is very small. For example, in model Rank 60 and 77 which almost have the same trend, the worst configuration is at 20% WWR which gives around 52.5 kWh/m^2 and the best configuration which is at 80% WWR gives around 51.9 kWh/m^2 . The worst configuration only gives around 1.16% increase in energy

per floor area. With this result, it can be said that applying too large or too small windows is not a major issue in the viewpoint of total energy consumption. This also means that in optimizing window size for west-facing windows, daylighting assessment will be useful in deciding to the optimum WWR since the energy consumption does not change really that much.

4.3.4.2 Daylighting Assessment

Figure 4.32 present the Useful Daylight Illuminance as a function of WWR for west-facing windows when south WWR is set to 20% and north WWR is set to 40%.

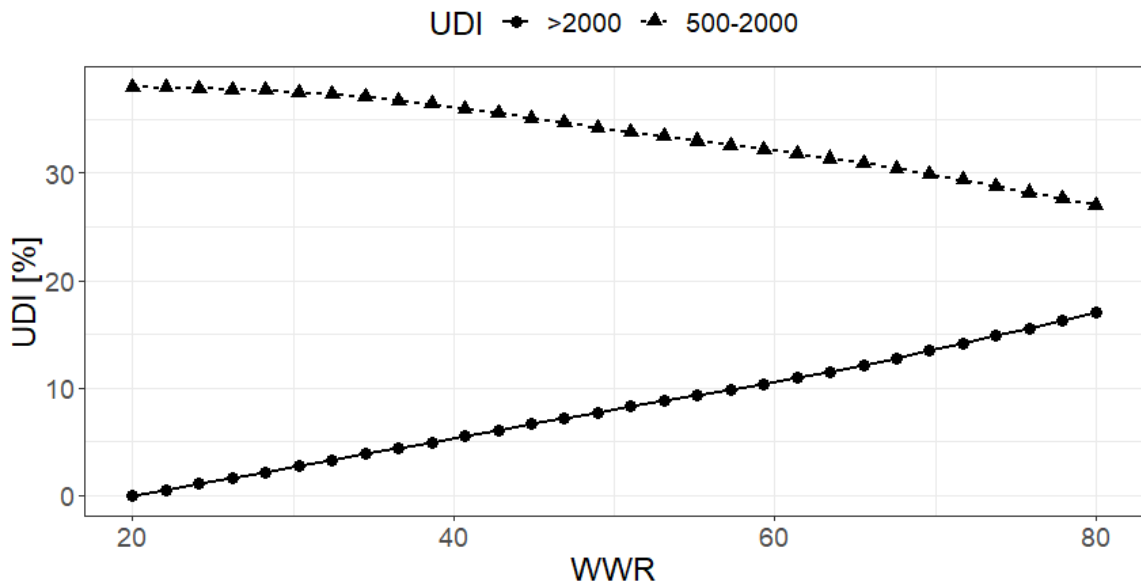


Figure 4.32 Useful Daylight Illuminance for West-facing Windows

Looking at the $UDI_{>2000}$, visual discomfort would only be a slight issue when the WWR is at 80%. The $UDI_{>2000}$ is near 20% when WWR is at the largest. The larger the WWR, the larger also the percentage of $UDI_{>2000}$, which is expected. On the other hand, $UDI_{500-2000}$ can be maximized if the WWR is at the lower spectrum. The less WWR of west-facing windows, the more useful daylight enters the building space. The highest $UDI_{500-2000}$ can be seen at around 20-30% WWR which is around 37.5%. 37.5% $UDI_{500-2000}$ means that 37.5% of the whole daylighting hours in a year is between 500-2000 lux which

is said to be the useful daylight illuminance according to Nabil and Mardaljevic [16]. But it is worth noting that even the UDI 500-2000

4.3.2.3 Optimum WWR

Even though the energy consumption does not change that much, four of the five models suggest that the least energy consumption can be experienced if WWR of west-facing windows is at 40-80%. For the daylighting assessment, visual discomfort is also not a serious issue because based from the result, no WWR will cause the $UDI_{>2000}$ reach 20%. Looking at UDI 500-2000, the largest percentage is at around 37.5% at 20% WWR and the least percentage is around 26% at 80% WWR. Considering all of these results, 40% to 50% of west-facing WWR would be the best choice to minimize the total energy consumption and maximize the useful daylight while not having a concern for visual discomfort. Between this range, around 35% of the total daylighting hours can be provided by just daylight alone with only less than 10% of the total daylighting hours is said to cause visual discomfort. Also, this range is within the range of WWR that causes the least total energy consumption as seen in Figure 4.31.

Chapter 5

Conclusions and Recommendations

5.1 Conclusions

Using a variation of Monte Carlo methods, the study was able to establish calibrated models of the SAFAD building that conform to the requirements set for building energy models. Out from the many calibrated models produced, five different models were used for the analysis of WWR to test the consistency of the results.

The study was able to find the optimum WWR for every building orientation that gives the least total energy consumption while maximizing useful daylight and minimizing the daylight that causes visual discomfort. The optimum WWR is between 20% to 27% for east, 40% to 50% for north, 20% to 30% for south, and 40% to 50% for west.

For east-facing windows, four of the five models suggest a difference of energy consumptions between the best and the worst WWR configuration not more than 5%. For north, south, and west-facing windows, all models suggest a difference between the best and the worst WWR configuration not more than 4%, 5%, and 2% respectively. These results show that potential savings can still be made just by considering the window size during the design process of buildings. However, when planning for retrofit involving window size, careful analysis should be made to test if it is economically reasonable since it can be seen that the difference between the energy consumptions of best and worst configurations are not very large.

The daylighting assessment shows that visual discomfort is not an issue for north-facing windows. For west and south-facing windows, visual discomfort can only be an issue if WWR is around 80%. For east-facing windows, visual discomfort can be a concern if WWR is around 27%-80%. It is also worth noting that only east-facing windows can achieve useful daylight which is at least 50% of the total daylighting hours. This means that daylighting cannot be maximized very much for north, south, and west-facing windows with the existing location and the existing window material of the building.

5.2 Recommendations

There were five different calibrated building energy models used in this study to view the relationship of WWR and total energy consumption if different models were used. The WWR range that gives the least total energy consumption for every orientation can be considered as consistent for the five models used. However, to further test the consistency of the optimum WWR, the use of more calibrated building energy models is recommended.

Moreover, *EnergyPlus* was the only software used to compute the illuminance level for the daylighting assessment. However, it can be found in the literature and in this study that the software has a problem computing illuminance levels for reference points far from the window. This issue was addressed in this study by using only a single reference point which is near the window and was verified through a calibration procedure. However, it is recommended to use different software for the daylighting assessment capable of simulating illuminance levels from different reference points which uses a different sky model and computation method and compare the results to the results from *EnergyPlus*.

Furthermore, since climate is an important factor in optimizing building features, it is recommended that the weather data will be from a local weather station located in the location of the case study building.

Finally, the optimization process performed in this study used an existing school building as the case study building, therefore, the results are only applicable for the case study building or for other buildings with the same details. Since Philippines does not have its guidelines yet, this study is a good starting point in designing energy efficient buildings, however, it is recommended that optimization studies like this will also be performed for other buildings in the Philippines. It would be beneficial for energy efficiency in buildings (EEB) domain in the country to develop benchmark models that are great representatives of all building types in the country, so that research works in the domain of EEB will be easier to perform and the results that would be drawn from the studies would be relevant for all buildings in the whole Philippines.

References

- [1] IEA, “Buildings,” 2018. [Online]. Available: <https://www.iea.org/buildings/>. [Accessed: 30-Nov-2018].
- [2] DOE, “2016 Philippine Power Situation Report | DOE | Department of Energy Portal,” 2016. [Online]. Available: <https://www.doe.gov.ph/electric-power/2016-philippine-power-situation-report>. [Accessed: 30-Nov-2018].
- [3] J. Kneifel, “Life-cycle carbon and cost analysis of energy efficiency measures in new commercial buildings,” vol. 42, pp. 333–340, 2010.
- [4] R. Ruparathna, K. Hewage, and R. Sadiq, “Improving the energy efficiency of the existing building stock: A critical review of commercial and institutional buildings,” *Renew. Sustain. Energy Rev.*, vol. 53, no. 1, pp. 1032–1045, 2016.
- [5] S. Grynning, A. Gustavsen, B. Time, and B. Petter, “Windows in the buildings of tomorrow : Energy losers or energy gainers ?,” *Energy Build.*, vol. 61, pp. 185–192, 2013.
- [6] M. K. Urbikain and J. M. Sala, “Analysis of different models to estimate energy savings related to windows in residential buildings,” *Energy Build.*, vol. 41, no. 6, pp. 687–695, 2009.
- [7] Z. Djamel and Z. Noureddine, “The Impact of Window Configuration on the Overall Building Energy Consumption under Specific Climate Conditions,” *Energy Procedia*, vol. 115, pp. 162–172, 2017.
- [8] H. Shen and A. Tzempelikos, “Sensitivity analysis on daylighting and energy performance of perimeter offices with automated shading,” *Build. Environ.*, vol. 59, pp. 303–314, 2013.
- [9] R. A. Mangkuto, M. Rohmah, and A. D. Asri, “Design optimisation for window size, orientation, and wall reflectance with regard to various daylight metrics and lighting energy demand: A case study of buildings in the tropics,” *Appl. Energy*, vol. 164, pp. 211–219, 2016.
- [10] L. P. Rosa and L. L. B. Lomardo, “The Brazilian energy crisis and a study to support building efficiency legislation,” *Energy Build.*, vol. 36, no. 2, pp. 89–95, 2004.
- [11] R. Foroughi, E. Mostavi, and S. Asadi, “Determining the Optimum Geometrical Design Parameters of Windows in Commercial Buildings: Comparison between Humid Subtropical and Humid Continental Climate Zones in the United States,” *J. Archit. Eng.*, vol. 24, no. 4, p. 04018026, 2018.
- [12] A. Ghosh and S. Neogi, “Effect of fenestration geometrical factors on building energy consumption and performance evaluation of a new external solar shading

- device in warm and humid climatic condition,” *Sol. Energy*, vol. 169, no. March 2017, pp. 94–104, 2018.
- [13] L. G. Maltais and L. Gosselin, *Daylighting ‘energy and comfort’ performance in office buildings: Sensitivity analysis, metamodel and pareto front*, vol. 14. 2017.
 - [14] F. Goia, “Search for the optimal window-to-wall ratio in office buildings in different European climates and the implications on total energy saving potential,” *Sol. Energy*, vol. 132, pp. 467–492, 2016.
 - [15] B. Ross-Larson and Steven C Francis, “Regulatory indicators for Sustainable Energy: A Global Scorecard for Policy Makers,” *Int. Bank Reconstr. Dev. / World Bank*, p. 264, 2016.
 - [16] A. Nabil and J. Mardaljevic, “Useful daylight illuminance: a new paradigm for assessing daylight in buildings,” *Light. Res. Technol.*, vol. 37, no. 1, pp. 41–59, 2005.
 - [17] C. Lee and J. Won, “Analysis of combinations of glazing properties to improve economic efficiency of buildings,” *J. Clean. Prod.*, vol. 166, pp. 181–188, 2017.
 - [18] F. Arumi, “Day lighting as a factor in optimizing the energy performance of buildings,” *Energy Build.*, vol. 1, no. 2, pp. 175–182, 1977.
 - [19] R. Johnson, R. Sullivan, S. Selkowitz, S. Nozaki, C. Conner, and D. Arasteh, “Glazing Energy Performance and Design Optimization with Daylighting,” *Energy Build.*, vol. 6, no. 4, pp. 305–317, 1984.
 - [20] M. N. Inanici and F. N. Demirbilek, “Thermal performance optimization of building aspect ratio and south window size in ® ve cities having di € erent climatic characteristics of Turkey,” vol. 35, 2000.
 - [21] E. Ghisi and J. Tinker, “OPTIMISING ENERGY CONSUMPTION IN OFFICES AS A FUNCTION OF WINDOW AREA AND ROOM SIZE Enedir Ghisi and John Tinker School of Civil Engineering , University of Leeds,” *Seventh Int. IBPSA Conf.*, no. m, pp. 1307–1314, 2001.
 - [22] E. Ghisi and J. A. Tinker, “An Ideal Window Area concept for energy e cient integration of daylight and artiÿcial light in buildings,” vol. 40, pp. 51–61, 2005.
 - [23] F. U. Xiuzhang, “Architectural Strategies for Low Energy House in Nanjing hot-summer and cold-winter region in China . As an example , a typical multi-story house in Nanjing is energy analysis), and the result shows that the most effective strategy to reduce the energy n,” pp. 1–5, 2004.
 - [24] C. K. Cheung, R. J. Fuller, and M. B. Luther, “Energy-efficient envelope design for high-rise apartments,” vol. 37, no. March 2004, pp. 37–48, 2005.
 - [25] M. Persson, A. Roos, and M. Wall, “Influence of window size on the energy

- balance of low energy houses,” vol. 38, pp. 181–188, 2006.
- [26] A. Gasparella, G. Pernigotto, F. Cappelletti, P. Romagnoni, and P. Baggio, “Analysis and modelling of window and glazing systems energy performance for a well insulated residential building,” *Energy Build.*, vol. 43, no. 4, pp. 1030–1037, 2011.
 - [27] C. Bouden, “Influence of glass curtain walls on the building thermal energy consumption under Tunisian climatic conditions: The case of administrative buildings,” *Renew. Energy*, vol. 32, no. 1, pp. 141–156, 2007.
 - [28] G. Feng, D. Chi, X. Xu, B. Dou, Y. Sun, and Y. Fu, “Study on the Influence of Window-wall Ratio on the Energy Consumption of Nearly Zero Energy Buildings,” *Procedia Eng.*, vol. 205, pp. 730–737, 2017.
 - [29] S. K. Alghoul, H. G. Rijabo, and M. E. Mashena, “Energy consumption in buildings: A correlation for the influence of window to wall ratio and window orientation in Tripoli, Libya,” *J. Build. Eng.*, vol. 11, pp. 82–86, 2017.
 - [30] F. M. Abed, O. K. Ahmed, and A. E. Ahmed, “Effect of climate and design parameters on the temperature distribution of a room,” *J. Build. Eng.*, vol. 17, pp. 115–124, 2018.
 - [31] Y. Zhai, Y. Wang, Y. Huang, and X. Meng, “A multi-objective optimization methodology for window design considering energy consumption, thermal environment and visual performance,” *Renew. Energy*, 2018.
 - [32] J. W. Lee, H. J. Jung, J. Y. Park, J. B. Lee, and Y. Yoon, “Optimization of building window system in Asian regions by analyzing solar heat gain and daylighting elements,” *Renew. Energy*, vol. 50, pp. 522–531, 2013.
 - [33] C. E. Ochoa, M. B. C. Aries, E. J. van Loenen, and J. L. M. Hensen, “Considerations on design optimization criteria for windows providing low energy consumption and high visual comfort,” *Appl. Energy*, vol. 95, pp. 238–245, 2012.
 - [34] F. Goia, M. Haase, and M. Perino, “Optimizing the configuration of a façade module for office buildings by means of integrated thermal and lighting simulations in a total energy perspective,” *Appl. Energy*, vol. 108, pp. 515–527, 2013.
 - [35] C. F. Reinhart and O. Walkenhorst, “Validation of dynamic RADIANCE-based daylight simulations for a test office with external blinds,” *Energy Build.*, vol. 33, no. 7, pp. 683–697, 2001.
 - [36] B. Lartigue, B. Lasternas, and V. Loftness, “Indoor and Built Multi-objective optimization of building envelope for energy consumption and daylight,” vol. 23, no. 1, pp. 70–80, 2014.
 - [37] P. Xue, Q. Li, J. Xie, M. Zhao, and J. Liu, “Optimization of window-to-wall ratio

- with sunshades in China low latitude region considering daylighting and energy saving requirements,” *Appl. Energy*, vol. 233–234, no. 100, pp. 62–70, 2019.
- [38] “POWER Data Access Viewer.” [Online]. Available: <https://power.larc.nasa.gov/data-access-viewer/>. [Accessed: 07-Dec-2018].
 - [39] ASHRAE, “ANSI/ASHRAE Standard 169-2013 - Climatic Data for Building Design Standards,” p. 98, 2013.
 - [40] RISE, “Philippines | RISE.” [Online]. Available: <http://rise.worldbank.org/country/philippines>. [Accessed: 03-Dec-2018].
 - [41] “17th Congress - Senate Bill No. 1531 - Senate of the Philippines.” [Online]. Available: https://www.senate.gov/lis/bill_res.aspx?congress=17&q=SBN-1531. [Accessed: 03-Dec-2018].
 - [42] “THE PHILIPPINE GREEN BUILDING CODE,” 2015.
 - [43] “Guidelines For Energy Conserving Design of Buildings and Utility Systems | DOE | Department of Energy Portal.” [Online]. Available: <https://www.doe.gov.ph/guidelines-energy-conserving-design-buildings-and-utility-systems>. [Accessed: 03-Dec-2018].
 - [44] G. Ramos and E. Ghisi, “Analysis of daylight calculated using the EnergyPlus programme,” *Renew. Sustain. Energy Rev.*, vol. 14, no. 7, pp. 1948–1958, 2010.
 - [45] R. Perez, P. Ineichen, R. Seals, J. Michalsky, and R. Stewart, “Modeling daylight availability and irradiance components from direct and global irradiance,” *Sol. Energy*, vol. 44, no. 5, pp. 271–289, 1990.
 - [46] D. B. Crawley *et al.*, “EnergyPlus : creating a new-generation building energy simulation program,” vol. 33, 2001.
 - [47] D. K. K. Arasteh, M. S. S. Reilly, and M. D. Rubin, “A Versatile Procedure for Calculating Heat Transfer Through Windows,” *ASHRAE Transactions*, vol. 95.2, no. 2, pp. 755–765, 1989.
 - [48] D. Arasteh, E. Finlayson, J. Huang, C. Huizenga, R. Mitchell, and M. Rubin, “State-of-the-art software for window energy-efficiency rating and labeling,” no. July, pp. 1–5, 1998.
 - [49] F. C. Winkelmann, “Modeling Windows in Energyplus,” *Build. Simul. 2001*, no. May, pp. 457–464, 2001.
 - [50] F. C. Winkelmann and S. Selkowitz, “Daylighting simulation in the DOE-2 building energy analysis program,” *Energy Build.*, vol. 8, no. 4, pp. 271–286, 1985.
 - [51] T. A. Reddy, I. Maor, and C. Panjapornpon, “Calibrating Detailed Building Energy Simulation Programs with Measured Data — Part II : Application to Three Case

- Study Office Buildings (RP-1051) Simulation Programs with Measured Data — Part II : Application to Three Case Study,” vol. 9669, no. April, 2016.
- [52] D. Coakley, P. Raftery, and M. Keane, “A review of methods to match building energy simulation models to measured data,” *Renewable and Sustainable Energy Reviews*, vol. 37. Elsevier, pp. 123–141, 2014.
 - [53] E. Fabrizio and V. Monetti, “Methodologies and Advancements in the Calibration of Building Energy Models,” pp. 2548–2574, 2015.
 - [54] T. A. Reddy, I. Maor, C. Panjapornpon, and T. A. Reddy, “Calibrating Detailed Building Energy Simulation Programs with Measured Data — Part I : General Methodology (RP-1051) Simulation Programs with Measured Data — Part I : General Methodology (RP-1051),” vol. 9669, no. April, 2016.
 - [55] ASHRAE, *ASHRAE 14*. 2002.
 - [56] IPMVP New Construction Subcommittee, “IPMVP - Efficiency Valuation Organization (EVO),” 2001. [Online]. Available: <https://evo-world.org/en/products-services-mainmenu-en/protocols/ipmvp>. [Accessed: 03-Dec-2018].
 - [57] FEMP, “M&V Guidelines: Measurement and Verification for Performance-Based Contracts (Version 4.0) | Department of Energy,” 2008. [Online]. Available: <https://www.energy.gov/eere/femp/downloads/mv-guidelines-measurement-and-verification-performance-based-contracts-version>. [Accessed: 03-Dec-2018].
 - [58] T. A. Reddy, “Literature Review on Calibration of Building Energy Simulation ...,” 2006.
 - [59] A. Pedrini, F. S. Westphal, and R. Lamberts, “A methodology for building energy modelling and calibration in warm climates,” vol. 37, pp. 903–912, 2002.
 - [60] M. Manfren, N. Aste, and R. Moshksar, “Calibration and uncertainty analysis for computer models – A meta-model based approach for integrated building energy simulation,” *Appl. Energy*, vol. 103, pp. 627–641, 2013.
 - [61] Z. Yang and B. Becerik-gerber, “A model calibration framework for simultaneous multi-level building energy simulation,” *Appl. Energy*, vol. 149, pp. 415–431, 2015.
 - [62] W. Tian, “A review of sensitivity analysis methods in building energy analysis,” *Renew. Sustain. Energy Rev.*, vol. 20, pp. 411–419, 2013.
 - [63] D. M. King and B. J. C. Perera, “Morris method of sensitivity analysis applied to assess the importance of input variables on urban water supply yield – A case study,” *J. Hydrol.*, vol. 477, pp. 17–32, 2013.
 - [64] P. Taylor, M. D. Morris, and M. D. Morris, “Computational Experiments Factorial

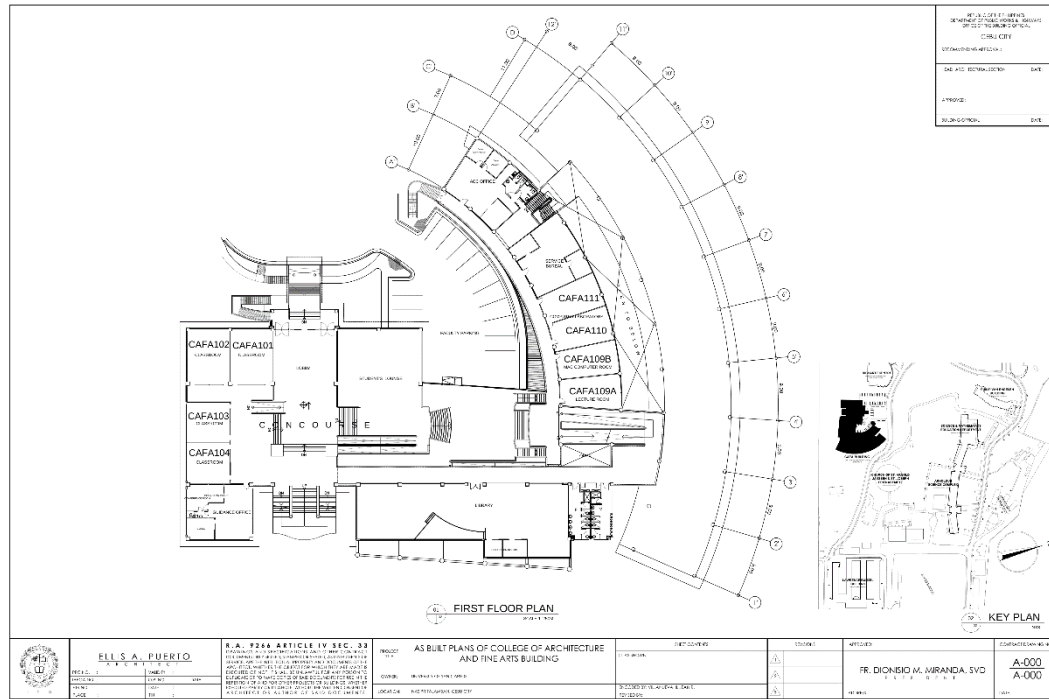
- Sampling Plans for Preliminary Computational Experiments,” no. September 2013, pp. 37–41, 2012.
- [65] J. C. Helton and F. J. Davis, “Latin hypercube sampling and the propagation of uncertainty in analyses of complex systems,” vol. 81, pp. 23–69, 2003.
 - [66] “ISO 13786:2017 - Thermal performance of building components -- Dynamic thermal characteristics -- Calculation methods.” [Online]. Available: <https://www.iso.org/standard/65711.html>. [Accessed: 14-Jan-2019].
 - [67] F. Campolongo, J. Cariboni, and A. Saltelli, “An effective screening design for sensitivity analysis of large models,” vol. 22, 2007.

APPENDICES

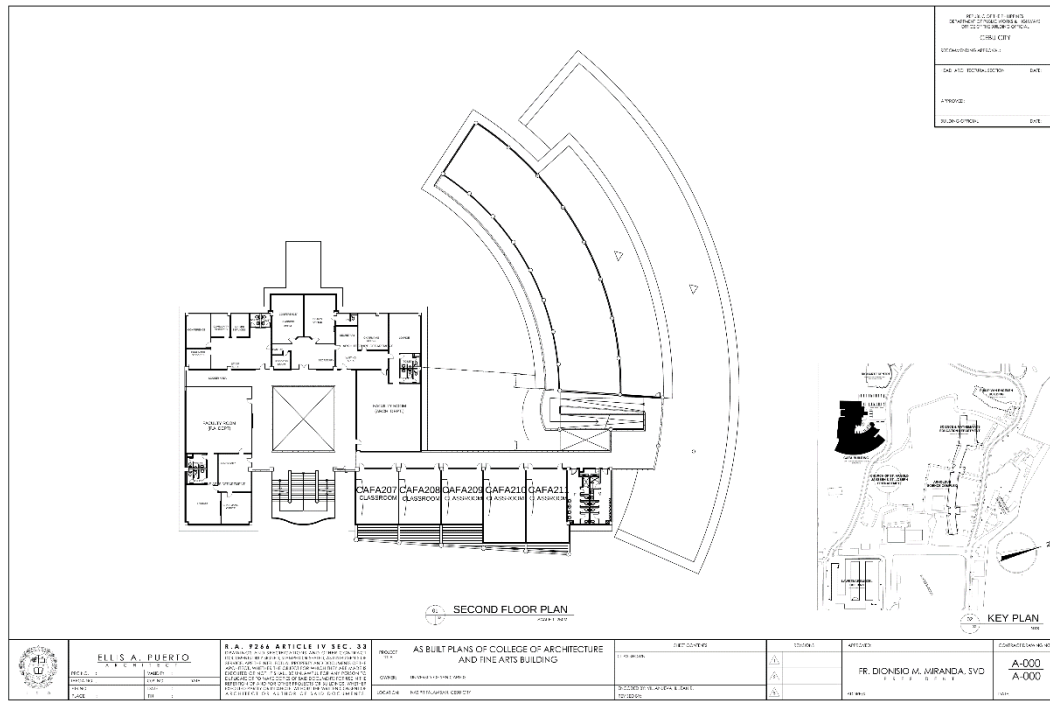
Appendix A. Case Study Building Details

Appendix A.1 Floor Plan Layout of SAFAD Building

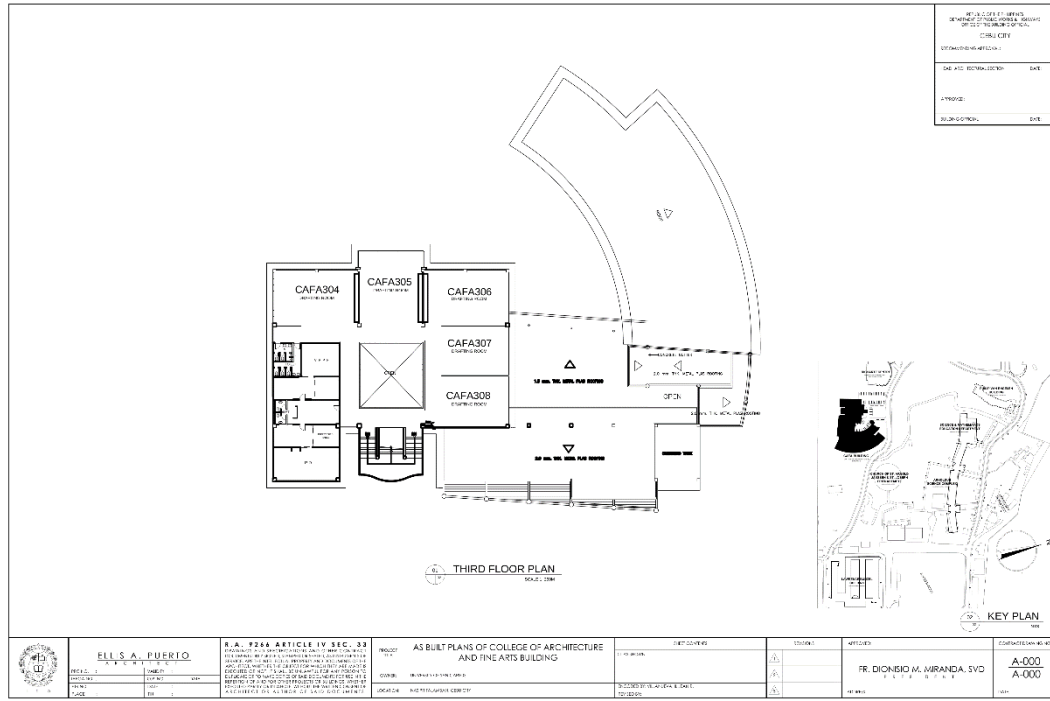
Appendix A.1.1 First Floor Plan Layout



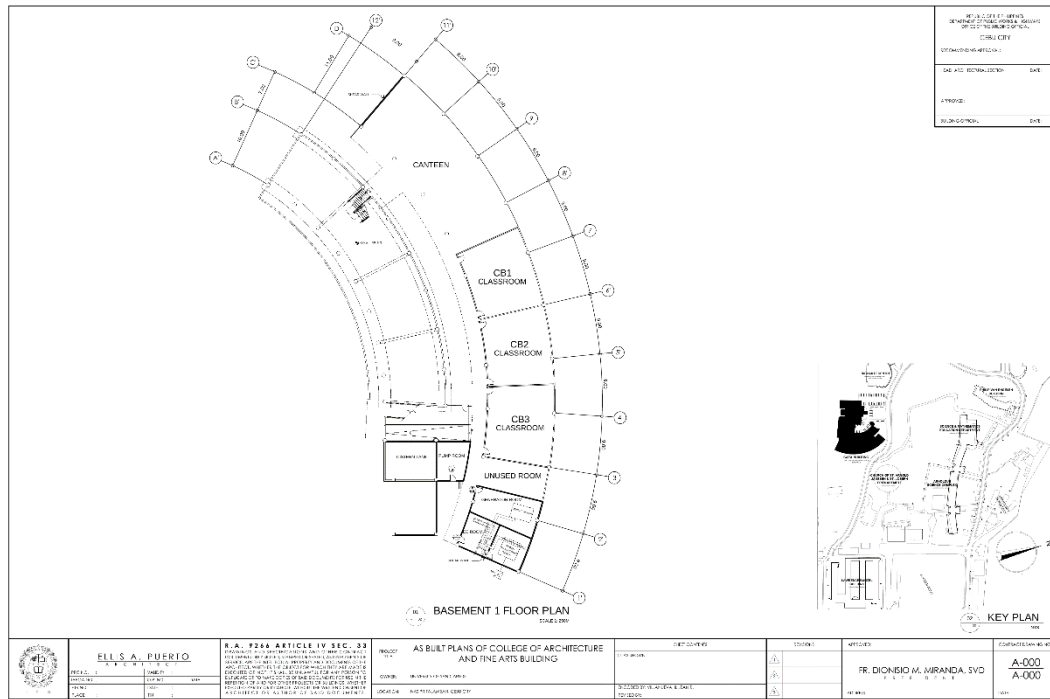
Appendix A.1.2 Second Floor Plan Layout



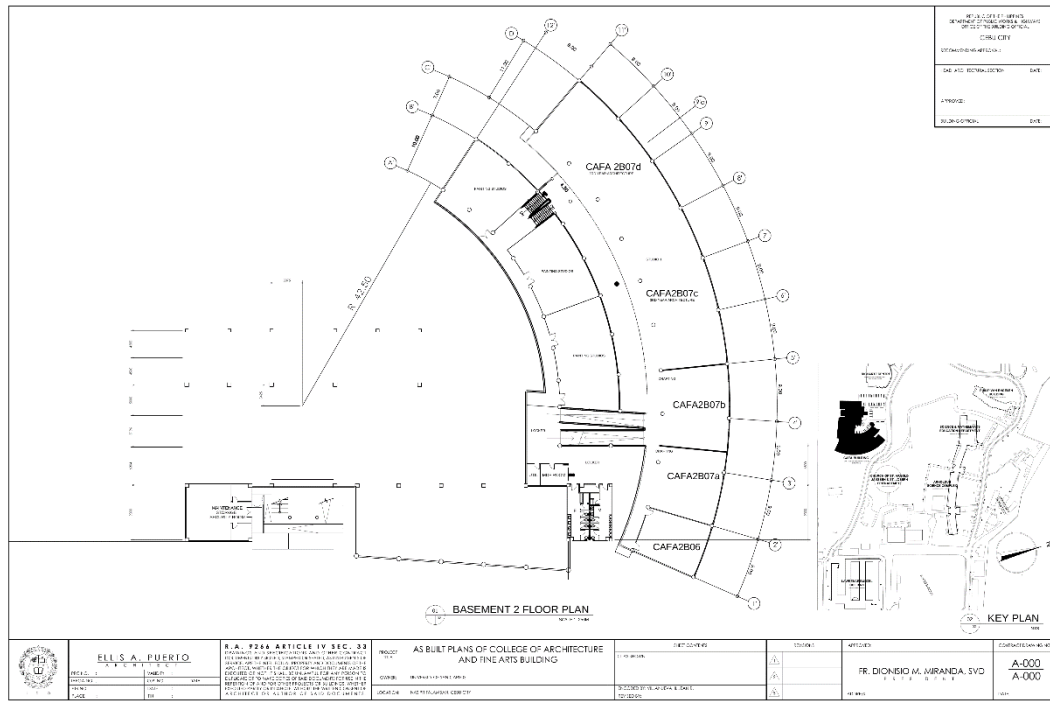
Appendix A.1.3 Third Floor Plan Layout



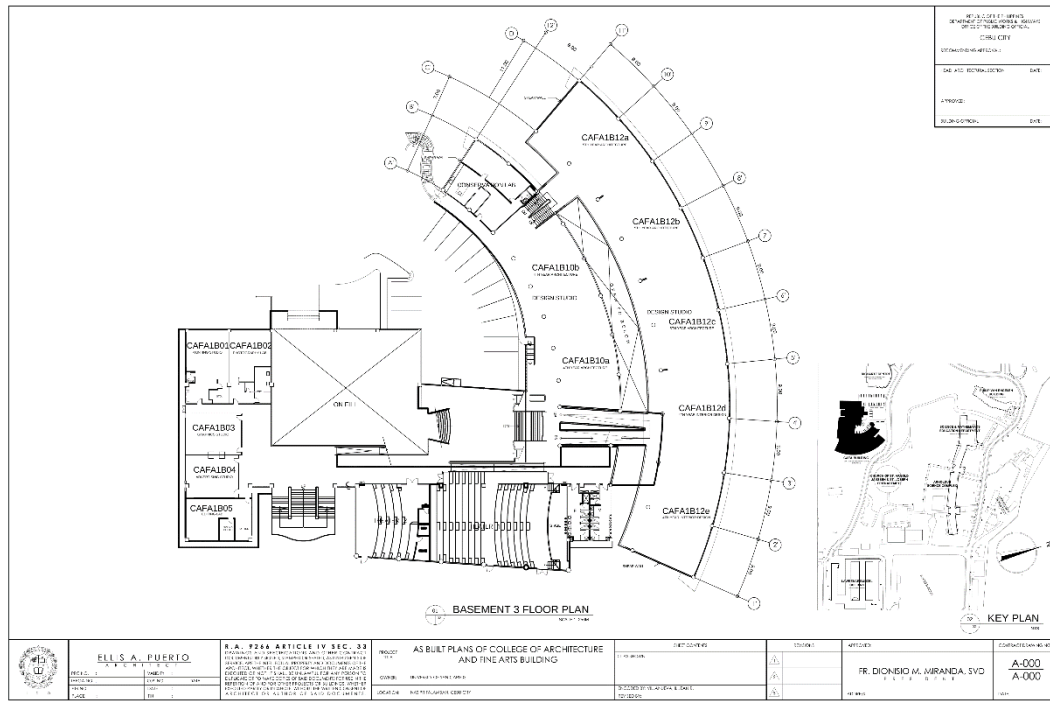
Appendix A.1.4 Basement 1 Floor Plan Layout



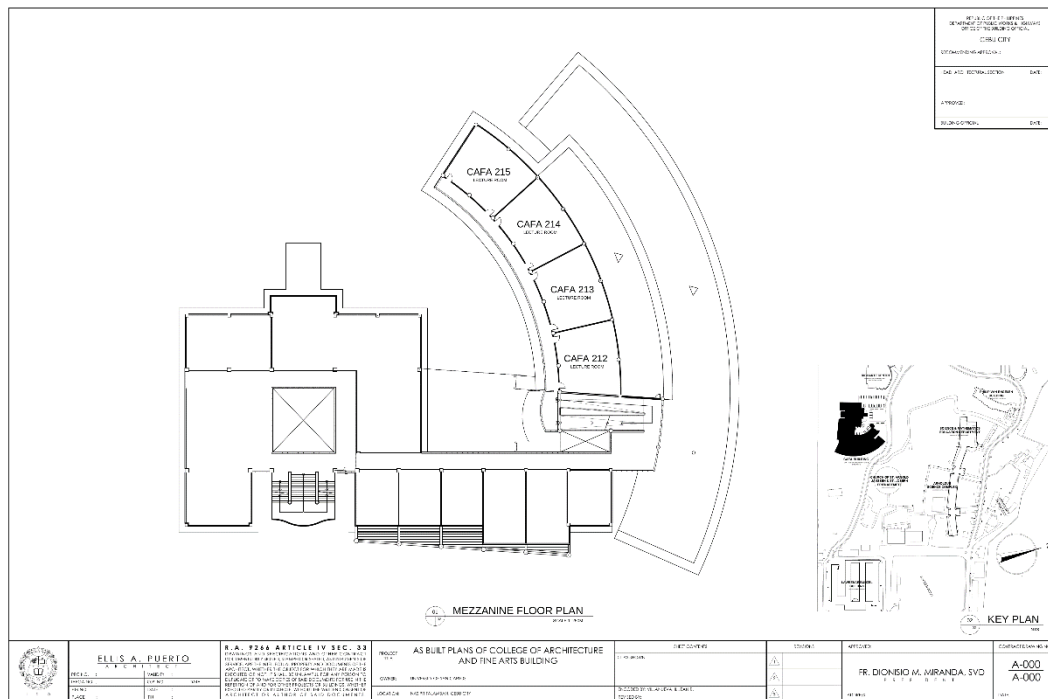
Appendix A.1.5 Basement 2 Floor Plan Layout



Appendix A.1.6 Basement 3 Floor Plan Layout



Appendix A.1.7 Mezzanine Floor Plan Layout



Appendix A.2 Window, Lighting, Equipment, and ACU Details

The images below present the window area, number of artificial lightings, number of air conditioners, and the plugged equipment in each room. For the walls, it can be observed that all rooms have uniform construction of walls, the walls are all cement except for walls that separate two different rooms which are made up of plyboards, this is explained carefully in Chapter 3.

Rooms	Wall	Window	Loads		
			Lighting	ACU	Equipment
ACC Service Bureau	out cement in plyboard	5x2east	20 T5	4 split ACU	8 PC, 1 apple computer, 5 printers
ACC Office	out cement in plyboard	5x2east	14 T5	2 split ACU	1 refrigerator, 4 apple computer, 4 PC, 3 printers
First Floor M CR	out cement in plyboard	6x2south	4 T5		
First Floor F CR	out cement in plyboard				
AF 207	out cement in plyboard	.697x 4.676north, 2x6.3south	6 T5, 3 Pinlight	2split ACU	1 Panasonic Projector
AF 208	out cement in plyboard	.697x 4.676north, 2x6.3south	6 T5, 3 Pinlight	2split ACU	1 Panasonic Projector
AF 209	out cement in plyboard	.697x 4.676north, 2x6.3south	6 T5, 3 Pinlight	2split ACU	1 Panasonic Projector
AF 210	out cement in plyboard	.697x 4.676north, 2x6.3south	8 T5, 3 Pinlight	2split ACU	1 Epson Projector
AF 211	out cement in plyboard	.697x 4.676north, 2x6.3south	8 T5, 3 Pinlight	2split ACU	1 Epson Projector
AF 212	out cement in plyboard	.635x4.936west	18 T5, 3 5watss Pinlight LED	2split ACU	1 Panasonic projector

AF 213	out cement in plyboard	.635x4.936west	18 T5, 3 5watss Pinlight LED	2split ACU	1 Panasonic projector
AF 214	out cement in plyboard	.635x4.936west	18 LED philips (19W), 16 28W philips light, 2pinlights(9 W)	2split ACU	1 sanyo projector, 20 sewing machines - Juki DDL 8700
AF 215	out cement in plyboard	.635x4.936west	18 LED philips (19W), 16 28W philips light, 2pinlights(9 W)	2split ACU	1 sanyo projector, 20 sewing machines - Juki DDL 8700
FINE ARTS DEPARTMENT	out cement in plyboard	7.3x2east, 10x2south, 8.4x2west, 1.87x2west	6 T5	2 split ACU	1 PC, 1 apple computer, 2 printers
FINE ARTS FACULTY	out cement in plyboard	10.75x2west	19 T5	2 split ACU	1 projector, 1 TV, 1 water dispenser, 1 ref

FINE ARTS FACULTY	out cement in plyboard	10.75x2west	19 T5	2 split ACU	1 projector, 1 TV, 1 water dispenser, 1 ref
ARCHITECTURE FACULTY	out cement in plyboard	4.4x2north, 8.4x2east, 13x2east	20 T5, 2 pinlights	3 split ACU	13 PC, 1 water dispenser, 1 refrigerator, 1 printer
ARCHITECTURE DEPT	out cement in plyboard	5.7x2north, 1.3x2north	8 T5, 5 pinlights	2 split ACU	3 PC, 3 apple computer, 1 printer
DEAN SECRETARY OFFICE	out cement in plyboard		4 T5, 4 pinlights	1 split ACU	1 PC, 1 refrigerator, 2 printers
CONFERENCE ROOM	out cement in plyboard	5x2north, 2.5x2west	2 T5, 6 pinlight	1 split ACU	1 water dispenser, 1 projector
DEAN OFFICE	out cement in plyboard	5x2north, 2.5x2east	2 T5, 6 pinlights	1 split ACU	1 apple computer
AUXILLIARY OFFICES	out cement in plyboard	5.7x2north, 5.7x2north	16 T5, 3 pinlight	3 split ACU	1 TV, 5 PC, 3 apple computer
2ND M CR	out cement in plyboard	5.35x2south	1 pinlight, 2 T5		
2ND FM CR	out cement in plyboard		1 pinlight, 2 T5		
AF 304	out cement in plyboard	5.7x2north, 5.7x2north, 8.4x2west	18 T5	2split ACU	1 Epson projector, 4ceiling fan
AF 305	out cement in plyboard	10x2north, 2.5x2east, 2.5x2west	24 T5, 3 Pinlight		4 wall fans
AF 306	out cement in plyboard	5.7x2north, 5.7x2north, 8.4x2east	24 T5, 3 Pinlight	2split ACU	1 Panasonic projector, 4 wall fans
AF 307	out cement in plyboard	.85x7.6east	24 T5 (26W), 3 Pinlight		4 wall fans
AF 308	out cement in plyboard		24 T5 (26W), 3 Pinlight		4 wall fans
IPD	out cement in plyboard	7.3x2east, 10x2south, 8.4x2west	22 T5, 3 120watts light	2 split acu	9 pc, 1 electric fan, 3 printers

IPD CR	out cement in plyboard	3.36x2west	2 T5		
VPPF	out cement in plyboard	9.24x2west	6 T5	1 split ACU	1 projector, 1 laptop, 4 PC
AF 1B01	out cement in plyboard	6.4x2west			
AF 1B02	out cement in plyboard				
AF 1B03	out cement in plyboard	6.4x2west	8 t5	4 ceiling fans	
AF 1B04	out cement in plyboard	6.4x2west, 0.5x2west	8 T5	4 ceiling fans	
AF 1B05	out cement in plyboard	7x2west,10x2south	10 t5		
AF 1B10A	out cement in plyboard	5.4x2east,5.4x2east,5.4x2	66 T5 LED Philips		
AF 1B10B	out cement in plyboard	east,5.4x2east,5.4x2east		8 ceiling fans	
AF 1B12A	out cement in plyboard	16.3x2east	18 T5	2 ACU Daikin	1 projector, 4 Ceiling Fans
AF 1B12B	out cement in plyboard	17x2east	18 T5	2 ACU Daikin	1 projector, 4 Ceiling Fans
AF 1B12C	out cement in plyboard	11x2east	18 T5	2 ACU Daikin	1 projector, 4 Ceiling Fans

AF 1B12C	out cement in plyboard	11x2east	18 T5	2 ACU Daikin	1 projector, 4 Ceiling Fans
AF 1B12D	out cement in plyboard	11x2east	18 T5	2 ACU Daikin	1 projector, 4 Ceiling Fans
AF 1B12E	out cement in plyboard	11x2east	18 T5	2 ACU Daikin	1 projector, 4 Ceiling Fans
AF 1B12F	out cement in plyboard	13.2x2east	18 T5	2 ACU Daikin	1 projector, 4 Ceiling Fans
BASEMENT 3 CR	out cement in plyboard	6x2south	4 T5		
CONSERVATION LAB	out cement in plyboard	5x2east, 5x2east			
2B06	out cement in plyboard	7x2east	12 t5		2 ceiling fans
2B07A	out cement in plyboard	10.5x2east	18 t5		4 ceiling fans
2B07B	out cement in plyboard	10.5x2east	18 t5		5 ceiling fans
2B07C	out cement in plyboard	10.5x2east	12 t5		3 ceiling fans
2B07D	out cement in plyboard	10.5x2east	24 t5		4 ceiling fans
2B07E	out cement in plyboard	10.5x2east	12 t5		2 ceiling fans
2B07F	out cement in plyboard	10.5x2east	24 t5		4 ceiling fans

PAINTING STUDIO	out cement in plyboard		seldom used	
1				
PAINTING STUDIO	out cement in plyboard		seldom used	
2				
PAINTING STUDIO	out cement in plyboard		seldom used	
3				
CB2	out cement in plyboard	8x2east	18 T5	2 split ACU
CB1	out cement in plyboard	8x2east	18 T5	2 split ACU
CB3	out cement in plyboard	8x2east	18 T5	2 split ACU
CB4	out cement in plyboard	8x2east	18 T5	2 split ACU
PUMP ROOM	out cement in plyboard		1 T5	3 HP motor
BARRACKS	out cement in plyboard		1 T5	
ELECTRICAL ROOM	out cement in plyboard		2 T5	

Appendix A.3 Class Schedules for Each Room and Enrollees for Each Subject

The images below present the number of enrollees for each subject and the rooms used for these classes.

No. of Enrollees	SCHEDULE
5	F (08:30 AM) - (12:30 PM) AF2B08B(Dummy) F (12:30 PM) - (04:30 PM) AFCHTC
14	W (09:30 AM) - (12:30 PM) AF207TC
3	F (09:30 AM) - (12:30 PM) AF104TC
5	M (01:30 PM) - (05:30 PM) AF109A
0	T (04:00 PM) - (07:00 PM) AF104TC
13	F (12:30 PM) - (03:30 PM) AF207TC
22	Sat (08:30 AM) - (12:30 PM) AF210TC
7	Sat (08:30 AM) - (11:30 AM) AF207TC
14	F (12:30 PM) - (04:30 PM) AF109A
18	F (04:30 PM) - (08:30 PM) AF109A
2	T (12:30 PM) - (03:30 PM) AF104TC
18	Th (07:30 AM) - (11:30 AM) AF104TC Th (12:30 PM) - (04:30 PM) AF104TC
25	T (01:30 PM) - (05:30 PM) AF207TC
33	T (08:30 AM) - (12:30 PM) AF207TC
18	M (01:30 PM) - (05:30 PM) AF1B04TC
36	T (05:30 PM) - (07:30 PM) AFCHTC Th (05:30 PM) - (07:30 PM) AFCHTC
19	W (08:30 AM) - (12:30 PM) AF210TC W (01:30 PM) - (05:30 PM) AF210TC
19	F (08:30 AM) - (12:30 PM) AF207TC
33	M (08:30 AM) - (12:30 PM) AF1B04TC
30	Sat (01:30 PM) - (05:30 PM) AFCHTC
6	TTh (09:00 AM) - (10:30 AM) 1B12a
14	MWF (09:30 AM) - (10:30 AM) 1B12d
0	Sat (08:30 AM) - (03:30 PM) 1B10a
22	Sat (08:30 AM) - (03:30 PM) 1B12b
5	MWF (11:30 AM) - (12:30 PM) AF208

No. of Enrollees	SCHEDULE
5	MWF (11:30 AM) - (12:30 PM) AF208
18	TTh (12:00 PM) - (01:30 PM) AF208
37	MWF (10:30 AM) - (11:30 AM) 1B12b
28	MWF (12:30 PM) - (01:30 PM) AF208
40	Sat (08:30 AM) - (11:30 AM) AF208
38	Sat (01:30 PM) - (04:30 PM) AF210C
0	TTh (12:00 PM) - (01:30 PM) 1B12E
19	TTh (12:00 PM) - (01:30 PM) AF305
13	MWF (08:30 AM) - (09:30 AM) 1B12d
44	TTh (01:30 PM) - (03:00 PM) AF101
45	TTh (12:00 PM) - (01:30 PM) AF101
2	MW (04:00 PM) - (05:30 PM) AF101
1	F (02:30 PM) - (05:30 PM) AF101
2	Sat (09:00 AM) - (12:00 PM) CB3
0	TTh (06:30 PM) - (08:00 PM) CB3
0	TTh (01:30 PM) - (03:00 PM) AF3B01
17	TTh (09:00 AM) - (10:30 AM) AF208
46	TTh (12:00 PM) - (01:30 PM) CB3
0	MWF (08:30 AM) - (09:30 AM) 1B12d
34	Sat (12:30 PM) - (03:30 PM) CB3
2	MW (12:30 PM) - (02:00 PM) 1B10a F (12:30 PM) - (02:30 PM) 1B10a
33	MW (08:00 AM) - (10:30 AM) 2B07F
2	M (02:30 PM) - (05:00 PM) AF305 W (03:30 PM) - (05:00 PM) AF305 W (02:30 PM) - (03:30 PM) AF110
40	T (08:00 AM) - (09:30 AM) AF305 Th (08:00 AM) - (10:30 AM) AF305 T (09:30 AM) - (10:30 AM) AF111
29	MW (01:30 PM) - (04:00 PM) 1B12d

No. of Enrollees	SCHEDULE	
29	MW (01:30 PM) - (04:00 PM) 1B12d	
21	MW (08:00 AM) - (10:30 AM) 1B12b	
15	MW (08:00 AM) - (10:30 AM) AF110	
30	TTh (03:00 PM) - (05:30 PM) AF111	
30	TTh (03:00 PM) - (05:30 PM) AF110	
28	TTh (05:30 PM) - (08:00 PM) AF111	
30	TTh (05:30 PM) - (08:00 PM) AF110	
30	MW (10:30 AM) - (01:00 PM) AF111	
0	F (07:30 AM) - (12:30 PM) 1B06	
7	F (09:30 AM) - (10:30 AM) AF209	
0	Sat (08:00 AM) - (01:00 PM) AF306TC	
42	TTh (01:30 PM) - (05:30 PM) AF1B05TC	
2	Sat (08:30 AM) - (11:30 AM) AF215TC	
1	W (12:30 PM) - (03:30 PM) 1B10c	
39	MWF (10:30 AM) - (11:30 AM) AFCB4TC	
41	MW (09:00 AM) - (10:30 AM) AF211TC	
44	TTh (12:00 PM) - (06:30 PM) 1B12a	
23	TTh (01:30 PM) - (06:30 PM) 1B10c	
51	TTh (01:30 PM) - (06:30 PM) 1B12b	
49	TTh (01:30 PM) - (06:30 PM) 1B12c	
0	TTh (01:30 PM) - (06:30 PM) 1B10a	
0	TTh (01:30 PM) - (06:30 PM) 2B07c	
44	MW (02:30 PM) - (05:30 PM) 1B12b	F (02:30 PM) - (06:30 PM) 1B12b
45	MW (02:30 PM) - (05:30 PM) 1B12a	F (02:30 PM) - (06:30 PM) 1B12a
44	MW (02:30 PM) - (05:30 PM) 1B10a	F (02:30 PM) - (06:30 PM) 1B10a

No. of Enrollees	SCHEDULE	
44	MW (02:30 PM) - (05:30 PM) 1B10a	F (02:30 PM) - (06:30 PM) 1B10a
0	MW (02:30 PM) - (05:30 PM) 1B10b	F (02:30 PM) - (06:30 PM) 1B10b
40	TTh (01:30 PM) - (03:00 PM) AFCB4TC	
40	MWF (01:00 PM) - (02:00 PM) AF211TC	
45	TTh (04:30 PM) - (06:00 PM) AF3B02	
45	MW (05:30 PM) - (07:00 PM) AF209	
19	Sat (10:30 AM) - (01:30 PM) AFCB4TC	
19	MW (04:30 PM) - (06:00 PM) 1B12E	
46	MW (04:30 PM) - (06:00 PM) AF3B02	
0	TTh (09:00 AM) - (10:30 AM) 1B12b	
20	TTh (09:00 AM) - (10:30 AM) AF102	
27	TTh (10:30 AM) - (12:00 PM) AF209	
7	Sat (09:00 AM) - (12:00 PM) AF103TC	
1	T (01:30 PM) - (04:30 PM) AF307TC	
3	Sat (01:30 PM) - (04:30 PM) AF306TC	Sat (04:30 PM) - (06:30 PM) AF306TC
6	T (08:00 AM) - (01:00 PM) AF306TC	
7	M (01:30 PM) - (05:30 PM) AF1B03TC	
8	F (08:30 AM) - (11:30 AM) AF208	
14	F (01:30 PM) - (05:30 PM) AF1B03TC	
5	W (01:30 PM) - (03:30 PM) AF213TC	
2	T (12:30 PM) - (05:30 PM) AF214TC	
2	W (08:30 AM) - (12:30 PM) AF214TC	W (01:30 PM) - (05:30 PM) AF214TC
33	M (08:30 AM) - (12:30 PM) AF214TC	M (01:30 PM) - (05:30 PM) AF214TC
2	Th (01:30 PM) - (05:30 PM) AF109A	
14	F (08:30 AM) - (12:30 PM) AF214TC	F (01:30 PM) - (05:30 PM) AF214TC

No. of Enrollees	SCHEDULE
14	F (08:30 AM) - (12:30 PM) AF214TC F (01:30 PM) - (05:30 PM) AF214TC
40	MWF (02:00 PM) - (03:00 PM) AFCB4TC
2	TTh (07:30 AM) - (09:00 AM) AF211TC
8	MWF (07:30 AM) - (08:30 AM) AF210TC
1	F (07:30 AM) - (12:30 PM) AF110
0	MWF (10:30 AM) - (11:30 AM) AF102
0	MWF (08:30 AM) - (09:30 AM) AF102
0	TTh (03:00 PM) - (04:30 PM) AF3802
27	MWF (08:30 AM) - (09:30 AM) AF3802
39	TTh (03:00 PM) - (04:30 PM) AF3802
35	MWF (02:30 PM) - (03:30 PM) AF3802
41	MWF (01:30 PM) - (02:30 PM) AF3802
39	TTh (10:30 AM) - (12:00 PM) AF3801
38	TTh (09:00 AM) - (10:30 AM) CB3
10	Sat (08:30 AM) - (03:30 PM) AF308TC
40	TTh (03:00 PM) - (04:30 PM) AF101
14	MW (04:30 PM) - (08:30 PM) AF305
4	Th (08:30 AM) - (01:30 PM) 1B10c
21	MW (08:30 AM) - (10:00 AM) 1B12F1
9	T (08:30 AM) - (01:30 PM) 1B10c
11	MW (10:30 AM) - (11:30 AM) AF208
35	MW (08:30 AM) - (12:30 PM) AF307TC
36	MW (12:30 PM) - (04:30 PM) AF307TC
28	T (08:30 AM) - (01:30 PM) 1B12F1
25	Th (08:30 AM) - (01:30 PM) 1B12F1

No. of Enrollees	SCHEDULE
25	Th (08:30 AM) - (01:30 PM) 1B12F1
2	TTh (05:30 PM) - (08:00 PM) AF101
33	Th (08:30 AM) - (01:30 PM) AF307TC
23	T (08:30 AM) - (01:30 PM) AF307TC
8	MW (04:30 PM) - (06:00 PM) 1B12F1
3	TTh (04:30 PM) - (05:30 PM) 1B12F1
5	Sat (01:30 PM) - (05:30 PM) 1B12F1
27	MW (12:30 PM) - (04:30 PM) 1B12E
26	MW (12:30 PM) - (04:30 PM) 1B12F1
0	TTh (05:30 PM) - (06:30 PM) AF101
41	TTh (04:30 PM) - (05:30 PM) AF101
25	F (01:30 PM) - (05:30 PM) 1B12F1
23	F (08:30 AM) - (12:30 PM) 1B12F1
7	F (08:30 AM) - (01:30 PM) AF111
44	TTh (09:00 AM) - (10:00 AM) AF101
46	MW (01:30 PM) - (02:30 PM) AF102
10	TTh (08:00 AM) - (12:00 PM) 1B12d
20	MW (08:00 AM) - (12:00 PM) 1B12c
1	TTh (04:30 PM) - (07:00 PM) 1B12E
13	TTh (01:30 PM) - (03:00 PM) AF305
19	TTh (09:30 AM) - (12:00 PM) 1B12c
9	TTh (01:30 PM) - (04:00 PM) 1B12d
4	FSat (01:30 PM) - (05:30 PM) 1B12E
38	MWF (12:30 PM) - (01:30 PM) AF101
2	Sat (05:00 PM) - (08:00 PM) AF103TC

No. of Enrollees	SCHEDULE
2	Sat (05:00 PM) - (08:00 PM) AF103TC
1	TTh (10:30 AM) - (12:00 PM) AF102
0	MWF (10:30 AM) - (11:30 AM) 2B06
0	MWF (02:30 PM) - (03:30 PM) AF101
0	TTh (09:00 AM) - (10:30 AM) AF209
0	TTh (10:30 AM) - (12:00 PM) CB3
44	TTh (10:30 AM) - (12:00 PM) AF101
44	MWF (10:30 AM) - (11:30 AM) AF101
45	MWF (03:30 PM) - (04:30 PM) AF3B02
2	MWF (09:30 AM) - (10:30 AM) 1B12E
10	Sat (02:30 PM) - (05:30 PM) AF101
7	Sat (02:30 PM) - (05:30 PM) AF208
6	Sat (06:00 PM) - (09:00 PM) AF208
7	Sat (11:30 AM) - (05:30 PM) 1B12a
3	Sat (08:00 AM) - (11:00 AM) AF102
2	Sat (11:30 AM) - (02:30 PM) AF102
39	MWF (09:30 AM) - (10:30 AM) AFCB4TC
36	TTh (01:30 PM) - (03:00 PM) AF211TC
3	Sat (08:00 AM) - (11:00 AM) AF101
1	Sat (11:30 AM) - (02:30 PM) AF209
1	TTh (04:30 PM) - (06:00 PM) 1B12d
0	TTh (06:00 PM) - (07:30 PM) 1B12d
13	Sat (08:00 AM) - (11:00 AM) AF209
2	Sat (11:30 AM) - (02:30 PM) AF101
8	Sat (06:00 PM) - (09:00 PM) AF209

No. of Enrollees	SCHEDULE
8	Sat (06:00 PM) - (09:00 PM) AF209
8	Sat (11:30 AM) - (02:30 PM) AF208
2	Sat (06:00 PM) - (09:00 PM) AF101
0	Sat (02:30 PM) - (05:30 PM) 1B12c
0	Sat (08:00 AM) - (11:00 AM) 1B12c Sat (11:30 AM) - (02:30 PM) 1B12c
0	Sat (08:00 AM) - (11:00 AM) 1B12c
30	TTh (01:30 PM) - (03:00 PM) AF102
27	MWF (07:30 AM) - (08:30 AM) AF103TC
0	Sat (03:00 PM) - (06:00 PM) AF104TC
44	Sat (01:30 PM) - (04:30 PM) AF103TC
45	Sat (03:30 PM) - (06:30 PM) AF104TC
6	W (08:30 AM) - (12:30 PM) AF2B11TC
12	W (01:30 PM) - (05:30 PM) AF2B11TC
39	TTh (03:00 PM) - (04:30 PM) AFCB4TC
2	MW (07:30 AM) - (09:00 AM) AF211TC
10	TTh (09:00 AM) - (10:30 AM) 2B06
1	MWF (02:30 PM) - (03:30 PM) AF3B02
0	MWF (02:30 PM) - (03:30 PM) AF101
26	MWF (02:30 PM) - (03:30 PM) AF102
3	MWF (01:30 PM) - (02:30 PM) 1B12c
50	MWF (02:30 PM) - (03:30 PM) 1B12c
5	MW (11:00 AM) - (12:30 PM) AF209
39	MWF (01:30 PM) - (02:30 PM) AF101
41	MWF (12:30 PM) - (01:30 PM) AF102
40	MWF (12:30 PM) - (01:30 PM) 2B06

No. of Enrollees	SCHEDULE
40	MWF (12:30 PM) - (01:30 PM) 2B06
0	MWF (12:30 PM) - (01:30 PM) AF3B02
34	Sat (01:30 PM) - (04:30 PM) 2B06
9	MWF (08:30 AM) - (09:30 AM) AF208
45	TTh (10:30 AM) - (12:00 PM) AF208
30	MWF (10:30 AM) - (11:30 AM) CB3
4	MWF (03:30 PM) - (04:30 PM) AF101
14	TTh (10:30 AM) - (12:00 PM) 1B12E
39	MWF (07:30 AM) - (08:30 AM) AFCB4TC
40	TTh (03:00 PM) - (04:30 PM) AF211TC
0	MWF (01:30 PM) - (02:30 PM) 2B06
46	MWF (11:30 AM) - (12:30 PM) AF101
0	MWF (11:30 AM) - (12:30 PM) AF102
0	MWF (11:30 AM) - (12:30 PM) 2B06
46	MWF (11:30 AM) - (12:30 PM) AF3B02
30	TTh (01:30 PM) - (03:00 PM) CB3
4	TTh (09:00 AM) - (10:30 AM) AF3B02
41	Sat (09:30 AM) - (12:00 PM) AF211TC
3	TTh (03:00 PM) - (04:30 PM) AF103TC
39	MWF (01:00 PM) - (02:00 PM) AFCB4TC
40	TTh (09:00 AM) - (10:30 AM) AF211TC
1	MWF (01:30 PM) - (02:30 PM) 2B07A
39	MWF (08:30 AM) - (09:30 AM) AFCB4TC
38	MW (03:00 PM) - (04:30 PM) AF211TC
39	TTh (12:00 PM) - (01:30 PM) AFCB4TC

No. of Enrollees	SCHEDULE
41	MWF (03:30 PM) - (04:30 PM) AF102
40	MWF (05:30 PM) - (06:30 PM) AF102
35	TTh (07:30 AM) - (09:00 AM) AF209
41	MWF (04:30 PM) - (05:30 PM) AF102
41	MWF (04:30 PM) - (05:30 PM) CB3
41	MWF (07:30 AM) - (08:30 AM) AF104TC
45	MWF (10:30 AM) - (11:30 AM) AF103TC
40	TTh (07:30 AM) - (09:00 AM) AF103TC
3	TTh (04:30 PM) - (06:00 PM) CB3
43	MWF (02:30 PM) - (03:30 PM) AF3B01
46	TTh (04:30 PM) - (06:00 PM) AF209
40	MWF (12:30 PM) - (01:30 PM) AF212TC
39	MWF (12:30 PM) - (01:30 PM) AF103TC
40	TTh (01:30 PM) - (03:00 PM) AF212TC
42	MWF (12:30 PM) - (01:30 PM) AF209
33	TTh (01:30 PM) - (03:00 PM) AF3B02
40	TTh (03:00 PM) - (04:30 PM) AF102
10	Sat (08:00 AM) - (12:00 PM) AF1B05TC
0	Sat (08:00 AM) - (12:00 PM) AF304TC
35	T (08:30 AM) - (12:30 PM) AF304TC
34	T (01:30 PM) - (05:30 PM) AF210TC
19	M (01:30 PM) - (05:30 PM) AF304TC
31	M (01:30 PM) - (05:30 PM) AF210TC
34	Th (08:30 AM) - (12:30 PM) AF304TC
33	Th (08:30 AM) - (12:30 PM) AF1B04TC

No. of Enrollees	SCHEDULE
33	Th (08:30 AM) - (12:30 PM) AF1B04TC
17	W (01:30 PM) - (05:30 PM) AF304TC
26	W (01:30 PM) - (05:30 PM) AF1B03TC
35	T (01:30 PM) - (05:30 PM) AF304TC
34	T (08:30 AM) - (12:30 PM) AF1B04TC
18	F (08:30 AM) - (12:30 PM) AF1B04TC
29	F (08:30 AM) - (12:30 PM) AF210TC
36	Th (01:30 PM) - (04:30 PM) AF304TC
33	Th (01:30 PM) - (04:30 PM) AF210TC
16	F (01:30 PM) - (04:30 PM) AF210TC
31	F (01:30 PM) - (04:30 PM) AF304TC
28	TTh (01:00 PM) - (04:30 PM) AF308TC
34	FSat (09:00 AM) - (11:30 AM) AF305
16	Sat (09:30 AM) - (12:30 PM) CB3
41	Sat (09:30 AM) - (12:30 PM) 2B06
33	Sat (09:30 AM) - (12:30 PM) AF3B01
27	Sat (09:30 AM) - (12:30 PM) AF3B02
38	TTh (09:00 AM) - (10:30 AM) AF3B01
45	MWF (07:30 AM) - (08:30 AM) CB3
39	TTh (04:30 PM) - (06:00 PM) AF102
44	TTh (09:00 AM) - (12:30 PM) 2B07c
45	TTh (12:30 PM) - (04:00 PM) 2B07b
11	TTh (12:30 PM) - (04:00 PM) 2B07c
9	MW (01:30 PM) - (05:00 PM) 2B07A
45	TTh (03:00 PM) - (06:30 PM) AF305

No. of Enrollees	SCHEDULE	
45	TTh (03:00 PM) - (06:30 PM) AF305	
36	TTh (09:00 AM) - (12:30 PM) 2B07b	
31	TTh (08:00 AM) - (11:30 AM) 2B07d	
31	F (08:30 AM) - (12:00 PM) AF307TC	F (01:00 PM) - (04:30 PM) AF307TC
35	F (08:30 AM) - (12:00 PM) AF308TC	F (01:00 PM) - (04:30 PM) AF308TC
45	MW (01:30 PM) - (05:00 PM) 2B07c	
44	MW (01:00 PM) - (04:30 PM) 2B07b	
44	TTh (04:00 PM) - (07:30 PM) 2B07A	
11	F (12:30 PM) - (04:30 PM) 2B07A	Sat (01:30 PM) - (04:30 PM) 2B07A
9	TTh (11:30 AM) - (03:00 PM) 2B07A	
41	FSat (09:30 AM) - (01:00 PM) 1B10b	
33	MW (08:00 AM) - (11:30 AM) 1B10a	
27	TTh (08:30 AM) - (12:00 PM) AF308TC	
34	TTh (08:30 AM) - (12:00 PM) 2B07e	
29	MW (08:30 AM) - (09:30 AM) AF308TC	
32	MW (12:30 PM) - (01:30 PM) AF308TC	
29	MW (09:30 AM) - (12:30 PM) AF308TC	
32	MW (01:30 PM) - (04:30 PM) AF308TC	
25	MW (01:30 PM) - (04:00 PM) CB3	
31	MW (08:30 AM) - (11:00 AM) AF209	
26	TTh (03:00 PM) - (04:30 PM) AF3B01	
31	TTh (01:30 PM) - (03:00 PM) AF3B01	
44	TTh (01:30 PM) - (03:00 PM) AF208	
37	MWF (04:30 PM) - (05:30 PM) AF208	
47	MW (05:30 PM) - (07:00 PM) AF211TC	

No. of Enrollees	SCHEDULE
47	MW (05:30 PM) - (07:00 PM) AF211TC
12	MWF (03:30 PM) - (04:30 PM) AF209
10	TTh (04:30 PM) - (06:00 PM) AF208
6	TTh (03:00 PM) - (04:30 PM) AF208
14	MW (08:30 AM) - (12:30 PM) 2B07F
40	MW (08:30 AM) - (12:30 PM) 2B07A
37	MW (08:30 AM) - (12:30 PM) 2B07b
39	MW (08:30 AM) - (12:30 PM) 2B07c
37	MW (08:30 AM) - (12:30 PM) 2B07d
34	MW (08:30 AM) - (12:30 PM) 2B07e
12	F (04:00 PM) - (06:00 PM) 2B07b Sat (02:30 PM) - (06:00 PM) 2B07b F (02:30 PM) - (04:00 PM) 2B07b
39	T (09:00 AM) - (12:30 PM) 1B12b Th (09:00 AM) - (11:00 AM) 1B12b Th (11:00 AM) - (12:30 PM) 1B12b
39	T (03:00 PM) - (05:00 PM) AF306TC Th (01:30 PM) - (05:00 PM) AF306TC T (01:30 PM) - (03:00 PM) AF306TC
43	T (03:00 PM) - (05:00 PM) 2B07c Th (01:30 PM) - (05:00 PM) 2B07c T (01:30 PM) - (03:00 PM) 2B07c
34	F (09:30 AM) - (01:00 PM) 2B07b Sat (11:00 AM) - (01:00 PM) 2B07b Sat (09:30 AM) - (11:00 AM) 2B07b
24	T (08:00 AM) - (11:30 AM) 2B07A Th (09:30 AM) - (11:30 AM) 2B07A Th (08:00 AM) - (09:30 AM) 2B07A
10	MW (03:30 PM) - (04:30 PM) AF208
12	TTh (09:30 AM) - (10:30 AM) AF208
31	F (04:30 PM) - (06:30 PM) AF209
39	F (10:30 AM) - (12:30 PM) AF209
30	MW (01:30 PM) - (02:30 PM) AF208
44	MW (02:30 PM) - (03:30 PM) AF208
15	MW (01:30 PM) - (02:30 PM) AF102
7	F (12:30 PM) - (02:30 PM) AF208
38	F (08:30 AM) - (10:30 AM) 1B12b

No. of Enrollees	SCHEDULE
38	F (08:30 AM) - (10:30 AM) 1B12b
33	F (01:30 PM) - (03:30 PM) AF209
29	MW (04:30 PM) - (05:30 PM) AF209
44	MW (01:30 PM) - (02:30 PM) AF209
39	T (08:00 AM) - (09:00 AM) AFCB4TC
1	M (10:30 AM) - (11:30 AM) AF211TC
33	M (01:30 PM) - (03:30 PM) AF103TC
24	M (05:30 PM) - (07:30 PM) AF103TC

Appendix B. Calibration Certificate

Appendix B.1 Illuminance Meter Calibration Certificate

The images below present the calibration certificate of the illuminance meter used in this study.



MICRO PRECISION CALIBRATION CEBU, INC.
U-201 IMEZ BLDG., OSMENA ST.
MEZ II BASAK, LAPU-LAPU CITY PHILIPPINES 6015



Certificate of Calibration

Date: Oct 1, 2019

Cert No. 551220083242550

Customer:

IVAN JOHN A. NAPAROTA
PUROK 1 TIPTIP DISTRICT
TAGBILARAN, BOHOL 6300

Work Order #: CEB-WO-1000001660

MPC Control #: 2685895

Received Date: Sep 25, 2019

Asset ID: NONE

Serial Number: 2685895

Gage Type: DIGITAL LUX METER

Department: N/A

Performed By: PATRICK A. DOYUGAN

Manufacturer: BENETECH

Received Condition: IN TOLERANCE

Model Number: GM1020

Returned Condition: IN TOLERANCE

Temp/RH: 20.4°C / 49.0%

Cal. Date: September 30, 2019

Location: Calibration performed at MPC facility

Cal. Interval: 12 MONTHS

Cal. Due Date: September 30, 2020

Calibration Notes:

See attached 1 page of calibration data.

Standards Used to Calibrate Equipment

I.D.	Description.	Model	Serial	Manufacturer	Cal. Due Date	Traceability #
AS9391	DIGITAL LIGHT METER	93-172	00000721	GREENLEE INSTRUMENTS	Jun 11, 2020	551220083064234

Procedures Used in this Event

Procedure Name	Description
MPCLUX-001	Lux Meters (Luminance/Illuminance), General, Nov-06-2017, rev01

Calibrating Technician:

PATRICK A. DOYUGAN

QC Approval:

BEVERLYNE C. SANDOVAL

Statements of Pass or Fail Conformance: The uncertainty of measurement has been taken into account when determining compliance with specification, as per ILAC-G8:03/2009. All measurements and test results guard banded to ensure the probability of false-accept does not exceed 2% in compliance with ANSI/NCISL Z540.3-2006.

The status of compliance with the acceptance criteria is reported as:

Pass - Compliant with specification;

Fail - Not compliant with specification;

Fail - The measured value is not within the acceptance limits. However, a portion of the expanded uncertainty of measurement at 95% is within the specified tolerance.

Pass - The measured value is within acceptance limits. However, a portion of the expanded uncertainty of measurement at 95% exceeds the specified tolerance.

The expanded uncertainty of measurement is stated as the standard uncertainty of measurement multiplied by the coverage factor k=2, which for a normal distribution corresponds to a coverage probability of approximately 95%, unless otherwise stated. This calibration report complies with ISO/IEC 17025:2017 and ANSI/NCSL Z540.3 Method 6-Guard Bands based on Test Uncertainty.

Calibration cycles are typically set to one week. Any number of cycles may be requested before the next scheduled calibration. Recalibration cycles should be based on frequency of use, environmental conditions and customer's established systematic accuracy. All standards are traceable to SI through the National Institute of Standards and Technology (NIST) and/or recognized national or international standards laboratories. Services rendered include proper manufacturer's service instruction and are warranted for no less than thirty (30) days. The information on this report pertains only to the instrument identified; this may not be reproduced in part or in a whole without the prior written approval of the issuing MP Calibration Laboratory.

Page 1 of 1

(CERT, Rev 6)



Calibration Report of Benetech GM1020 Digital Lux Meter

MPC Control #:	2685895	Serial Number:	2685895
Asset ID:	NONE	Calibration Date:	September 30, 2019

Light Accuracy

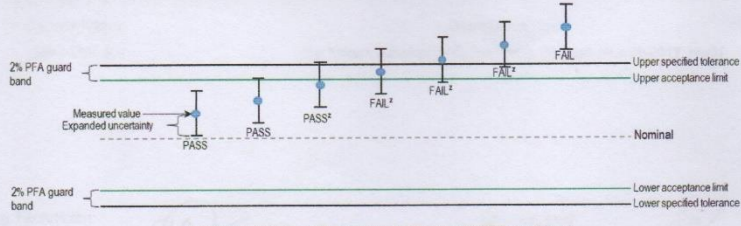
Range	Reference Measured Value	Lower Limit	As Found	As Left	Upper Limit	Result	Uncertainty (\pm)
200.0 Lux	20.2 Lux	19.6 Lux	20.4 Lux	20.4 Lux	20.8 Lux	PASS	0.61 Lux
	100.9 Lux	97.9 Lux	101.6 Lux	101.6 Lux	103.9 Lux	PASS	3.03 Lux
	180.3 Lux	174.9 Lux	181.2 Lux	181.2 Lux	185.7 Lux	PASS	5.41 Lux
2000.0 Lux	200 Lux	194 Lux	203 Lux	203 Lux	206 Lux	PASS	6.00 Lux
	1000 Lux	970 Lux	1006 Lux	1006 Lux	1030 Lux	PASS	30.00 Lux
	1800 Lux	1746 Lux	1812 Lux	1812 Lux	1854 Lux	PASS	54.00 Lux
20000.0 Lux	2000 Lux	1940 Lux	2020 Lux	2020 Lux	2060 Lux	PASS	80.00 Lux
	10000 Lux	9600 Lux	10030 Lux	10030 Lux	10400 Lux	PASS	400.00 Lux
	18000 Lux	17280 Lux	18030 Lux	18030 Lux	18720 Lux	PASS	720.00 Lux
200000.0 Lux	20000 Lux	19200 Lux	20100 Lux	20100 Lux	20800 Lux	PASS	980.00 Lux
	25000 Lux	24000 Lux	25200 Lux	25200 Lux	26000 Lux	PASS	1000.00 Lux
	30000 Lux	28800 Lux	30300 Lux	30300 Lux	31200 Lux	PASS	1200.00 Lux

Statements of Pass or Fail Conformance

The uncertainty of measurement has been taken into account when determining compliance with specification, as per ILAC-G8:03/2009.
All measurements and test results guard banded to ensure the probability of false-accept does not exceed 2% in compliance with ANSI/NCSL Z540.3-2006.

The status of compliance with the acceptance criteria is reported as:

- PASS - Compliant with specification
- FAIL - Not compliant with specification.
- FAIL² - The measured value is not within the acceptance limits. However, a portion of the expanded uncertainty of measurement at 95% is within the specified tolerance.
- PASS² - The measured value is within acceptance limits. However, a portion of the expanded uncertainty of measurement at 95% exceeds the specified tolerance.



Acceptance limits for $\leq 2\%$ probability of false accept (PFA) guard band

The expanded uncertainty of measurement is stated as the standard uncertainty of measurement multiplied by the coverage factor $k=2$, which for a normal distribution corresponds to a coverage probability of approximately 95%, unless otherwise stated.
This calibration report complies with ISO/IEC 17025:2017 and ANSI/NCSL Z540.3 Method 6-Guard Bands based on Test Uncertainty Ratio.

- End of Calibration Report -



Appendix C. R Software Codes

Appendix C.1 Morris Method

The image below presents the code written in R to build the trajectory for Morris method and for solving the indices. Lines 1 to 4 are the code for building the trajectory. *morris* is the function from the package *sensitivity*. *#factors* is the number of parameters. *#r* is the number of elementary effects per parameter. *#levels* is the number of levels. *#grid.jump* is the number of levels per step. *#binf* is a vector specifying the lower bounds of the parameters. *#bsup* is a vector specifying the upper bounds of the parameters. *#Morris\$X* is the returned final matrix that defines the trajectory. On the other hand, lines 7 to 21 are the code for computing the indices. *#tell(Morris,c(...))* defines the simulation results in total energy consumption using the trajectory matrix earlier. *#mu <- apply(Morris\$ee, 2, mean)*, *#sigma <- apply(Morris\$ee, 2, sd)*, and *#mu.star <- apply(Morris\$ee, 2, function(Morris) mean(abs(Morris)))* are the returned vectors for the indices, mean of elementary effects, standard deviation of elementary effects, and mean* of elementary effects.

```
1 Morris <- morris(model = NULL, factors = 15, r = 5, design = list(type = "oat", levels = 4, grid.jump = 1),
2   binf = c(0.001,0,0.001,0,0.001,0,100,100,100,0,0,0.1,0.3,30,1),
3   bsup = c(0.999,1,0.999,1,1,1,150,150,150,1,1,6,0.9,120,5), scale =T)
4 design <- Morris$X
5 write.csv(design, file = "GG.csv")
6
7 tell(Morris,c(43351.17,87404.83,92487.72,92142.59,92561.71,93161.28,91449.5,
8   91255.38,91828.64,91518.12,91546.77,91237.84,89975.08,90010.29,
9   89521.16,89234.36,54075.03,54365.18,54111.04,55630.76,55540.84,
10  55466.01,55952.95,77811.09,77307.67,77027.97,77023.13,76742.89,
11  38799.58,39121.81,38441.4,36156.6,30948.1,30919.87,30124.19,
12  24482.02,24468.77,24509.97,32303,32598.29,32593.84,32453.56,
13  32710.54,32529.72,32910.79,33952.14,33559.72,34574.46,88001.88,
14  88347.13,88548.77,87116.22,78707.55,79424.08,39999.57,39610.2,
15  39538.36,39421.65,39890.19,39683.97,39666.9,39922.72,39915.07,
16  38038.51,41007.81,31990.59,32192.56,32082.49,31626.06,31506.53,
17  31767.89,32030.71,33147.68,33144.57,32387.05,60948.84,54585.93,
18  53879.27,54407.26,54359.07))
19 mu <- apply(Morris$ee, 2, mean)
20 sigma <- apply(Morris$ee, 2, sd)
21 mu.star <- apply(Morris$ee, 2, function(Morris) mean(abs(Morris)))
22
23 write.csv(mu, file = "mu.csv")
24 write.csv(sigma, file = "sigma.csv")
25 write.csv(mu.star, file = "mu.star.csv")
```

The final matrix is presented below.

Appendix C.2 Design Matrix Construction via Latin Hypercube Sampling

The image below presents the code for making the design matrix through Latin Hypercube Sampling for the Monte Carlo simulation. The used function is *randomLHS* from the package *lhs* in R. #randomLHS(5,7) means that there are 5 samples for each parameter and there are 7 parameters. The sampling was repeated 80 times to have a total of 400 combinations of parameter values.

```
a <- replicate(80, {
  randomLHS(5,7)
}, simplify = FALSE)
write.csv(a, file = "Design Matrix_3.csv")
```

The images below present the first 200 combinations of the 7 parameters. These values are not yet scaled to the respective value ranges of the parameters in *EnergyPlus*.

Column1	1	2	3	4	5
X1	0.492746	0.852841	0.112502	0.681693	0.251739
X2	0.078608	0.339976	0.815696	0.480615	0.680534
X3	0.103754	0.477178	0.682332	0.905262	0.334257
X4	0.926612	0.230705	0.771481	0.546553	0.127813
X5	0.159221	0.999944	0.683412	0.387104	0.467658
X6	0.882397	0.796148	0.535863	0.399116	0.185351
X7	0.938084	0.314878	0.093712	0.694034	0.504287
X1.1	0.684853	0.35248	0.445336	0.012645	0.977878
X2.1	0.565252	0.676527	0.145952	0.8832	0.326446
X3.1	0.915125	0.087262	0.490762	0.303231	0.694745
X4.1	0.93797	0.126213	0.435129	0.67961	0.378688
X5.1	0.464786	0.906006	0.146455	0.631991	0.343448
X6.1	0.352744	0.60286	0.582042	0.884944	0.139243
X7.1	0.508443	0.121687	0.794655	0.965458	0.238207
X1.2	0.071355	0.703093	0.589157	0.829054	0.214637
X2.2	0.610683	0.108665	0.226928	0.591797	0.863561
X3.2	0.029039	0.44063	0.806583	0.259665	0.717349
X4.2	0.843524	0.014444	0.785206	0.277577	0.582991
X5.2	0.246171	0.880006	0.193648	0.781393	0.421437
X6.2	0.29748	0.955963	0.643206	0.595814	0.053354
X7.2	0.585078	0.886636	0.063586	0.231598	0.62906
X1.3	0.433972	0.707421	0.009613	0.283622	0.984646
X2.3	0.65673	0.197963	0.268373	0.496766	0.992409
X3.3	0.481278	0.936433	0.648654	0.324063	0.157524
X4.3	0.188435	0.578413	0.350048	0.914437	0.659252
X5.3	0.805494	0.237001	0.415974	0.050846	0.786506

X6.3	0.490597	0.091145	0.766188	0.982525	0.359146
X7.3	0.343627	0.186466	0.838079	0.410875	0.696443
X1.4	0.21596	0.588376	0.795843	0.115423	0.894613
X2.4	0.512293	0.291958	0.834988	0.788483	0.010305
X3.4	0.201328	0.430107	0.605306	0.973615	0.188877
X4.4	0.531041	0.376016	0.970517	0.110646	0.601456
X5.4	0.408122	0.161879	0.368277	0.703203	0.901483
X6.4	0.949225	0.160385	0.516982	0.395122	0.655816
X7.4	0.760726	0.332969	0.541939	0.105265	0.953058
X1.5	0.383726	0.70083	0.167423	0.564104	0.870183
X2.5	0.090281	0.399812	0.763415	0.974368	0.431601
X3.5	0.788354	0.216232	0.517148	0.995566	0.1322
X4.5	0.500344	0.076585	0.74842	0.364733	0.889989
X5.5	0.991308	0.354254	0.431356	0.011475	0.718511
X6.5	0.721411	0.874413	0.315353	0.021296	0.577063
X7.5	0.986136	0.05941	0.300795	0.709389	0.533346
X1.6	0.890013	0.656242	0.407386	0.369155	0.159123
X2.6	0.729072	0.099644	0.908287	0.370005	0.482941
X3.6	0.222861	0.420917	0.731837	0.831116	0.076799
X4.6	0.590503	0.920902	0.132869	0.214077	0.710777
X5.6	0.849944	0.789858	0.154081	0.494819	0.229735
X6.6	0.257078	0.454909	0.088668	0.704931	0.85626
X7.6	0.011527	0.809306	0.313682	0.601694	0.57416
X1.7	0.698905	0.942684	0.573329	0.133446	0.227096
X2.7	0.608209	0.498974	0.112777	0.907341	0.386333
X3.7	0.416676	0.659448	0.099082	0.92319	0.278365
X4.7	0.256106	0.961016	0.093924	0.607435	0.459687

X5.7	0.554019	0.879479	0.227289	0.191476	0.661946
X6.7	0.798846	0.187674	0.48668	0.320733	0.905845
X7.7	0.359367	0.092182	0.940658	0.52185	0.700586
X1.8	0.511289	0.308797	0.074831	0.730517	0.983232
X2.8	0.069657	0.243773	0.443967	0.685223	0.923078
X3.8	0.969737	0.435064	0.146233	0.229507	0.621525
X4.8	0.081213	0.605082	0.23376	0.852073	0.537057
X5.8	0.24432	0.733536	0.05741	0.562321	0.958304
X6.8	0.643288	0.456616	0.985676	0.307425	0.048646
X7.8	0.484727	0.011839	0.669496	0.251837	0.90011
X1.9	0.688393	0.407551	0.977659	0.324298	0.040204
X2.9	0.024828	0.278165	0.476291	0.968958	0.70284
X3.9	0.066764	0.629604	0.828446	0.540129	0.212261
X4.9	0.510387	0.36834	0.993619	0.786071	0.037436
X5.9	0.170895	0.209342	0.663757	0.831203	0.52372
X6.9	0.27581	0.938269	0.747306	0.037038	0.42147
X7.9	0.399648	0.808171	0.779343	0.047217	0.520991
X1.10	0.449281	0.865906	0.370519	0.054105	0.788744
X2.10	0.871374	0.013926	0.262517	0.43288	0.748496
X3.10	0.595348	0.064738	0.947592	0.797468	0.287029
X4.10	0.974275	0.416225	0.72634	0.385285	0.110127
X5.10	0.285614	0.05265	0.540692	0.759508	0.955698
X6.10	0.569371	0.101611	0.259435	0.677311	0.881386
X7.10	0.943833	0.658398	0.310851	0.07195	0.420711
X1.11	0.507565	0.26149	0.795412	0.041002	0.815886
X2.11	0.234223	0.794898	0.575145	0.011605	0.805512
X3.11	0.129267	0.266671	0.509224	0.851161	0.723736

X4.11	0.259824	0.953106	0.024551	0.742738	0.45304
X5.11	0.235175	0.070692	0.620666	0.936254	0.453834
X6.11	0.972577	0.142128	0.718008	0.300668	0.507589
X7.11	0.010018	0.475526	0.36378	0.742885	0.893781
X1.12	0.782056	0.833974	0.179194	0.419354	0.263935
X2.12	0.320094	0.125027	0.896369	0.499404	0.651544
X3.12	0.893747	0.232793	0.730203	0.126832	0.487895
X4.12	0.165238	0.687877	0.288144	0.546007	0.909841
X5.12	0.848998	0.540658	0.156377	0.317127	0.727538
X6.12	0.828824	0.487985	0.363226	0.651724	0.154846
X7.12	0.812938	0.458473	0.255796	0.072217	0.623663
X1.13	0.959843	0.208474	0.52104	0.748208	0.054849
X2.13	0.646255	0.535908	0.001456	0.929104	0.228964
X3.13	0.810064	0.606322	0.4315	0.092217	0.37266
X4.13	0.280382	0.10579	0.981931	0.49747	0.718033
X5.13	0.757822	0.238212	0.191505	0.810905	0.501761
X6.13	0.149346	0.547417	0.277873	0.978981	0.707959
X7.13	0.155084	0.228558	0.486876	0.958358	0.651056
X1.14	0.303202	0.108167	0.825173	0.442641	0.750089
X2.14	0.53645	0.259396	0.129869	0.979813	0.724782
X3.14	0.665947	0.548513	0.230784	0.046082	0.958908
X4.14	0.820417	0.676952	0.394593	0.483315	0.149166
X5.14	0.951036	0.373411	0.663209	0.535912	0.187839
X6.14	0.153449	0.631603	0.524516	0.248203	0.872471
X7.14	0.000195	0.903401	0.388105	0.416543	0.604221
X1.15	0.743946	0.049951	0.499801	0.914589	0.311586
X2.15	0.077668	0.957085	0.695551	0.468314	0.315612

X3.15	0.07637	0.729476	0.395303	0.914719	0.473238
X4.15	0.157945	0.993802	0.321834	0.559372	0.730712
X5.15	0.139759	0.855157	0.235706	0.569779	0.691338
X6.15	0.20605	0.469334	0.868789	0.026878	0.635507
X7.15	0.991427	0.56212	0.387372	0.742238	0.022016
X1.16	0.022008	0.70287	0.901244	0.340515	0.480172
X2.16	0.096201	0.389798	0.657311	0.904419	0.51443
X3.16	0.423447	0.11307	0.78987	0.823961	0.327341
X4.16	0.219069	0.469946	0.60507	0.0626	0.81432
X5.16	0.336117	0.778308	0.973368	0.159263	0.595171
X6.16	0.518505	0.966353	0.144646	0.376269	0.768213
X7.16	0.351739	0.867191	0.092586	0.756838	0.524681
X1.17	0.370123	0.530929	0.761049	0.894929	0.079441
X2.17	0.101089	0.418052	0.280603	0.648481	0.965902
X3.17	0.424793	0.230109	0.16971	0.769137	0.811413
X4.17	0.116549	0.509186	0.7242	0.363881	0.853699
X5.17	0.359603	0.432078	0.722277	0.946455	0.092294
X6.17	0.982951	0.627722	0.556701	0.270176	0.088664
X7.17	0.036127	0.492573	0.933641	0.379076	0.72399
X1.18	0.99308	0.70013	0.109437	0.227014	0.4573
X2.18	0.103174	0.735613	0.568127	0.86585	0.275856
X3.18	0.120665	0.74535	0.413042	0.8932	0.304462
X4.18	0.434535	0.821445	0.665567	0.288758	0.051137
X5.18	0.765727	0.124356	0.373306	0.451669	0.855898
X6.18	0.677305	0.562997	0.327553	0.932651	0.096993
X7.18	0.303636	0.534212	0.90834	0.638199	0.193528
X1.19	0.200318	0.108573	0.950156	0.612031	0.429553
X2.19	0.087378	0.347126	0.670756	0.456722	0.882845
X3.19	0.203104	0.781796	0.064927	0.958835	0.431377
X4.19	0.776933	0.446815	0.326441	0.842852	0.072453
X5.19	0.993857	0.746126	0.116815	0.333928	0.47268
X6.19	0.250791	0.496966	0.740923	0.887148	0.037038
X7.19	0.36405	0.640724	0.976743	0.046204	0.534379

X1.20	0.581391	0.944022	0.300665	0.140703	0.746523
X2.20	0.841116	0.310256	0.179054	0.5464	0.651663
X3.20	0.94487	0.618869	0.021577	0.596887	0.372937
X4.20	0.539988	0.321608	0.70008	0.827194	0.106799
X5.20	0.247605	0.107507	0.623445	0.474084	0.999956
X6.20	0.007227	0.954189	0.345159	0.505495	0.744043
X7.20	0.202681	0.105037	0.91888	0.754577	0.500184
X1.21	0.775731	0.191854	0.374995	0.517042	0.801948
X2.21	0.789411	0.389153	0.824307	0.124362	0.471832
X3.21	0.176923	0.586711	0.339355	0.801804	0.709347
X4.21	0.108356	0.763741	0.376177	0.857275	0.541446
X5.21	0.161409	0.241842	0.583271	0.951218	0.61432
X6.21	0.04671	0.689214	0.53385	0.881991	0.227376
X7.21	0.868292	0.088417	0.387666	0.638463	0.579198
X1.22	0.432773	0.974178	0.664211	0.083846	0.358088
X2.22	0.403294	0.946724	0.06215	0.671005	0.262528
X3.22	0.630858	0.399616	0.047563	0.599048	0.875153
X4.22	0.602608	0.967497	0.231393	0.588856	0.13345
X5.22	0.701078	0.586564	0.392391	0.861551	0.036427
X6.22	0.618087	0.135808	0.948643	0.49614	0.257811
X7.22	0.205809	0.101548	0.546691	0.819261	0.702228
X1.23	0.565939	0.657241	0.811857	0.055278	0.396264
X2.23	0.922855	0.341756	0.573963	0.676365	0.189342
X3.23	0.323897	0.489296	0.673524	0.958766	0.101914
X4.23	0.319018	0.52325	0.841182	0.008199	0.673273
X5.23	0.110813	0.93493	0.229937	0.465715	0.77064
X6.23	0.353946	0.435831	0.006062	0.658678	0.95321

X7.23	0.508723	0.705749	0.809794	0.049445	0.213236
X1.24	0.041881	0.89246	0.383033	0.742778	0.571588
X2.24	0.992672	0.33498	0.070244	0.473641	0.779852
X3.24	0.896136	0.643745	0.199253	0.389122	0.41862
X4.24	0.31693	0.888064	0.410062	0.633917	0.004347
X5.24	0.30255	0.145191	0.563431	0.663359	0.987206
X6.24	0.600966	0.382491	0.907019	0.020364	0.532921
X7.24	0.781535	0.569598	0.134405	0.310509	0.977893
X1.25	0.314824	0.91478	0.538866	0.14768	0.668342
X2.25	0.903287	0.776871	0.33832	0.543249	0.157482
X3.25	0.987037	0.777057	0.469193	0.013193	0.357059
X4.25	0.603432	0.991075	0.091548	0.448524	0.275785
X5.25	0.53044	0.660072	0.225796	0.052823	0.877494
X6.25	0.291727	0.436703	0.880706	0.747307	0.087927
X7.25	0.279156	0.491655	0.634794	0.862054	0.034062
X1.26	0.252024	0.964174	0.091585	0.713238	0.421454
X2.26	0.2642	0.683566	0.875594	0.000488	0.552262
X3.26	0.925804	0.524161	0.060419	0.617687	0.353703
X4.26	0.367909	0.565781	0.084653	0.871975	0.77322
X5.26	0.397037	0.832409	0.682467	0.506186	0.04357
X6.26	0.366299	0.814987	0.775187	0.443596	0.04297
X7.26	0.175718	0.311196	0.950402	0.571528	0.721098
X1.27	0.497854	0.892331	0.102782	0.771036	0.36299
X2.27	0.50516	0.969843	0.277292	0.776279	0.087931
X3.27	0.82186	0.135279	0.769682	0.54325	0.358307
X4.27	0.681166	0.81567	0.361244	0.449481	0.032154
X5.27	0.028298	0.881739	0.605847	0.578005	0.30303

X6.27	0.171035	0.676694	0.968912	0.533367	0.25265
X7.27	0.423068	0.240545	0.693611	0.191485	0.831224
X1.28	0.388392	0.838201	0.453372	0.653298	0.158183
X2.28	0.852037	0.727109	0.070441	0.577149	0.357161
X3.28	0.576734	0.632591	0.89387	0.172181	0.254314
X4.28	0.800223	0.187949	0.743056	0.284416	0.539614
X5.28	0.751916	0.057846	0.432799	0.80024	0.284373
X6.28	0.476499	0.619022	0.302805	0.824143	0.056971
X7.28	0.747568	0.960209	0.172886	0.518814	0.212064
X1.29	0.792553	0.229879	0.825482	0.028737	0.441733
X2.29	0.146958	0.219406	0.881686	0.460732	0.663178
X3.29	0.010844	0.812579	0.244081	0.538241	0.690414
X4.29	0.173321	0.676936	0.232171	0.93255	0.474459
X5.29	0.388982	0.447297	0.001682	0.963836	0.68066
X6.29	0.870381	0.659408	0.422285	0.197502	0.386948
X7.29	0.602181	0.157847	0.991626	0.254169	0.497834
X1.30	0.402943	0.284254	0.139388	0.69788	0.82903
X2.30	0.772676	0.053582	0.500239	0.93955	0.234485
X3.30	0.73126	0.192727	0.300283	0.873615	0.558263
X4.30	0.127334	0.810624	0.75844	0.276795	0.505921
X5.30	0.015533	0.854679	0.311885	0.677017	0.500424
X6.30	0.935532	0.484336	0.651176	0.201251	0.184842
X7.30	0.56425	0.35012	0.925716	0.685799	0.163463
X1.31	0.383241	0.633019	0.9875	0.532401	0.115056
X2.31	0.302651	0.691227	0.480754	0.184286	0.854616
X3.31	0.8597	0.412109	0.165524	0.372108	0.684544
X4.31	0.396317	0.094924	0.871346	0.449118	0.731652

X5.31	0.882522	0.49868	0.221917	0.021411	0.665155
X6.31	0.67552	0.48696	0.16285	0.91491	0.254168
X7.31	0.037717	0.476754	0.310689	0.759362	0.858175
X1.32	0.302934	0.471605	0.770002	0.995953	0.026448
X2.32	0.371595	0.022847	0.886211	0.517031	0.664319
X3.32	0.917242	0.227235	0.777886	0.516866	0.139753
X4.32	0.275195	0.867842	0.598056	0.010286	0.73254
X5.32	0.049622	0.399369	0.461815	0.955695	0.732824
X6.32	0.021803	0.762287	0.480573	0.206245	0.848215
X1.33	0.797671	0.826879	0.374574	0.170349	0.543387
X2.33	0.673874	0.474458	0.351107	0.118428	0.81467
X3.33	0.994898	0.575679	0.179523	0.35154	0.774575
X4.33	0.71698	0.975318	0.265586	0.55873	0.016074
X5.33	0.295064	0.543216	0.778573	0.874261	0.105833
X6.33	0.913217	0.136616	0.39777	0.719114	0.487018
X7.33	0.882224	0.043709	0.377192	0.420974	0.662546
X1.34	0.179847	0.540843	0.690396	0.972129	0.388085
X2.34	0.362643	0.459114	0.195371	0.617867	0.922108
X3.34	0.732037	0.423544	0.324928	0.131275	0.981041
X4.34	0.157959	0.557763	0.880072	0.73733	0.209995
X5.34	0.314731	0.469623	0.07728	0.896073	0.746277
X6.34	0.278987	0.989779	0.167712	0.520096	0.725253
X7.34	0.490346	0.640144	0.327558	0.180862	0.923691
X1.35	0.206376	0.457017	0.847166	0.061479	0.737881
X2.35	0.386646	0.97373	0.49003	0.657796	0.096998
X3.35	0.145676	0.498553	0.97564	0.214632	0.738206
X4.35	0.991031	0.040175	0.668542	0.538896	0.20807

X5.35	0.908048	0.407815	0.716967	0.385434	0.096534
X6.35	0.976575	0.224631	0.167318	0.705676	0.532158
X7.35	0.442498	0.603542	0.862135	0.270446	0.163498
X1.36	0.910211	0.646061	0.490862	0.234944	0.174432
X2.36	0.789317	0.444534	0.881512	0.114937	0.380314
X3.36	0.972314	0.179629	0.693242	0.278852	0.563269
X4.36	0.28144	0.60199	0.90355	0.591275	0.055912
X5.36	0.141573	0.439537	0.982498	0.686923	0.277943
X6.36	0.693573	0.902409	0.282441	0.170019	0.424538
X7.36	0.571324	0.032729	0.204081	0.965549	0.632712
X1.37	0.099469	0.248832	0.515406	0.75563	0.84115
X2.37	0.165376	0.49867	0.317199	0.987107	0.757264
X3.37	0.77656	0.029525	0.289075	0.801943	0.479939
X4.37	0.658698	0.991072	0.277738	0.133597	0.518448
X5.37	0.452433	0.977633	0.625448	0.202061	0.007948
X6.37	0.316295	0.950237	0.792018	0.501267	0.184672
X7.37	0.885061	0.016591	0.667205	0.224295	0.47265
X1.38	0.416067	0.618715	0.976608	0.394766	0.104841
X2.38	0.864204	0.18984	0.227659	0.750152	0.428962
X3.38	0.941269	0.601883	0.16424	0.4249	0.257846
X4.38	0.09924	0.890391	0.297999	0.449294	0.747546
X5.38	0.653217	0.970983	0.587011	0.088102	0.219416
X6.38	0.77648	0.203909	0.918647	0.582996	0.012894
X7.38	0.062954	0.631281	0.402134	0.824972	0.390364
X1.39	0.490771	0.102536	0.690799	0.289611	0.824744
X2.39	0.074735	0.848041	0.445045	0.673177	0.289774
X3.39	0.358668	0.981699	0.020306	0.671348	0.468535
X4.39	0.262552	0.860133	0.522376	0.739967	0.090586
X5.39	0.327758	0.030107	0.939172	0.730961	0.422154
X6.39	0.65744	0.231348	0.812379	0.595852	0.042829
X7.39	0.538299	0.178565	0.316394	0.652312	0.800781

The images below present the second 200 combinations of the 7 parameters. These values are not yet scaled to the respective value ranges of the parameters in *EnergyPlus*.

X1	0.668806	0.518429	0.227391	0.814163	0.05596
X2	0.567632	0.359772	0.067656	0.701741	0.932497
X3	0.112828	0.258147	0.838789	0.722085	0.582025
X4	0.37805	0.645042	0.046377	0.927332	0.527427
X5	0.258868	0.830832	0.544163	0.125328	0.605851
X6	0.557326	0.985104	0.147496	0.727302	0.212763
X7	0.62139	0.597438	0.25025	0.833884	0.175951
X1.1	0.008085	0.457845	0.200739	0.638903	0.837626
X2.1	0.918511	0.534199	0.020202	0.365494	0.779543
X3.1	0.770391	0.816796	0.335757	0.082249	0.424512
X4.1	0.878251	0.478487	0.069453	0.779939	0.2995
X5.1	0.13079	0.527911	0.783779	0.225534	0.826169
X6.1	0.996536	0.623335	0.574595	0.288848	0.16909
X7.1	0.617826	0.923814	0.595705	0.010892	0.341463
X1.2	0.932268	0.541522	0.076032	0.231742	0.782089
X2.2	0.575557	0.1846	0.823122	0.609572	0.385418
X3.2	0.58792	0.886569	0.613622	0.051373	0.398441
X4.2	0.690318	0.081113	0.879743	0.3475	0.565604
X5.2	0.94716	0.667517	0.276707	0.510475	0.117672
X6.2	0.163634	0.347172	0.70027	0.914415	0.483018
X7.2	0.621055	0.407358	0.916593	0.010001	0.230232
X1.3	0.217163	0.966001	0.79069	0.549577	0.198514
X2.3	0.152253	0.419219	0.669954	0.976548	0.220215
X3.3	0.977543	0.101592	0.272776	0.571416	0.733501
X4.3	0.717751	0.030053	0.989843	0.327735	0.479569
X5.3	0.877201	0.212214	0.649554	0.466027	0.031387
X6.3	0.585395	0.113695	0.842962	0.289579	0.777428

X7.3	0.137252	0.757309	0.503749	0.341576	0.853633
X1.4	0.465406	0.795289	0.896334	0.077698	0.250488
X2.4	0.971256	0.376578	0.414662	0.645091	0.030647
X3.4	0.641859	0.41535	0.093202	0.957987	0.225399
X4.4	0.718528	0.0658	0.517737	0.89992	0.340286
X5.4	0.123056	0.326052	0.448719	0.649626	0.816046
X6.4	0.727139	0.547545	0.835633	0.032888	0.225656
X7.4	0.41587	0.011162	0.303962	0.952305	0.623861
X1.5	0.679008	0.569263	0.963124	0.350159	0.062349
X2.5	0.393815	0.165967	0.999121	0.785266	0.412434
X3.5	0.806868	0.359783	0.683619	0.547826	0.188968
X4.5	0.024949	0.205817	0.600643	0.447627	0.93616
X5.5	0.454387	0.198151	0.342263	0.996033	0.663322
X6.5	0.515668	0.878837	0.027481	0.720041	0.359105
X7.5	0.514763	0.698573	0.897472	0.072529	0.271788
X1.6	0.439026	0.937593	0.347438	0.671907	0.157996
X2.6	0.515525	0.81318	0.335303	0.799	0.031791
X3.6	0.132929	0.317925	0.43828	0.997478	0.664248
X4.6	0.819332	0.712027	0.308661	0.491087	0.012289
X5.6	0.022593	0.991881	0.287907	0.425715	0.749072
X6.6	0.923075	0.387988	0.085501	0.618842	0.5223
X7.6	0.01057	0.528778	0.380619	0.942313	0.679509
X1.7	0.66755	0.265336	0.029686	0.942439	0.536265
X2.7	0.874064	0.722753	0.388323	0.404905	0.107901
X3.7	0.143991	0.231342	0.431975	0.972337	0.776446
X4.7	0.373479	0.165102	0.771945	0.405181	0.842792
X5.7	0.506661	0.26705	0.600454	0.863472	0.186196

X6.7	0.70022	0.514056	0.122725	0.368599	0.964579
X7.7	0.165858	0.464149	0.727838	0.357741	0.987048
X1.8	0.833173	0.74324	0.034717	0.344683	0.574232
X2.8	0.861493	0.129493	0.586658	0.76562	0.362299
X3.8	0.740701	0.286454	0.461139	0.072927	0.84835
X4.8	0.441179	0.158614	0.660081	0.903011	0.347174
X5.8	0.615159	0.969219	0.390325	0.440483	0.021542
X6.8	0.797768	0.075966	0.267645	0.976435	0.47647
X7.8	0.903846	0.392515	0.06946	0.721981	0.527221
X1.9	0.380043	0.177589	0.789623	0.804416	0.41402
X2.9	0.634659	0.595857	0.88418	0.138207	0.250508
X3.9	0.198005	0.471647	0.245458	0.6415	0.823033
X4.9	0.114918	0.932305	0.575206	0.729804	0.374314
X5.9	0.598336	0.008506	0.782481	0.258504	0.832312
X6.9	0.75412	0.346673	0.184876	0.941838	0.566858
X7.9	0.52719	0.009964	0.814509	0.739102	0.321327
X1.10	0.641428	0.128723	0.47393	0.279317	0.914316
X2.10	0.878248	0.723611	0.129049	0.446668	0.375977
X3.10	0.489834	0.364664	0.057743	0.967755	0.714678
X4.10	0.799057	0.889271	0.218462	0.521028	0.043989
X5.10	0.85685	0.582545	0.703175	0.336781	0.17354
X6.10	0.333576	0.601516	0.90548	0.530441	0.171942
X7.10	0.661839	0.474015	0.98053	0.189643	0.291786
X1.11	0.455025	0.249375	0.754968	0.862164	0.089954
X2.11	0.137198	0.868248	0.501259	0.680706	0.235941
X3.11	0.832127	0.357535	0.768847	0.020859	0.466706
X4.11	0.410117	0.358218	0.884335	0.060145	0.603569

X5.11	0.496047	0.2866	0.935089	0.760873	0.037075
X6.11	0.092232	0.635927	0.897422	0.376192	0.527938
X7.11	0.596822	0.890664	0.386611	0.680278	0.006789
X1.12	0.115864	0.858205	0.78382	0.373961	0.409494
X2.12	0.726854	0.545188	0.103395	0.248956	0.876988
X3.12	0.392518	0.594084	0.068215	0.708435	0.968128
X4.12	0.497434	0.182947	0.318705	0.872466	0.703419
X5.12	0.322774	0.000131	0.621728	0.899662	0.56644
X6.12	0.486621	0.752374	0.241704	0.198999	0.809244
X7.12	0.689063	0.474467	0.072207	0.236627	0.858171
X1.13	0.708757	0.867887	0.442985	0.196247	0.21547
X2.13	0.546871	0.352598	0.650261	0.843412	0.139047
X3.13	0.02082	0.710094	0.25714	0.980137	0.504647
X4.13	0.354507	0.153627	0.484179	0.622925	0.853551
X5.13	0.712264	0.463757	0.002331	0.395506	0.906912
X6.13	0.842263	0.369235	0.575582	0.745682	0.185302
X7.13	0.223258	0.773176	0.923022	0.157618	0.502576
X1.14	0.45647	0.798398	0.354884	0.176507	0.824935
X2.14	0.476946	0.76851	0.163144	0.976775	0.202041
X3.14	0.586533	0.347012	0.724997	0.015112	0.812662
X4.14	0.950092	0.215967	0.527285	0.672146	0.128839
X5.14	0.402364	0.791746	0.22708	0.115595	0.937515
X6.14	0.80328	0.686748	0.22295	0.445245	0.16322
X7.14	0.196454	0.237699	0.911729	0.489463	0.741517
X1.15	0.408875	0.214466	0.97844	0.625763	0.043698
X2.15	0.970578	0.584089	0.027608	0.796559	0.200146
X3.15	0.774457	0.31191	0.557846	0.042365	0.871513

X4.15	0.791421	0.991219	0.136261	0.203276	0.442626
X5.15	0.071209	0.427737	0.207511	0.720939	0.862256
X6.15	0.538248	0.716264	0.001502	0.356683	0.854782
X7.15	0.421326	0.836669	0.672987	0.160872	0.273557
X1.16	0.786179	0.366044	0.038832	0.412061	0.888367
X2.16	0.386391	0.787181	0.425693	0.159242	0.953119
X3.16	0.963734	0.141159	0.34061	0.726509	0.586009
X4.16	0.013152	0.813022	0.534656	0.394026	0.725527
X5.16	0.711648	0.162688	0.344688	0.868836	0.519501
X6.16	0.694162	0.239245	0.977435	0.166006	0.422678
X7.16	0.569004	0.98248	0.640871	0.039847	0.39814
X1.17	0.458248	0.315292	0.171421	0.894862	0.783439
X2.17	0.407729	0.734831	0.123865	0.830584	0.246825
X3.17	0.939906	0.142919	0.428037	0.762248	0.222206
X4.17	0.053898	0.812172	0.449228	0.216943	0.785448
X5.17	0.636472	0.049553	0.944064	0.452817	0.33546
X6.17	0.294761	0.438733	0.602735	0.138614	0.934389
X7.17	0.378133	0.575883	0.706214	0.974783	0.003621
X1.18	0.848729	0.385708	0.511966	0.12707	0.777639
X2.18	0.563007	0.972608	0.046745	0.249914	0.740133
X3.18	0.322586	0.811077	0.036302	0.453641	0.709444
X4.18	0.394546	0.534194	0.941831	0.749697	0.110147
X5.18	0.152384	0.562924	0.396092	0.709589	0.840519
X6.18	0.498397	0.927087	0.056038	0.614508	0.224851
X7.18	0.899199	0.410833	0.194184	0.78919	0.287404
X1.19	0.897378	0.526121	0.792211	0.179843	0.398262
X2.19	0.205838	0.748933	0.942403	0.102647	0.527883

X3.19	0.493106	0.16445	0.278916	0.989796	0.73925
X4.19	0.388621	0.903441	0.182101	0.567773	0.751039
X5.19	0.537936	0.684193	0.336762	0.928165	0.128877
X6.19	0.661417	0.133461	0.460187	0.8386	0.289514
X7.19	0.554497	0.614208	0.136153	0.814403	0.356409
X1.20	0.958111	0.479248	0.201061	0.101776	0.617892
X2.20	0.222873	0.4487	0.856357	0.734765	0.142208
X3.20	0.585408	0.382417	0.771649	0.063517	0.976262
X4.20	0.451579	0.645138	0.056334	0.283193	0.918611
X5.20	0.600711	0.987593	0.038451	0.304355	0.505546
X6.20	0.352754	0.664603	0.995229	0.402579	0.085591
X7.20	0.693516	0.07085	0.331017	0.551812	0.905847
X1.21	0.114776	0.316199	0.876975	0.785539	0.556729
X2.21	0.069319	0.776632	0.495281	0.209112	0.97685
X3.21	0.407749	0.957074	0.169003	0.205143	0.703371
X4.21	0.018261	0.904072	0.713429	0.309186	0.524261
X5.21	0.781038	0.986812	0.378258	0.577813	0.050693
X6.21	0.906303	0.002286	0.444596	0.778111	0.379694
X7.21	0.246482	0.990667	0.440277	0.129612	0.754912
X1.22	0.584537	0.049275	0.979694	0.607111	0.23603
X2.22	0.807564	0.070011	0.781745	0.246232	0.430967
X3.22	0.073526	0.88039	0.655394	0.278247	0.401035
X4.22	0.660227	0.403595	0.268065	0.84788	0.115754
X5.22	0.145511	0.6108	0.429432	0.836087	0.301395
X6.22	0.187112	0.259194	0.602642	0.40815	0.914034
X7.22	0.478128	0.607907	0.188222	0.955223	0.375334
X1.23	0.878426	0.421473	0.264628	0.703664	0.101165

X2.23	0.546458	0.155054	0.851755	0.703567	0.296994
X3.23	0.600742	0.146287	0.293209	0.429564	0.987591
X4.23	0.095955	0.360282	0.437311	0.834118	0.714195
X5.23	0.154596	0.692526	0.513744	0.888739	0.331365
X6.23	0.560608	0.997938	0.337794	0.093916	0.725743
X7.23	0.164426	0.373891	0.904435	0.767845	0.507384
X1.24	0.429834	0.700911	0.091701	0.967107	0.327823
X2.24	0.332839	0.428123	0.720638	0.073615	0.873205
X3.24	0.625026	0.904776	0.595322	0.238153	0.152445
X4.24	0.728839	0.015734	0.323924	0.457518	0.956258
X5.24	0.949546	0.617894	0.527399	0.247384	0.006362
X6.24	0.837069	0.554348	0.630173	0.146188	0.219145
X7.24	0.06184	0.397724	0.819955	0.620007	0.438687
X1.25	0.19174	0.83562	0.20905	0.579825	0.720622
X2.25	0.594989	0.855497	0.015677	0.365539	0.74696
X3.25	0.209914	0.490333	0.162491	0.880096	0.729821
X4.25	0.257981	0.191477	0.892343	0.650458	0.405051
X5.25	0.865634	0.401774	0.153619	0.721262	0.290288
X6.25	0.48176	0.703662	0.941484	0.196785	0.227348
X7.25	0.828904	0.110317	0.396449	0.498354	0.689551
X1.26	0.615161	0.072173	0.38414	0.464471	0.831308
X2.26	0.289735	0.096961	0.553636	0.802951	0.667527
X3.26	0.554602	0.246504	0.033895	0.737721	0.897867
X4.26	0.036759	0.680646	0.366359	0.851834	0.426928
X5.26	0.496438	0.011346	0.384916	0.939116	0.612772
X6.26	0.320875	0.611779	0.801498	0.016007	0.42812
X7.26	0.120653	0.536506	0.920849	0.341174	0.750598

X1.27	0.796957	0.443372	0.185045	0.247532	0.860318
X2.27	0.292471	0.689609	0.570113	0.838546	0.093208
X3.27	0.856624	0.041795	0.580547	0.754078	0.240227
X4.27	0.768634	0.338492	0.039812	0.826987	0.419234
X5.27	0.266422	0.903584	0.570257	0.108378	0.782182
X6.27	0.500137	0.281776	0.874337	0.018743	0.714764
X7.27	0.348767	0.965525	0.640377	0.467191	0.163506
X1.28	0.383185	0.673066	0.593863	0.980288	0.164305
X2.28	0.831204	0.547519	0.388179	0.011749	0.697101
X3.28	0.237878	0.718507	0.853879	0.175759	0.439806
X4.28	0.933047	0.362595	0.157951	0.538845	0.646894
X5.28	0.080579	0.896233	0.616882	0.464811	0.268346
X6.28	0.905805	0.1356	0.622168	0.530887	0.385324
X7.28	0.871251	0.227838	0.467282	0.667687	0.13227
X1.29	0.322063	0.493808	0.73641	0.103731	0.887926
X2.29	0.290342	0.590965	0.734194	0.067249	0.865143
X3.29	0.695101	0.875621	0.498077	0.078491	0.234182
X4.29	0.967336	0.347911	0.625139	0.165081	0.412735
X5.29	0.653984	0.961342	0.524515	0.207343	0.093451
X6.29	0.273715	0.532041	0.848694	0.704484	0.177603
X7.29	0.253168	0.425603	0.171818	0.739341	0.966746
X1.30	0.858867	0.344129	0.491438	0.682662	0.119943
X2.30	0.946618	0.287056	0.457862	0.130666	0.774387
X3.30	0.70131	0.997865	0.112786	0.398202	0.434788
X4.30	0.190033	0.447224	0.960201	0.269452	0.742026
X5.30	0.078158	0.655259	0.389358	0.813956	0.43381
X6.30	0.276327	0.729729	0.557621	0.903134	0.109688

X7.30	0.17144	0.294345	0.773958	0.567063	0.971122
X1.31	0.470333	0.304246	0.158009	0.867484	0.717813
X2.31	0.95377	0.191384	0.586094	0.791781	0.244981
X3.31	0.010119	0.642552	0.963507	0.542543	0.317306
X4.31	0.449735	0.989573	0.32367	0.601007	0.156992
X5.31	0.538941	0.85626	0.735461	0.105358	0.239828
X6.31	0.582924	0.93577	0.79124	0.25241	0.093209
X7.31	0.462169	0.273304	0.970741	0.650296	0.130781
X1.32	0.815239	0.238306	0.086888	0.460738	0.670635
X2.32	0.71868	0.33217	0.957241	0.436525	0.124972
X3.32	0.195485	0.416691	0.327011	0.638929	0.99492
X4.32	0.298514	0.082386	0.736777	0.979552	0.431874
X5.32	0.024606	0.717692	0.269035	0.57817	0.949558
X6.32	0.686996	0.524277	0.159864	0.895683	0.295467
X7.32	0.819132	0.064939	0.384438	0.631052	0.510376
X1.33	0.2763	0.029064	0.801609	0.744824	0.554465
X2.33	0.675436	0.829574	0.393562	0.187652	0.474226
X3.33	0.222737	0.690287	0.008803	0.522309	0.867377
X4.33	0.275543	0.68157	0.858273	0.112178	0.596928
X5.33	0.581854	0.213981	0.061258	0.72794	0.993012
X6.33	0.413728	0.10391	0.399161	0.960968	0.770674
X7.33	0.142618	0.888546	0.685946	0.518418	0.352276
X1.34	0.583175	0.968188	0.27584	0.675965	0.009266
X2.34	0.354035	0.707089	0.972799	0.032679	0.587439
X3.34	0.457097	0.169265	0.285539	0.91705	0.774993
X4.34	0.215004	0.889839	0.078577	0.759283	0.408619
X5.34	0.728136	0.857629	0.02077	0.461468	0.25956

X6.34	0.099723	0.334156	0.975074	0.797613	0.413592
X7.34	0.996311	0.526537	0.252109	0.774008	0.195208
X1.35	0.144301	0.536046	0.234984	0.702558	0.996987
X2.35	0.975401	0.663848	0.244775	0.147805	0.421323
X3.35	0.272996	0.088386	0.628238	0.824516	0.511884
X4.35	0.444657	0.017169	0.747026	0.840371	0.288503
X5.35	0.718238	0.248976	0.988315	0.413539	0.046718
X6.35	0.134298	0.552806	0.337833	0.636617	0.987964
X7.35	0.419898	0.83965	0.005715	0.613027	0.26857
X1.36	0.266374	0.783633	0.551791	0.93437	0.021131
X2.36	0.737463	0.881111	0.073172	0.430187	0.222242
X3.36	0.907927	0.356724	0.599521	0.152151	0.669604
X4.36	0.40578	0.653691	0.211714	0.972931	0.154665
X5.36	0.505134	0.687323	0.192613	0.317323	0.881174
X6.36	0.501262	0.853791	0.653834	0.234929	0.003163
X7.36	0.335598	0.102557	0.92222	0.676239	0.580537
X1.37	0.928102	0.640365	0.525794	0.353879	0.056191
X2.37	0.801276	0.709058	0.508217	0.220803	0.077942
X3.37	0.947953	0.385735	0.643818	0.498825	0.022257
X4.37	0.793039	0.166419	0.231127	0.847667	0.412278
X5.37	0.417441	0.14256	0.604422	0.328764	0.855753
X6.37	0.733719	0.949643	0.333609	0.177059	0.583037
X7.37	0.741966	0.183949	0.567512	0.224474	0.915979
X1.38	0.543191	0.261618	0.99257	0.195642	0.774081
X2.38	0.409386	0.137092	0.783268	0.21728	0.960549
X3.38	0.099072	0.275568	0.407835	0.756111	0.807606
X4.38	0.476749	0.02174	0.249147	0.815089	0.606106

X5.38	0.626809	0.397724	0.439441	0.161283	0.811588
X6.38	0.029914	0.781905	0.458358	0.810243	0.213989
X7.38	0.830387	0.730692	0.17458	0.347309	0.55664
X1.39	0.58512	0.916998	0.142697	0.709722	0.263975
X2.39	0.028713	0.52013	0.948211	0.222131	0.612192
X3.39	0.82068	0.571844	0.17558	0.633097	0.242327
X4.39	0.016603	0.565228	0.621479	0.997562	0.210903
X5.39	0.745102	0.482725	0.213848	0.116702	0.951786
X6.39	0.863822	0.154958	0.679643	0.474777	0.380631
X7.39	0.006511	0.537513	0.605491	0.848332	0.369481

Appendix C.3 Spline Interpolation

The image below presents the code used for performing the spline interpolation for interpolating the UDI and total energy consumption as functions of WWR. The function used was *spline* function which is a built-in R function. #x is a vector that defines the WWR values, and #y is a vector that defines the UDI or energy consumption.

```
1 x <- c(20,35,50,65,80)
2 y <- c(52.58131221,52.16050564,52.05350427,52.0041033,51.98205232)
3
4 spline(x, y, n = 30, method = "natural", xmin = min(x), xmax = max(x))
```